Contraction fatigue and motor unit overlap in the tibialis anterior during different intensities of interleaved electrical stimulation

by

Emily Noelle Ainsley

A thesis submitted in partial fulfillment of the requirements for the degree of

Master of Science

Faculty of Kinesiology, Sport, and Recreation and
Neuroscience

University of Alberta

ABSTRACT

Interleaved neuromuscular electrical stimulation (iNMES), which involves alternating stimulus pulses between a nerve (nNMES) and muscle belly (mNMES), has been demonstrated to reduce fatigue of the ankle dorsiflexors when used with relatively low contraction amplitudes. However, the amount of fatigue accrued at higher intensities of NMES has not been investigated, when theoretically higher overlap between the motor units (MUs) recruited with stimulation at each site may reduce its effectiveness. The present experiments were designed to determine the effect of contraction amplitude on the amount of fatigue and MU overlap in the tibialis anterior muscle. Fourteen participants completed 3 testing sessions on 3 separate days during which fatigue protocols of iNMES were delivered over the common peroneal nerve and tibialis anterior muscle belly at one of (LOW: ~5% MVC, MID: ~15% MVC, MAX: the greatest tolerable stimulation amplitude; ~30% MVC) were administered. Each fatigue protocol consisted of 180 iNMES-evoked contractions (40 Hz; 500μs; 0.3 s "on", 0.7 s "off"). Fatigue was quantified as the percent decline in torque from beginning to the end of the fatigue protocol. MU overlap (%) was quantified by comparing the amount of torque produced at each stimulation site separately to that produced when stimulation was delivered over both sites at the same time. Contraction fatigue was found to be not different across the three contraction amplitudes. MU overlap was higher during MAX than during LOW and was found to have a significant positive correlation with contraction amplitude. However, no significant relationship was found between MU overlap and contraction fatigue. These data suggest that across a moderate range of contraction amplitudes, contraction fatigue remains consistent during iNMES and does appear to be influenced by the amount of overlap in MUs recruited by each stimulation site.

PREFACE

This thesis is an original work by Emily Noelle Ainsley. The research projects described here received approval from the University of Alberta Research Ethics Board under the project name "Contraction fatigue during different intensities of electrical stimulation" (No. Pro00054857).

ACKNOWLEDGEMENTS

I would like to first thank my supervisor, Dr. David Collins, for his continued guidance and support throughout the several years I have known him, as well as for setting an exemplary teaching style for which I have tried to mirror myself. I would also like to thank my committee members, Dr. Monica Gorassini and Dr. Francois Roy, for their valuable input on this thesis, as well as sharing their knowledge and expertise with me in both the classroom and the operating room.

I would also like to extend my deepest gratitude to my many labmates both past and present, for their immense support and input on this thesis project and for making my Master's experience far more enjoyable. I would also like to thank many of the graduate students and faculty members in the Faculty of Physical Education and Recreation and the Neuroscience Mental Health Institute for sharing their experiences and knowledge with me and providing much-appreciated support along the way. Finally, much gratitude for my family and friends for standing beside me these past two-and-a-half years and ensuring I maintained a school-life balance.

TABLE OF CONTENTS

LIST OF FIGURES

CHAPTER 1

CHAPTER 2

LIST OF ABBREVIATIONS

PL, peroneus (fibularis) longus muscle

H-reflex, Hoffmann reflex

LOW, stimulation intensity to achieve a contraction amplitude of ~5% MVC

MAX maximal tolerated stimulation amplitude

MID, stimulation intensity to achieve a contraction amplitude of ~ 15% MVC

MU, motor unit

MVC, maximum voluntary contraction

M-wave, motor wave

NMES, neuromuscular electrical stimulation

mNMES, neuromuscular electrical stimulation delivered over the muscle belly

nNMES, neuromuscular electrical stimulation delivered over the nerve trunk

iNMES, interleaved neuromuscular electrical stimulation (delivered over both the muscle belly and nerve trunk)

m+nNMES, mNMES and nNMES delivered simultaneously

TA, tibialis anterior muscle

$\mathbf{T_{mNMES}}$**,** torque evoked by stimulation over the mNMES site alone

$\mathbf{T_{nNMES}}$**,** torque evoked by stimulation over the nNMES site alone

$\mathbf{T_{m+nNMES}}$**,** torque evoked when mNMES and nNMES are delivered simultaneously

CHAPTER 1: GENERAL INTRODUCTION

1.1 PREFACE

Following neuromuscular injury or disease to the central or peripheral nervous systems, individuals may experience loss or complete abolishment of voluntary motor control. This loss of function can result in a lack of ability to execute various movements requisite for activities of daily living, including reaching and grasping, standing, walking, and, ultimately, a diminished quality of life. A muscle commonly affected by neuromuscular trauma including stroke (cerebral vascular accident; CVA) and spinal cord injury (SCI) is the tibialis anterior located on the anterior portion of the lower leg (Stein, Rolf, Everaert, Bobet, & Chong, 2008). The tibialis anterior is fundamental to dorsiflex the ankle during walking to ensure efficiency of gait and prevent dragging of the foot, trips and falls.

One way to produce contractions and mitigate secondary complications following a SCI or CVA is using neuromuscular electrical stimulation (NMES). While NMES has been used in the tibialis anterior since the 1960s, one persistent issue with its use is the rapid fatigue that develops with multiple contractions. This fatigue may limit walking over a longer duration or at a higher intensity, therein attenuating the potential cardiovascular, neuromuscular and functional benefits of NMES and hindering its widespread clinical use. One method developed to reduce fatigue during NMES, is interleaved NMES (iNMES), which involves alternating stimulating pulses over the tibialis anterior muscle belly and the common peroneal nerve trunk in an attempt to reduce the firing rates of individual motor units (MU). Although iNMES has been shown to reduce fatigue in the tibialis anterior compared to stimulating over the muscle belly or nerve trunk alone at low contraction amplitudes (Lou, Bergquist, Aldayel, Czitron, & Collins, 2016), how fatigue changes during iNMES over a range of contraction amplitudes has not been

elucidated. In addition, the mechanisms responsible for reducing fatigue during iNMES have not been fully investigated.

This thesis contains one study that will be submitted for publication (Chapter 2). One main goal of this study was to compare the amount of contraction fatigue of the ankle dorsiflexors during iNMES delivered to generate a range of contraction amplitudes. We also estimated the proportion of MUs recruited by both the nerve and muscle stimulation sites at this range of contraction amplitudes, to determine if a significant relationship exists between contraction fatigue and MU overlap. This general introduction is comprised of five main sections. The following section (1.2) provides a brief history of NMES as well as a description of how NMES generates muscle contractions when administered transcutaneously. The next section (1.3) discusses the various parameters of NMES, including stimulation amplitude, pulse duration, stimulation frequency, duty cycle and stimulation waveform and their respective effects on torque generation during NMES. Subsequently, a description of clinical populations who currently or could benefit from NMES is provided (1.4) with a particular focus on individuals with CVA or SCI. The final two sections of this chapter focus on a main limitation of present NMES use, which is rapid contraction fatigue and the many mechanisms that contribute to it (1.5); and introduces a method of NMES that has been developed to combat this fatigue, known as iNMES (1.6). While NMES is used in a wide range of muscles located in both the upper and lower limbs, as well as the trunk, this thesis centers primarily around NMES used in lower limb musculature, in particular the tibialis anterior muscle, due to its importance in rehabilitation for standing and ambulation.

1.2 NEUROMUSCULAR ELECTRICAL STIMULATION (NMES)

1.2.1 Brief History and Contemporary Use of NMES

Electrical stimulation is currently used primarily for rehabilitative purposes following a SCI or stroke. However, the use of electrical stimulation is not a novel medium in the treatment of medical ailments and was first used almost two millennia ago when Torpedo fish were used to treat headaches and gout (Fodstad & Hariz, 2007). However, the breakthrough of electrical stimulation to induce muscle contractions in paralyzed muscles did not occur until the eighteenth century. Although the beginnings of electrical stimulation are often attributed to Italian scientist Luigi Galvani based on his classic experiments involving the sciatic nerve of frog legs in the early 1790s, the origins of electrophysiology revolve around the discovery of the Leyden jar in 1746 (Fodstad & Hariz, 2007; Hoff, 1936). It is thought that Kruger (JG) and Antoine Louis, among others, were the first to use this technique to elicit contractions in both intact and paralyzed muscles, with Louis first noting that contractions may be impossible to elicit in muscles with significant atrophy (Hoff, 1936).

Regardless of the exact origin of electrical stimulation, at the turn of the nineteenth century, much division remained in the scientific community about how such muscle contractions were elicited. In particular, Galvani postulated that the muscle twitches of frog legs were due to an intrinsic form of electrical force within the muscle tissue or nerves themselves, in what was referred to as “animal electricity” (Finkelstein, 2015; Piccolino & Bresadola, 2013). In contrast, Alessandro Volta, a physicist and inventor of the electric battery (1800), contended that the contractions were due to the contact between two different metals inserted into the tissue of the animal, a concept which he termed “the special theory of contact electricity” (Finkelstein, 2015; Fodstad & Hariz, 2007; Piccolino & Bresadola, 2013). The debate between these theories

persisted until Emil Du Bois-Reymond (1941-1943) demonstrated that, under resting conditions, the surface of a nerve fibre was positive, while its center was negative (Smith, Frixione, Finger, & Clower, 2012). He argued that, this polarity can be disrupted by natural signals, leading to a propagated wave of excitation, in what is referred to today as the action potential (Smith et al., 2012). The speed of action potentials was later determined by Hermann Helmholtz (1849) to be ~30 m/s and the activity of sodium (Na^+) and potassium (K^+) channels during action potentials was later elucidated by Andrew Huxley and Alan Hodgkin (Finkelstein & Finkelstein, 2014; Häusser, 2000).

The first application of electrical stimulation to evoke functional contractions was the foot drop stimulator, designed by Waldimir Liberson in 1961 to elicit dorsiflexion contractions in individuals with hemiplegia. This device involved stimulation over the common peroneal nerve which was triggered by a heel switch located in the shoe of the affected leg. Subsequent to use of the foot drop stimulator among individuals with stroke, it was postulated that the effectiveness of electrical stimulation in producing functional contractions could be extended to individuals with SCI. As such, the 1970s-1990s saw an emergence of research into electrical stimulation typically over the quadriceps femoris to restore functional movements following neuromuscular impairment (Hamid & Hayek, 2008), including standing (Grobelnik & Kralj, 1973) and walking (Bajd, Kralj, Turk, Benko, & Šega, 1989; Granat, Ferguson, Andrews, & Delargy, 1993). While the term "functional electrotherapy" was used originally by Liberson (1961), it was later replaced by "functional electrical stimulation" by Mo & Post in 1962 (Moe & Post, 1962) and is presently more generally referred to as neuromuscular electrical stimulation (NMES). However, the term NMES typically encompasses of a variety of subtypes. NMES used to produce functional contractions such as those to enable walking, cycling, rowing, grasping, or reaching has been

referred to as functional electrical stimulation (FES). NMES used for more therapeutic purposes, wherein the effects of stimulation persist subsequent to the stimulation being turned off, is referred to as therapeutic electrical stimulation (TES).

1.2.2 Elicitation of Muscular Contractions using NMES

The following section outlines how NMES delivered transcutaneously evokes muscular contractions. Briefly, a description of the action potential (1.2.2.1) is provided, along with a description of conduction along a nerve axon from the site of stimulation to deep within the muscle, leading to excitation-contraction coupling. Next, a description of MUs, including their various types is given (1.2.2.2). The typical recruitment order of these MUs during NMES is then described (1.2.2.3) along with an explanation of the differing spatial distribution of MU recruitment when NMES is delivered over a nerve trunk versus a muscle belly (1.2.2.4). Finally, a brief discussion of the central and peripheral neural pathways involved in NMES-generated contractions is included (1.2.2.5).

1.2.2.1 Biophysics and the Action Potential

During NMES, electrical current is typically delivered through a pair of electrodes consisting of one anode (positively charged electrode) and one cathode (negatively charged electrode). These electrodes act as an interface between the external power source (i.e. stimulator) and the tissues of the nervous system and imitate natural neural triggers (Hamid & Hayek, 2008; Ho et al., 2014). Stimulating electrodes can be implanted intramuscularly, or can be positioned around a nerve trunk via a nerve cuff. However, these methods of NMES delivery are invasive and require medical expertise and surgical procedures. Therefore, the focus of this

thesis will involve a more common and less invasive administration of NMES, known as surface NMES, where electrodes are affixed to the skin over a nerve trunk (nNMES) or over a muscle belly (mNMES). Regardless of whether electrodes are positioned above a nerve trunk or muscle belly, surface NMES activates nerve axons, and not muscle fibres themselves as it would take approximately 10 times the current to activate muscle fibres as it does nerve axons (Hamid & Hayek, 2008). Consequently, substantially smaller currents are required to activate the muscle, thereby reducing power consumption and reducing the risk of tissue damage (Ho et al., 2014). In addition, it is important to recognize that stimulation using surface electrodes is appreciably different than direct stimulation of motor axons since axons and axonal branches are more disseminated and thus receive different densities of current when indirectly activated over the skin (Bickel, Gregory, & Dean, 2011). For the remainder of this thesis document, surface NMES will be referred to more simply as NMES.

The generation of muscle contractions during NMES is initiated when charge transfer occurs between the anode and cathode, regardless of whether these electrodes are configured in a monopolar or bipolar arrangement (Ho et al., 2014). Specifically, positively-charge ions (cations) move from the anode to the cathode and negatively-charged ions (anions) flow from the cathode to the anode. As this occurs, ions are repelled or attracted to the nerve membrane depending on their charge, resulting in perturbations in the membrane potential of the axon which typically remains around -65mV at rest. The resting membrane potential is determined by the relative abundance of various non-gated ion channels, where slow or "leak" potassium (K^+) channels are primarily responsible for the maintenance of the resting potential. If the stimulation amplitude delivered is sufficiently large enough to depolarize the membrane potential to approximately

-50mV (i.e. the threshold for an action potential), fast Na^+ channels open and Na^+ enters the cell (Sandow, 1965). As this influx of Na^+ occurs, the membrane potential continues to progressively depolarize in what is often referred to as the "rising phase" of the action potential (Kandel, Schwartz, & Jessell, 1991). When the membrane potential peaks in depolarization and approaches approximately +30mV (often referred to as the "overshoot"), Na^+ channels inactivate rapidly (Sandow, 1965). As this occurs, voltage-gated K^+ channels open leading to a net efflux of K^+ ions which lowers the membrane potential consecutively more negative, often referred to as "repolarizing" the membrane potential. Importantly, the opening of voltage-gated K+ channels leads to a pronounced membrane permeability to K^+, therefore causing an "extra" efflux of K^+ such that the membrane potential becomes even more negative than at rest and approaches the equilibrium potential of K^+ at -93 mV. Because the membrane potential becomes more negative than at rest, this phase of the action potential is termed "hyperpolarization" and prevents action potentials from occurring in too quick of succession.

In myelinated motor axons, action potentials propagate via saltatory conduction where signals travel from node of Ranvier to node of Ranvier. This saltatory conduction is attributable to the specialized distribution of ion channels along the nodal, paranodal and internodal regions of the myelinated axon. Specifically, Na^+ channels (both transient and persistent) along with slow K^+ channels are concentrated more densely in the nodal regions, whereas fast K^+ channels are found almost exclusively in the paranodal regions (Kiernan & Lin, 2012). Once action potentials reach the terminal boutons of the axon, voltage-gated Ca^{2+} channels open, allowing Ca^{2+} to enter the terminal bouton. This influx of Ca^{2+} causes vesicles containing acetylcholine fuse to the pre-synaptic membrane before acetylcholine is released into the synaptic cleft. Once in the synaptic cleft, acetylcholine diffuses to the motor end plate and binds to ligand-gated

nicotinic receptors. This binding of acetylcholine leads to a net cation influx into the post-synaptic cell, thereby depolarizing the end plate potential and activating voltage-gated Na+ channels. Accordingly, an excitatory post-synaptic potential is generated and propagation of the action potential occurs along the sarcolemma of the muscle fibre. Thereafter, the action potential propagates through the T-system, which is comprised of transverse tubules (i.e. T-tubules) ~0.03 nm in diameter which infiltrate into each muscle fiber in a lateral or transverse direction (Sandow, 1965). As there typically exists one neuromuscular junction per muscle fibre, T-tubules enable the action potential to reach all parts of the cell and, therefore, myofibrils, at the same time to enable synchronous contraction (Mann, 2011). As the action potential travels down each T-tubule, it activates dihydropyridine (DHP) receptors, which are L-type voltage-activated Ca^{2+} channels located along the membrane of the T-tubule (Westerblad & Allen, 2009). When these DHP receptors are activated, L-type Ca^{2+} channels open, allowing Ca^{2+} to enter the cell and bind to ryanodine receptors (RyR) located on the sarcoplasmic reticulum. Concomitantly, activation of DHP receptors leads to activation of RyR directly, due to a mechanical coupling mechanism between DHP and RyR receptors (Westerblad & Allen, 2009).

Once RyR receptors are activated, Ca^{2+} is released from the terminal cisternae of the sarcoplasmic reticulum into the myoplasm where it binds to troponin (Westerblad & Allen, 2009). This binding of Ca^{2+} results in a conformational change of the troponin complex causing tropomyosin to disengage from the myosin-binding site on actin myofilaments, thereby enabling attachment of the myosin head and cross-bridge formation. The coordinated cyclic attachment and detachment of these cross-bridges along the actin results in in coordinated sarcomere shortening (Binder, Hirokawa, & Windhorst, 2009). Sarcomeres return to their resting length

when Ca^{2+} ions are pumped back into the sarcoplasmic reticulum and troponin regains its block over the myosin head binding site, instigating global muscle relaxation.

1.2.2.2 The Motor Unit

A single muscle within the human body can consist of hundreds of thousands of muscle fibres. These muscle fibres are organized into groups and innervated by a single α-motoneuron located in the spinal cord (Bickel, Gregory, & Dean, 2011). These functional units (i.e. one single α-motoneuron and all the muscle fibres it innervates) are referred to as motor units (MU) (Burke, 1967), a term first described by Sir Charles Sherrington (Floeter, 2010). Comparatively, the term "muscle unit" refers specifically to the population of muscle fibres innervated by a single motor neuron (Burke, 1967). The number of MUs per muscle varies extensively across muscles, depending on the size and function of the muscle itself. For example, the TA muscle has been estimated to consist of ~ 120-450 MUs depending on the methodology used to quantify the number of MUs, while considerably larger muscles such as the vastus lateralis can contain several thousand MUs. The size of these MUs can be estimated by dividing the total number of muscle fibres within a given muscle belly by the number of motor axons innervating that muscle. Larger innervation ratios would indicate more muscle fibres are part of a MU and are typically present for muscles that require greater force generation. For example, while the tibialis anterior and medial gastrocnemius contain a similar number of MUs (~445 vs 579, respectively (Feinstein, Lindegard, Nyman, & Wohlfart, 1955)), the innervation ratio for the tibialis anterior is 562, while the innervation ration for the medial gastrocnemius is 1934.

Within the human spinal cord, motoneurons are clustered into motor nuclei located in the ventral horn (Rexed lamina IX), with motoneurons innervating more distal muscles located more laterally within the horn (Floeter, 2010; Molander, Xu, & Grant, 1984; Rexed, 1952). It is

currently thought that three types of motoneurons exist within the human spinal cord including the large α-motoneurons that innervate extrafusal muscle fibres and gamma (or fusimotor) motoneurons that innervate fibres of the muscle spindles (Floeter, 2010; Kanning, Kaplan, & Henderson, 2010). The third type of motoneuron have been called either the skeleto-fusimotor or beta motor neurons and likely innervate both extra- and intrafusal muscle fibres, however these have been poorly described in humans (Floeter, 2010; Kanning et al., 2010). The most abundant of the three subtypes, α-motoneurons, are organized into clusters of motor nuclei which form elongated columns, spanning several segments of the spinal cord, and innervate the same muscle (Floeter, 2010; Kanning et al., 2010). Each α-motoneuron innervates or synapses with a collection of muscle fibres which all share the same histochemistry and contractile characteristics including the isoform of myosin heavy chain, ATPase activity and metabolic enzyme capacities (Purves, Augustine, Fitzpatrick, & Katz, 1997). Classic experiments by Burke et al. (1967) in the cat soleus and gastrocnemius muscle examined these characteristics in relation to peak twitch force, tetanic force, "sag" and fatigability profiles and classified MUs into three main subtypes (Floeter, 2010). These subtypes include Type S (slow twitch, fatigue resistant), Type FR (fast twitch, fatigue resistant) and Type FF (fast twitch, fatigable) (Floeter, 2010). Although resistant to fatigue, Type S MUs generate smaller levels of torque and therefore, are more prevalent in muscles under sustained or repetitive contractions such as those responsible for posture and walking (Purves et al., 1997). Conversely, Type FF produce the most torque and are thus, important for explosive activities such as running and jumping, yet fatigue the most rapidly (Purves et al., 1997). Correspondingly, Type S MUs typically have the lowest threshold of depolarization while Type FF have the highest threshold (Purves et al., 1997).

Although a single MU is comprised of a single type of muscle fibre, whole muscles themselves are heterogeneous, meaning they contain a combination of MU types. Inaddition, the distribution of MU types within each muscle is not uniform. For example, in the TA muscle which is comprised of approximately 70% Type S MUs, studies of cadaver muscle tissue have established that the Type S MUs are located in the superficial portions of the muscle, while Type FR ad Type FF muscle fibers are distributed deeper within the muscle contiguous to the tibia bone (Henriksson-Larsén, Lexell, & Sjöström, 1983; Johnson, Polgar, Weightman, & Appleton, 1973). Within the muscle itself, the fibres activated by each MU occupy a certain portion, or "territory" of each muscle and intermix with muscle fibres of other MUs (Heckman & Enoka, 2012) in what is often referred to as a "mosaic" fibre distribution (Gordon & de Zepetnek, 2016). The spread of these MU territories is thought to extend differently across muscles. For example, in the rat tibialis anterior it has been demonstrated that MU territories extend roughly 3.7 to 22.6 mm^2 (Gordon & de Zepetnek, 2016), while MU territories in the medial gastrocnemius have been shown to span 14 - 70 mm^2 (Rafuse & Gordon, 1996). Despite these absolute differences in MU territory size, the relative area of these MU territories to the total muscle cross-sectional areas of the tibialis anterior and medial gastrocnemius are very similar (i.e. 17% in the tibialis anterior (Edström & Kugelberg, 1968) vs. 15-20% in the medial gastrocnemius (Rafuse & Gordon, 1996), thus, it has been suggested that the extent of axonal branching may be matched to the muscle size of which it innervates (Gordon & de Zepetnek, 2016).

1.2.2.3 MU Recruitment Order During NMES

Given that MUs are the "final common pathway" between the central and peripheral nervous systems, as described by Sherrington in 1904, it is ultimately the activity and characteristics of the α-motoneuron that determines the magnitude of torque generation of the

ensuing muscle contraction (Heckman & Enoka, 2012). Augmentation of torque output of a given muscle during voluntary contractions can be achieved in one of two ways. First, a greater number of MUs can be activated, which is typically referred to as "recruitment." Under voluntary conditions, MUs are recruited in an orderly pattern, known as Henneman's size principle, where Type S MUs are recruited first and followed by Type FR and Type FF, should greater torque generation be required. The second strategy to increase torque production during voluntary contractions is by increasing the rates at which individual MUs discharge, in what is referred to as "rate coding" (Milner-Brown, Stein, & Yemm, 1973). Briefly, while firing rates of MUs are typically < 10 Hz at recruitment, MUs can typically fire 20-40 Hz during maximal voluntary contractions depending on the muscle in question. Mean maximal firing rates of MUs have been demonstrated to be relatively higher in the tibialis anterior compared to other muscles including its plantarflexor counterpart, the soleus, and can even exceed firing rates of 40 Hz.

The following section provides a brief description of how recruitment during NMES differs greatly from that during voluntary contractions. First, a description of the random recruitment order of MUs during NMES is provided. Secondly, how MUs are recruited spatially, in particular during stimulation over a nerve trunk versus over a muscle belly, is described. An explanation of firing rates during NMES is provided in Section 1.3 and will, thus, not be discussed in the present section.

1.2.2.4 Random Order of MU Recruitment During NMES

During NMES, the way in which MUs are recruited has not been fully elucidated, despite investigation for a number of decades. Earlier work suggested that during NMES, MUs are recruited in a reversed order to that described by Henneman's size principle (Enoka, 2002).

Specifically, it was postulated that MUs with larger diameters (i.e. Type FF MUs) were more easily activated using NMES than smaller diameter axons (i.e. Type S MUs), as according to Ohm's Law (V = IR), those axons with a larger diameter would have a lower threshold of recruitment due to a lower resistance. This reversed order fit with consistent findings that contractions evoked via NMES fatigued to a greater extent than those elicited volitionally (Gregory & Bickel, 2005). However, the studies demonstrating this reversed order were conducted primarily in animal models where direct activation of axons was employed which markedly differs from transcutaneous stimulation utilized with human participants (Gregory & Bickel, 2005; Kim, Bangsbo, Strange, Karpakka, & Saltin, 1995). In addition, in the tibialis anterior muscle it was found that MU recruitment followed a reversed order only ~28-35% of the time (Feinstein et al., 1955; Gregory & Bickel, 2005).

Thus, the support for a reversed order of MU recruitment began to lose strength, and it was suggested that rather than a reversal of Henneman's size principle, MUs may be recruited in a pattern without obvious sequencing related to MU type during NMES (Jubeau, Gondin, Martin, Sartorio, & Maffiuletti, 2007). To verify this hypothesis, Jubeau et al. (2007) utilized a twitch-interpolation technique during various amplitudes of volitional and electrically-evoked contractions, whereby the time to peak torque of the superimposed doublet was measured. While the time to peak torque of the doublets decreased with increases in volitional contraction amplitudes, the time to peak torque was unchanged during the various amplitudes of NMES-generated contractions. Consequently, the authors concluded that MU recruitment during NMES is random with respect to MU type (Jubeau et al., 2007). Based on these various experiments, the more widely accepted theory of MU recruitment during NMES at present is that MUs are

recruited non-selectively or, in other words, randomly with respect to MU type (Gregory & Bickel, 2005; Jubeau et al., 2007).

1.2.2.5 Spatial Distribution when NMES is Delivered Over a Nerve Trunk Versus a Muscle Belly

There is a general consensus within the literature that nNMES and mNMES recruit largely spatially distinct motor units within a given muscle. In particular, it has been demonstrated that mNMES delivered at low stimulation amplitudes primarily recruits only those MUs closest to the surface of the skin (i.e. superficial MUs) in the tibialis anterior, quadriceps femoris and biceps brachii, rendering MUs located deep in the muscle largely inactive (Maffiuletti, 2010). However, one earlier study utilizing fMRI of the quadriceps muscles suggested that MUs located deep in the muscle can also be recruited during low contraction amplitudes of NMES (Adams, Harris, Woodard, Dudley, & Adams, 1993). As stimulation amplitude is increased, MUs located within deeper portions of the muscle are progressively recruited, however, even at very high stimulation amplitudes, previous work has demonstrated not all MUs deep within the muscle are recruited. This inactivity of deep MUs during mNMES occurs even in relatively thin muscles such as the tibialis anterior (Okuma, Bergquist, Hong, Chan, & Collins, 2013), and, as such, mNMES has been described as largely "incomplete" activation of a muscle (Maffiuletti, 2010).

In contrast, nNMES is thought to elicit MU activity more globally within a given muscle. For example, in a study conducted by Okuma et al. (2013) recording electrodes were positioned superficially and deep within the tibialis anterior muscle belly using ultrasound technology. Concomitantly, stimulation was delivered at increasing amplitudes over both the tibialis anterior muscle belly and the common peroneal nerve trunk and M-wave amplitudes were recorded from

various sites within the muscle (superficial to deep). Findings of this study suggested that while stimulation over the muscle belly recruited primarily superficial MUs at lower stimulation amplitudes, when stimulation was delivered over the common peroneal nerve trunk, MUs located both superficially and deep were recruited, regardless of stimulation amplitude (Okuma et al., 2013). Consequently, it is generally assumed that nNMES and mNMES recruit spatially distinct populations of MUs, at least at lower stimulation amplitudes.

Distributed types of stimulation, involving stimulation electrodes placed over multiple portions of the muscle belly or over a muscle belly *and* a nerve trunk innervating a given muscle may exploit this differential recruitment of MU populations in order to attenuate fatigue during NMES. However, these methods of NMES may only be effective in reducing fatigue when largely different populations of MUs are recruited at each stimulation site (i.e. when there is minimal or low overlap between the MUs recruited at multiple stimulation sites), as it is expected that when MUs are only activated with every other pulse (rather than with every pulse) MU discharge rates can be reduced by half. A recent study examined the magnitude of MU overlap of the tibialis anterior muscle at a range of stimulation amplitudes (10-100% peak twitch torque) during iNMES (Wiest, Bergquist, Schimidt, Jones, & Collins, 2017a). Even at the lowest stimulation intensity utilized (i.e. 10% peak twitch torque) there was on average ~5% MU overlap between the populations of MUs recruited at the common peroneal nerve and tibialis anterior muscle belly stimulation sites. This amount of MU overlap was significantly smaller than the MU overlap calculated at all other stimulation intensities used in the study, as depicted in Figure 1-1. This figure also shows that MU overlap increased until 50% peak twitch torque, after which the magnitude of MU overlap plateaued. Although this study demonstrates that, in general, larger stimulation amplitudes result in greater MU overlap between stimulation sites,

this study did not investigate directly whether these greater magnitudes of MU overlap achieved at higher stimulation amplitudes resulted in enhanced fatigue during iNMES compared to lower stimulation amplitudes. Accordingly, the present thesis was designed to assess whether the magnitude of MU overlap is related to the amount of fatigue during iNMES of the ankle dorsiflexors.

1.2.2.6 Neural Pathways involved in NMES

When stimulation is delivered over a mixed nerve trunk or muscle belly, signals can travel along peripheral axons in various ways. First, signals may be sent from the site of stimulation directly to the muscle along efferent fibres of the motor axon. Because this pathway bypasses the spinal cord completely, this pathway is often referred to as exclusively "peripheral." When axons are depolarized in such a way, a predictable and "time-locked" twitch response appears in the EMG referred to as a motor- or M-wave (Bergquist, Clair, & Collins, 2011). The latency of M-waves can vary extensively depending on the distance between the electrode site and the muscle, age and presence of injury, however, a typical M-wave latency in the tibialis anterior is ~ 6-8 ms. If stimulation amplitude is continually increased, a plateau in peak-to-peak M-wave amplitude will be established, representing the maximal motor response of the muscle (M_{max}).

Alternatively, orthodromic signals can travel along afferent pathways (from muscle spindles, Golgi tendon organs and cutaneous receptors) which project to the dorsal horn of the spinal cord. When large-diameter Ia afferents are activated in this way, excitation of the α-motoneuron within the ventral horn of the spinal cord occurs (either via mono- or oligosynaptic projections) and a subsequent volley is sent from the α-motoneuron to the target muscle

(Misiaszek, 2003; Palmieri, Ingersoll, & Hoffman, 2004). The resultant "time-locked" response in the EMG is typically referred to as a Hoffman reflex, or H-reflex as it was first described by Hoffman (Hoffmann, 1910) and this pathway is often referred to as the electrical analogue to the spindle stretch reflex (Palmieri et al., 2004). Due to the longer time required for the signal to travel to and from the spinal cord, the latencies of an H-reflex compared to an M-wave is considerably longer and range from ~ 15-30 ms, depending on the distance between the spinal cord, location of stimulating electrodes and muscle (Palmieri et al., 2004).

Using electrical stimulation, activation of afferent pathways can concomitantly lead to α-motoneuron discharge in a second way. It is currently thought that afferent pathways can activate persistent inward currents (PICs) on α-motoneurons leading to a sustained depolarization. In contrast to M-waves and H-reflexes, this activity appears in the EMG signal as activity not time-locked to each stimulus pulse and is therefore, often referred to as "asynchronous activity." Because an H-reflex and asynchronous activity involve signals traversing the spinal cord, these pathways are typically referred to as "central pathways" or "central contributions". Importantly, central contributions to contractions can vary greatly depending on stimulation parameters utilized, individual differences and the muscle in question. For instance, the soleus muscle can elicit relatively large central contributions where approximately 50% of its MUs can be recruited into the H-reflex response (Zehr, 2002) even while at rest. Conversely, the tibialis anterior generally lacks strong afferent connections to the CNS and typically requires a background voluntary contraction to elicit such a central response (Burke, 2016; Zehr, 2002).

In addition to orthodromic propagation of action potentials along sensory axons towards the spinal cord and along efferent axons towards the muscle, during electrical stimulation action potentials can also propagate from the site of stimulation back towards the soma of the neuron

located in the spinal cord. This antidromic conduction of action potentials along motor axons increases with larger stimulation amplitudes (described in the subsequent section) and these action potentials travelling antidromically can interfere with and cancel out orthodromically-conducting action potentials travelling along reflexive pathways (Kandel et al., 1991). Consequently, at higher stimulation amplitudes, typically only M-waves are present with minimal to no elicitation of H-reflexes.

1.3 PARAMETERS OF NMES

Protocols of NMES consist of a combination of stimulation pulse and time parameters which can be manipulated according to the specific goals of the participant and task at hand (Gorgey & Dudley, 2008). The following section describes the specific parameters of stimulation amplitude, frequency, pulse duration, waveform and duty cycle. Along with each parameter, a brief description of how each of these parameters can affect torque production during electrically-evoked contractions is provided.

1.3.1 Stimulation Amplitude

Stimulation amplitude refers to the amount of current delivered through the stimulating electrodes and is typically measured in milliamperes (mA) (Bickel et al., 2011; Doucet, Lam, & Griffin, 2012). Peak current outputs from common stimulators used in clinical and research settings can vary extensively, but typically range between 100 to 1000 mA. In populations that are able to generate volitional contractions, stimulation amplitude is often reported as the current intensity required to produce a certain percentage of an individual's maximum voluntary contraction (MVC), and is therefore reported as % MVC. When utilizing relatively low simulation amplitudes, only a small portion of MUs are recruited, resulting in typically low

torque output. As the stimulation amplitude is gradually increased, however, more MUs are progressively recruited. Therefore, higher stimulation amplitudes facilitate the activation of more MU's and, thus, greater force output of the muscle (Adams et al., 1993; Bickel et al., 2011; Doucet et al., 2012; Mesin, Merlo, Merletti, & Orizio, 2010). This apparent linear relationship between stimulation amplitude and force output persists in both neurologically-intact and paralyzed muscle tissue until a stimulation amplitude is reached in which all axons are depolarized and no more additional torque can be generated.

Generally, higher stimulation amplitudes are required to produce more functional contractions such as standing, walking or cycling, and it has been suggested that obtaining maximal benefits from NMES regimes is contingent on production of relatively high contractile forces. For example, when stimulating the quadriceps femoris muscle group in a variety of populations, increases in neuromuscular strength were observed when stimulation amplitudes of approximately 30-100% MVC were employed (Currier & Mann, 1983; Delitto, Strube, Shulman, & Minor, 1992; Petterson et al., 2009; Selkowitz, 1985; Stackhouse et al., 2007). However, while higher stimulation amplitudes generate greater torque outputs leading to more functional muscle contractions, they may provide a number of disadvantages. First, while relatively low stimulation amplitudes evoke contractions via both peripheral and central pathways, higher stimulation amplitudes may result in more peripherally-mediated contractions. This occurs as the amount of antidromic collisions increase with higher amplitudes, thereby reducing the central contribution to the contraction (Doucet et al., 2012). In addition, higher stimulation amplitudes typically result in greater discomfort (Delitto et al., 1992; Lake, 1992; Maffiuletti, 2010) due to activation of nociceptors. This discomfort may limit the use of NMES particularly in individuals with full sensation, or with conditions such as hypersensitivity or reduced pain tolerance. Importantly, the

location of stimulation can affect participant discomfort and it has been demonstrated that stimulation over a nerve trunk can elicit a desired contraction amplitude with lower current and lower participant discomfort compared to simulation over a muscle belly (Wiest, Bergquist, & Collins, 2017b).

In the present thesis, a range of stimulation amplitudes will be utilized to determine how altering stimulation amplitude affects the amount of contraction fatigue (described in Section 1.5) of the ankle dorsiflexors during iNMES. Specifically, we selected three stimulation amplitudes to generate low (~5% MVC) to the largest tolerable (which we termed our MAX condition) contraction amplitudes. Due to inter-individual differences in tolerability of iNMES, we expected that initial contraction amplitudes (as a % MVC) achieved during the MAX condition would vary widely across participants.

1.3.2 Stimulation Frequency

Stimulation frequency refers to the number of pulses delivered per second and is reported as pulses per second (pps) or in Hertz (Hz) (Bickel et al., 2011). It is well established that a sigmoidal relationship exists between stimulation frequency and muscular force production in unfatigued muscle tissue, a phenomenon referred to as the force-frequency relationship (Kernell, 1995; Lee, Russ, & Binder-Macleod, 2009). This increased force production is attributable to enhanced release of Ca^{2+} from the sarcoplasmic reticulum during higher frequencies, leading to greater cross-bridge formation between actin and myosin and resulting in greater force generation. During NMES, stimulation frequencies must be high enough to elicit smooth contractions (Ragnarsson, 2008), thus, stimulation frequencies of 20-50 Hz are typically employed in order to achieve fused tetanus (Bickel et al., 2011; Doucet et al., 2012) where the

contracting tension of the muscle achieves a steady-state. In addition to achieving tetany, however, it has been demonstrated that these higher frequencies of NMES are requisite to produce functionally-relevant contractions and NMES frequencies of 50-100 Hz are recommended to maximize muscle tension (Doucet et al., 2012; Maffiuletti, 2010; Vanderthommen & Duchateau, 2007).

1.3.3 Pulse Duration

Pulse duration, also referred to as pulse width, refers to the time span for which a single stimulus pulse is delivered (Doucet et al., 2012). The role of pulse duration on torque production has received less attention in the literature, consequently, its specific contribution to NMES protocols are less well understood. Early work suggested pulse durations of 20 – 200 μs could achieve motor activation without evoking pain responses (Alon, Allin & Inbar, 1983; Gorgey & Dudley, 2008) and the majority of research to date has utilized pulse durations of equal to or less than 300 μs (Gorgey & Dudley, 2008). However, more recent research has suggested that longer pulse durations can evoke larger amounts of torque. For example, it has been demonstrated that 40% greater torque production can be achieved using pulse durations of 500 μs in comparison to pulse durations of 150 μs (Hultman, Sjöholm, Jäderholm-Ek, & Krynicki, 1983). Similarly, a pulse duration of 450 μs was shown to result in greater cross-sectional activation of the quadriceps femoris compared the activation during pulse widths of 150 μs (Gorgey, Mahoney, Kendall, & Dudley, 2006). In addition, when longer pulse durations are utilized (~ 670 μs), sensory axons are preferentially recruited, compared to motor axons which tend to be recruited with shorter pulse durations (~460 μs; Bergquist et al., 2011; Kiernan & Lin, 2012; Neyroud et

al., 2014). This phenomenon is attributable to a greater amount of persistent Na^+ channels and, thus, the lower rheobase present in sensory axons.

1.3.4 Stimulation Waveform

Pulses of stimulation can be monophasic (one phase either positive or negative; current flows in only one direction), biphasic (positive and negative phases; charge flows in both directions) or polyphasic (more than two phases; charge flows in multiple directions). Typically, biphasic waveforms are recommended to balance the charge administered and prevent electrochemical decomposition of the tissue (Ho et al., 2014; Ragnarsson, 2008). In addition, it has been demonstrated that greater torque can be generated when using monophasic and biphasic waveforms during isometric contractions in the quadriceps femoris group in comparison to polyphasic waveforms (Laufer, Ries, Leininger, & Alon, 2001). The shape of the waveform can also be varied extensively, however, most common waveform shapes include rectangular or square, triangular and sinusoidal.

1.3.5 Duty Cycle

The duty cycle during NMES refers to the time in which stimulation is on or off and is most commonly reported as a ratio of the stimulus on time to the stimulus off time, or as a percentage of the stimulus on time in comparison to the total time (Doucet et al., 2012; Packman-Braun, 1988). For example, if stimulation is on for 3 seconds and off for 6 seconds, a ratio of 1:2 or 67% would be reported. Standard duty cycles utilized in clinical applications typically involve a 1:3 ratio. Stimulation patterns utilizing duty cycles where stimulation is interspersed with rest

periods, often referred to as intermittent stimulation, is typically used to maintain force development while ensuring the comfort of its users (Doucet et al., 2012).

1.4 USES OF NMES IN CLINICAL POPULATIONS

The uses for NMES span widely and encompass a multitude of clinical and non-clinical populations. Briefly, in uninjured populations, NMES has been utilized to attenuate reductions in strength and to prevent muscle atrophy following periods of space flight (Duvoisin, Convertino, Buchanan, Gollnick, & Dudley, 1989; Mayr et al., 1999; Yoshimitsu et al., 2010) to increase strength and anerobic power in a variety of athletic populations (Babault, Cometti, Bernardin, Pousson, & Chatard, 2007; Gondin, Cozzone, & Bendahan, 2011; Maffiuletti, 2006; Maffiuletti et al., 2009; Martínez-López, Benito-Martínez, Hita-Contreras, Lara-Sánchez, & Martínez-Amat, 2012) after periods of immobilization or bed rest (Gibson, Smith, & Rennie, 1988), and in elderly populations, either alone or in combination with other modes of exercise, to retain lower limb strength and balance needed for activities of daily living (Amiridis, Arabatzi, Violaris, Stavropoulos, & Hatzitaki, 2005; de Oliveira Melo, Aragão, & Vaz, 2013). Within more clinical populations, NMES has been utilized in patients with cancer (Ryu et al., 2009), hemophilia (Querol, Gallach, Toca-Herrera, Gomis, & Gonzalez, 2006), urinary incontinence (Bø, Talseth, & Holme, 1999; Moore, Griffiths, & Hughton, 1999; Yamanishi et al., 1997) and patients with a variety of cardiac and respiratory disorders (Harris, LeMaitre, Mackenzie, Fox, & Denvir, 2003; Quittan et al., 2001; Roig & Reid, 2009). NMES has also been implemented subsequent to a variety of orthopedic surgical interventions including total knee (Bade & Stevens-Lapsley, 2012; Stevens-Lapsley, Balter, Wolfe, Eckhoff, & Kohrt, 2012) and hip (Gremeaux et al., 2008) arthroplasty, anterior cruciate ligament reconstruction (Fitzgerald, Piva, & Irrgang, 2003; Kim,

Croy, Hertel, & Saliba, 2010) and has also been used pre-operatively (i.e. "pre-rehabilitation") to improve outcomes following surgical intervention (Walls, McHugh, O'Gorman, Moyna, & O'Byrne, 2010). More recently, NMES has also been implemented into intensive care units in an attempt to reduce the drastic muscle mass loss associated with hospital stays within these units (Gruther et al., 2010). Moreover, NMES has been used to assist in recovery of wounds in patients with ulcers due to a variety of etiologies (Baker, Rubayi, Villar, & Demuth, 1996; Houghton et al., 2003) and prevent of pressure sores in sedentary or mobility-restricted populations.

Perhaps the most common use of NMES, however, involves rehabilitation following neuromuscular injury or disease including SCI or CVA, and would be the target application of the results of the present thesis. The following two sections provide an overview of SCI (1.4.1) and CVA (1.4.2) including the physiological outcomes of each neurological injury. Thereafter, a discussion of the typical uses of NMES within these populations is provided including a brief background of the potential physiological and functional benefits that may be garnered for individuals in each population. Although it is important to consider the many benefits of NMES in SCI and CVA populations, as will be outlined below, it is concurrently important to recognize that NMES is not appropriate for all populations. Indeed, a number of contraindications exist for NMES that include, but are not limited to, conditions such as hypersensitivity, autonomic dysreflexia, poor thermoregulation or pregnancy. In addition, NMES is not advised when individuals have implanted metal devices, poor skin quality or a skin condition (such as occurs during diabetes), and/or a cancerous tumor close to the site of stimulation. Individuals with severe low bone mineral density are also typically excluded from NMES-based programming

due to fracture risk. As such, clinicians implementing NMES-based programs in clinical populations must ensure programs are individualized to each participant.

1.4.1 Spinal Cord Injury (SCI)

1.4.1.1 Clinical Outcomes of SCI

Spinal cord injury (SCI), either traumatic or non-traumatic, is a devastating lesion of the nervous system, resulting in mild to severe neurological deficits and substantial decreases in physical functioning (Silva, Sousa, Reis, & Salgado, 2014). Following a SCI, individuals typically experience sensory and/or motor loss, with partial or full muscle paralysis of muscles below the level of the lesion. Concomitantly, rapid "disuse" muscle atrophy (i.e. loss of size and/or number of muscle fibres) occurs, particularly in the first year subsequent to injury, much of which is thought to result from lack of volitionally-induced contractions against gravity, along with changes in length and loading conditions (Baldi, Jackson, Moraille, & Mysiw, 1998; Gibbons et al., 2014; Gordon & Mao, 1994). A conversion from Type S to Type FF MUs also occurs, typically beginning 2-4 months post-injury, eventually leading to muscles being almost exclusively comprised of fast-fatigable fibres. In fact, Type S MUs have been shown to be almost entirely non-existent 2-11 years post injury in the tibialis anterior, soleus vastus medialis, and rectus femoris muscles (Castro, Apple, Staron, Campos, & Dudley, 1999). While these physiological changes lead to decrements in physical functioning and functional independence (Griffin et al., 2009), these physiological changes coupled with a substantially sedentary lifestyle can lead to a variety of issues including orthostatic hypotension and autonomic dysreflexria as well as a high risk of cardiovascular and metabolic diseases and obesity (Garshick et al., 2005;

Yekutiel, Brooks, Ohry, Yarom, & Carel, 1989). Not only does this pose important implications on number and length of hospitalization stays for individuals with SCI, it also inflicts a profound risk of all-cause mortality. In fact, the leading cause of death among individuals with a chronic SCI is cardiovascular disease and individuals with an SCI have a rate of death 2.3 times higher than individuals without a SCI (Kocina, 1997).

1.4.1.2 NMES for Individuals with SCI

Physical activity and exercise may assist with mitigating the physiological, fitness and quality of life decrements following SCI, while potentially promoting beneficial synaptic plasticity of the brain and spinal cord following injury (Ragnarsson, 2008; Vaynman & Gomez-Pinilla, 2005; Ying, Roy, Edgerton, & Gómez-Pinilla, 2005). It is presently recommended that individuals with a SCI participate in at least 20 minutes of aerobic exercise at a moderate to vigorous intensity alongside resistance training (3 sets of 8-10 repetitions) at least two times per week (Ginis et al., 2011). However, given the muscle paralysis following SCI, involvement in exercise-based programs can be at times, impossible (Nash, 2005). In addition, as most SCIs involve paralysis of the lower limbs which constitute the larger proportion of muscle mass compared to the upper limbs, achieving the aerobic training stimulus sufficient to incur cardiovascular benefits can be impossible (Faghri, Glaser, & Figoni, 1992; Gibbons, Stock, Andrews, Gall, & Shave, 2016; Nash, 2005).

One method to enable exercise in paralyzed muscle is to evoke muscle contractions via NMES. For individuals with SCI, NMES is typically used to evoke functional contractions (i.e. termed FES) requisite for standing, walking, rowing and cycling but can also be used in conjunction with upper body volitional movements, in what is often called hybrid-FES (Gibbons

et al., 2016; Wheeler et al., 2002). FES has been demonstrated to evoke increases in cross sectional area (i.e. muscle hypertrophy) of a variety of leg musculature following FES-cycling (Scremin et al., 1999), resisted knee extension exercise (Mahoney et al., 2005), or a combination of both (Pacy et al., 1988) in individuals with complete and incomplete SCI. Notably, the greatest improvements in hypertrophy were found in muscles located in closest proximity to the stimulating electrodes (Scremin et al., 1999). Alongside to promotion of muscle mass, FES-based programming has been shown to prevent disuse atrophy, particularly if integrated into rehabilitation programs early after injury (Baldi et al., 1998). In addition to mitigating muscle mass loss, NMES has also been shown to reverse the conversion of type I muscle fibres to type II fibres within the quadriceps muscle group using muscle biopsies and intramuscular myosin heavy chain isoform content (Andersen, Mohr, Biering-Sørensen, Galbo, & Kjaer, 1996; Mohr et al., 1997) and, accordingly, may reduce some of the rapid muscle fatigue that occurs following SCI due to fibre-type conversion (Ragnarsson, 2008).

Although the neuromuscular benefits of NMES are marked, NMES has also been demonstrated to impose a variety of benefits in the skeletal system. FES rowing, in particular, has shown promise in attenuating bone loss following SCI, even in individuals with chronic SCI (Gibbons et al., 2014; Wheeler et al., 2002). Further, NMES has been shown to elicit a number of other multi-system benefits in this population including prevention (Regan et al., 2009) and facilitated healing of pressure ulcers (Regan et al., 2009; Houghton et al., 2010), as well as reduction of muscle spasticity (Krause et al., 2008; Carty et al., 2013). Moreover, cardiovascular and metabolic benefits of NMES training include improved venous return and increased arterial diameter (Gerrits et al., 2001), positive cardiac remodeling (Gibbons et al., 2016) and myocardial function (Wheeler et al., 1995), stabilization of heart rate and increased blood pressure (Faghri et

al., 1992; Sampson et al., 2000), and improved glucose tolerance (Griffin et al., 2009). Finally, NMES-based programs may improve sensory function, as assessed by ASIA scores, in the lower extremity (Griffin et al., 2009).

1.4.2 Stroke (CVA)

1.4.2.1 Clinical Outcomes of Stroke

A cerebral vascular accident (CVA), most commonly referred to as a stroke, involves the death of brain cells due to hypoxia as a result of either a blocked or ruptured cerebral artery. At present, strokes are considered the most common route to disability in developed nations (Ada, Dorsch, & Canning, 2006; Pollock et al., 2013; Warlow et al., 2008). Although impairment following a stroke is dependent on the area of the brain affected, motor deficits have been demonstrated to be the primary impairment following a stroke, with approximately ~70% of individuals experiencing deficits in motor function of the lower limb across stroke types. Importantly, approximately 20% of individuals will experience foot-drop subsequent to the injury (Everaert, Thompson, Chong, & Stein, 2010), which is typically characterized by an inability to dorsiflex the ankle, therefore, hindering toe clearance during the swing phase of gait (Kottink et al., 2004). This foot-drop can be compounded further by spasticity of the plantar flexors that commonly occurs following stroke (Burridge, Wood, Taylor, & McLellan, 2001; Embrey, Holtz, Alon, Brandsma, & McCoy, 2010; Lundström, Smits, Terént, & Borg, 2010; C. Stein, Fritsch, Robinson, Sbruzzi, & Plentz, 2015), and can lead to a variety of compensation patterns including hip hitching and hip circumduction, toe drag as well as decreased walking speed and an increased risk for falls (Kottink et al., 2004). These altered gait patterns can collectively lead to gait asymmetry and increased energy costs of walking, leading to an

impaired ability to walk far distances and participate in normal daily function (Stein et al., 2008; Cheng et al., 2010; Awad et al., 2016; Auchstaetter et al., 2016).

1.4.2.2 NMES for Individuals with Stroke

In order to combat the effects of foot drop, NMES devices are commonly utilized among individuals with a hemiparetic stroke. Specifically, foot drop stimulators, or NMES of the common peroneal nerve, involves appropriate-timed stimulation using a tilt accelerometer to elicit dorsiflexion during the swing phase of gait (Everaert et al., 2010; van Swigchem, van Duijnhoven, den Boer, Geurts, & Weerdesteyn, 2012). Some current models of foot drop stimulators utilized following stroke include the WalkAide, Odstock Dropped Foot Stimulator and the NESS L300, all of which are approved by the FDA (Sheffler & Chae, 2007; Stein et al., 2008).

To date, NMES over the common peroneal nerve has been demonstrated to elicit both orthotic and therapeutic improvements in gait speed (Kottink et al., 2004; Taylor et al., 1999; Robbins et al., 2006) and improve gait symmetry (Cheung et al., 2010) and decreased energy costs associated with walking (Awad et al., 2016). NMES may further improve balance during walking, particularly when it is repeatedly administered in a standing position versus supine (Kim et al., 2012). Moreover, NMES can improve volitional strength of the ankle dorsiflexors, and has even been shown to improve strength by over 75% following only 12-weeks of use. More recently, increases in strength have also been documented with NMES used in tandem with unstable surfaces, including standing on a rocker-board (Cheung et al., 2010) and these improvements were superior to those obtained with a traditional physiotherapy-based rehabilitation program. Concomitant to increases in strength of the ankle dorsiflexors, NMES has

been shown to increase range of motion of the ankle (Mesci et al., 2009) as assessed by goniometer measurements, as well as attenuate spasticity of the plantar flexor muscles (Sabut, Sikdar, Kumar, & Mahadevappa, 2011).

1.5 NEUROMUSCULAR FATIGUE DURING NMES

Despite the benefits of NMES among individuals with SCI and stroke, its benefits can be attenuated significantly due to a variety of limitations associated with NMES. For example, NMES can be uncomfortable and even painful for those individuals with partial or fully intact sensation (Chae & Hart, 1998; Delitto et al., 1992; Maffiuletti, 2010). In addition, NMES in laboratory settings is typically performed at set joint angles, therefore the translatability of these isometric contractions to functional movements may be limited (Maffiuletti, 2010). Finally, widespread implementation of NMES necessitates specialized equipment and exercise machines and expertise that is often associated with relatively high economic costs, rendering NMES inaccessible for many.

However, the main limitations associated with NMES and the primary focus of the present thesis, is the rapid contraction fatigue that develops during its use (Gondin et al., 2011). This fatigue manifests as a decline in torque with repeated contractions (Enoka & Duchateau, 2008) and is predominantly attributable to the "non-natural" or non-physiologically way in which MUs are recruited and discharge during NMES in comparison to volitional contractions. Although fatigue occurs during repeated electrically-evoked contractions of healthy, neurologically intact muscle, fatigue is more pronounced in individuals following a SCI such that the decline in torque far exceeds the decline observed in uninjured muscle tissue for the same intensity of stimulation (De Luca & Hostage, 2010; Pelletier & Hicks, 2011) which may be

explained by poor muscle quality and significant muscle atrophy, diminished perfusion of the muscle and the conversion of type I fibres to type II fibres (described in Section 1.4.1). This pronounced fatigue attenuates the effectiveness of NMES and hinders exercise of a prolonged duration, thereby decreasing the attainment of neuromuscular, cardiovascular and metabolic benefits and individuals' abilities to meet exercise guidelines.

The following two sections describe the strikingly different ways in which MUs are recruited and discharge during voluntary (1.5.1) and electrically-evoked contractions (1.5.2). This contrast is done to highlight the relatively simple behavior of MUs during NMES compared to the complex activity of MUs during volitional contractions and, therefore, emphasize the many aspects inherent to NMES that contribute to rapid fatigue during electrically-evoked contractions. Section 1.5.3 describes the various locations along the site of stimulation deep within the muscle belly that may contribute to fatigue.

1.5.1 MU Recruitment and Discharge During Voluntary Contractions

Although most muscular contractions exhibit fatigue, embedded in the neuromuscular system are a variety of strategies to mitigate fatigue during volitional contractions. Voluntary or volitional contractions are initiated primarily from the primary motor cortex (M1), a strip of cortex anterior to the central gyrus in the frontal lobe of the human brain (Kandel et al., 1991). The primary motor cortex is somatotopically organized such that specific regions of the motor cortex influence activity of particular muscle groups in the trunk and limbs. Axons from pyramidal cells (located in layer 5 of the cerebral cortex) project to cells of the corticospinal tract which then descend to the spinal cord (Kandel et al., 1991). Approximately 90% of corticospinal fibers decussate at the medulla, while the remaining 10% descend ipsilaterally. Once at the spinal

cord, corticospinal fibers project directly onto motoneurons or onto interneurons within the ventral horn.

During submaximal voluntary contractions, MUs are recruited in a specific orderly manner, known as Henneman's size principle, where activation of small (i.e. slow twitch) MUs are recruited first followed progressively by larger-diameter (i.e. FR and FF) MUs. This recruitment strategy is based on the proportional relationship between the membrane potential of the soma of a motoneuron and its input resistance, as described by Ohm's Law (Enoka, 2002). As Type S motoneurons have comparatively greater input resistances than their fast-twitch counterparts, Type S motoneurons achieve threshold for depolarization with lesser synaptic currents, and are, therefore, recruited earlier (Enoka, 2002). Importantly, recruiting MU's according to Henneman's size principle effectively ensures correct force output for a given task and preserves the most fatigable MUs for contractions requiring larger forces, thereby reducing neuromuscular fatigue during contractions.

Once recruited, instantaneous firing rates of MUs rise steeply and then plateau at a steady-state "optimal" frequency for a given contraction amplitude, typically within 0.4 – 3 s following recruitment (Allen, Lamb & Westerblad, 2008). Although MUs from various muscles tend to fire at similar average rates upon recruitment (6-12 Hz), mean MU firing rates during submaximal to maximal voluntary contractions can vary extensively across the lower limb musculature (Graham, Rice, & Dalton, 2016). For example, during low contraction amplitudes (i.e. ~ 25% MVC) MUs have been demonstrated to fire at 7-8 Hz in the soleus (Dalton, Harwood, Davidson, & Rice, 2009), ~ 9-15 Hz in the medial and lateral gastrocnemius (Graham et al., 2016; Kirk & Rice, 2017), ~ 15 Hz in the tibialis anterior and the quadriceps femoris (De Luca & Hostage, 2010; Roos, Rice, Connelly, & Vandervoort, 1999) and ~12-15 Hz in the

hamstrings (Kirk & Rice, 2017). During more moderate contractions (~ 50% MVC) MU's typically increase their firing rates to ~ 12 Hz in the soleus (Dalton et al., 2009), 11 – 13 Hz in the medial and lateral gastrocnemius (Graham et al., 2016; Kirk & Rice, 2017), 15-20 Hz in the tibialis anterior (Christie & Kamen, 2009; De Luca & Hostage, 2010), 15-21 Hz in the quadriceps (Kamen & Knight, 2004; Roos, Rice, Connelly & Vandervoort, 1999; Stock & Thompson, 2014) and ~ 16-23 Hz in the hamstrings (Kirk & Rice, 2017). During high to maximal contraction amplitudes (i.e. 100% MVC) MUs have been demonstrated to fire at ~ 16.5 Hz in the soleus (Dalton et al., 2009) ~ 23 Hz in the gastrocnemius (Graham et al., 2016), ~ 20-42 Hz in the tibialis anterior (Bigland-Ritchie, Furbush, Gandevia, & Thomas, 1992; Connelly, Rice, Roos, & Vandervoort, 1999; De Luca & Hostage, 2010; Rubinstein & Kamen, 2005), ~ 20-25 Hz in the quadriceps femoris (Kamen & Knight, 2004; Roos et al., 1999), and 25-31 Hz in the hamstrings (Kirk & Rice, 2017). Of note, even at the highest contraction amplitudes (i.e. 100% MVC) mean firing rates typically do not exceed 20-40 Hz.

While the above description provides a range of average MU discharge rates, individual MU behavior during volitional contractions can exhibit variations in discharge rates and firing patterns. For one, individual MUs have been demonstrated to discharge with variable inter-spike intervals, with coefficients of variation ranging between 6-33%. In doing so, individual MU discharge is asynchronous with respect to other MUs, permitting the occurrence of smooth, fused contractions even during low mean firing rates of MUs. In addition, during voluntary contractions it has been postulated that MUs with higher thresholds are recruited to replace previously active low-threshold MUs (Bawa & Murnaghan, 2009) and this phenomenon has been termed MU substitution (Person, 1974) or MU rotation (Sale, 1987). While this type of MU behavior has been specifically witnessed during postural changes (Person 1974) and prolonged

contractions (Westergaard & De Luca), replacement of fatigued MUs with "fresh" MUs may allow for recovery of fatigued MUs across a range of other contraction types. In tandem to replacement of fatigued MUs, individual MUs firing rates have been demonstrated to decrease during sustained contractions. This process likely occurs to enable achievement of tetanic forces at the lowest possible MU firing rates, lending the name "muscle wisdom" (Allen, Lamb & Westerblad, 2008). Finally, MUs have been demonstrated to discharge irregularly either two (i.e. doublet) or three (i.e. triplet) times in rapid succession. These doublets and triplets are particularly evident during contractions of a prolonged duration and therefore, may be used as a strategy to augment torque production during fatiguing contractions. Specifically, these doublets and triplets are thought to take advantage of the "catch-like" property of the muscle which leads to enhanced Ca^{2+} release from the SR, and thus, greater tension development of the contractile elements.

1.5.2 MU Recruitment and Discharge During NMES-evoked Contractions

During NMES, the way in which MUs are recruited and discharge only crudely mimics MU behavior during volitional contractions. For example, as described in Section 1.2.2.3, during NMES, MUs are recruited depending on their location and orientation in relation to the stimulating electrode and not on MU type (Gregory & Bickel, 2005; Neyroud et al., 2014). This means that even at low contraction amplitudes, MUs that exhibit greater rates of fatigue (i.e. Type FF and FR) are recruited, countering the largely fatigue-resistant MU recruitment of volitional contractions of equal magnitude (Neyroud et al., 2014). In addition to recruitment of less fatigue-resistant MUs, electrically-evoked contractions elicit repeated activation of the same subpopulation of MUs and discharge of these MUs is "time-locked" to each stimulus pulse, such

that activity of all activated MUs is largely temporally synchronous. Although it is possible that MUs do not fire with every single pulse and/or that MU rotational activity takes place as occurs during volitional contractions, the extent to which this occurs during NMES has not been fully investigated.

The assumed synchronicity of MU firing during NMES is problematic given that it greatly counters the "asynchronous" discharge during volitional contractions which is thought to enable fused contractions despite low average MU discharge rates. Consequently, higher stimulation frequencies are required to enable fused contractions of sufficient amplitude during NMES (Neyroud et al., 2014). Typically, muscle tetany is achieved using frequencies of at least 15-20 Hz during electrically-evoked contractions, and therefore, stimulation frequencies used for NMES protocols usually range between 20-50 Hz even for contractions of a low amplitude (Doucet et al., 2012; Neyroud et al., 2014). These high discharge rates relative to those that occur during voluntary contractions are problematic given that greater stimulation frequencies have been shown to elicit a greater magnitude of fatigue during NMES, thus, rendering the contraction with a greater propensity for fatigue.

The type of NMES used in the present thesis, iNMES, was designed with the specific goal of reducing MU discharge rates while maintaining contractions of appropriate amplitudes. By dividing stimulation over two locations, iNMES is speculated to reduce individual MU firing rates by approximately half the firing rates that would occur during stimulation over a single stimulation site, as has been done conventionally during nNMES or mNMES. In doing so, iNMES may pose a promising means to reduce some of the excessive contraction fatigue associated with electrical stimulation.

1.5.3 Mechanisms of Fatigue During NMES

While differences in MU recruitment and discharge behavior help explain the susceptibility of NMES-evoked contractions to rapid fatigue, it is important to understand the main mechanisms contributing to this fatigue during electrically-evoked contractions. Generally, impairments in excitation-contraction coupling considered to be one of the main contributors to the contraction fatigue that develops during electrical stimulation. However, it is important to consider that many factors contribute to EC coupling and, thus, during NMES, a myriad of locations from the site of stimulation at the nerve axon to regions deep within the muscle belly may contribute to fatigue (Westerblad & Allen, 2009). Briefly, during NMES, fatigue may potentially develop due to decreased excitability of the nerve axon, depletion of substrate at the neuromuscular junction or due to the failure of the action potential along the sarcolemma. Thereafter, fatigue may develop due to failure of transmission along the T-tubule and or impaired release of Ca^{2+} from the SR. The following paragraphs of this section provide an overview of these many different mechanisms

Although it has been demonstrated consistently for over three decades that subsequent to repeated pulses or trains of NMES, the membrane potential of axons may decrease in excitability (i.e. hyperpolarize), it is currently unclear whether this reduced excitability results in fatigue during NMES. Specifically, changes in the excitability of the membrane potential of nerve axons may develop during NMES due to activation of slow K^+ conductances or, more likely in animals, due to an inability of the Na^+-K^+ pump to maintain ionic balance (Bostock & Grafe, 1985; Gasser, 1935; Kiernan, Lin, & Burke, 2004; Kiernan, Mogyoros, & Burke, 1996; Matkowski, Lepers, & Martin, 2015). Specifically, the Na^+-K^+ pump exchanges three Na^+ ions for one K^+, resulting in an ionic imbalance and, ultimately, driving the membrane potential more negative

and farther away from threshold (Kiernan et al., 2004). Accordingly, this phenomenon has also been referred to as activity-dependent axonal hyperpolarization and has been demonstrated to occur in both sensory and motor axons, particularly under greater impulse loads such as during higher MU discharge rates and longer contraction durations (Kiernan et al., 2004; Vagg, Mogyoros, Kiernan, & Burke, 1998). When an axon undergoes hyperpolarization, greater current would need to be introduced for the membrane potential to reach threshold. However, because most NMES protocols consist of a set stimulation intensity, axons exhibiting more negative membrane potentials would be less likely to reach their threshold for depolarization, rendering these axons inactive during repeated contractions when appropriate adjustment of current throughout the duration of a NMES session is not conducted. The "drop out" of these axons would then lead to lesser torque output and, therefore, potentially greater fatigue during NMES.

In addition to reduced axonal excitability, repeated NMES contractions may fatigue as a result of depletion of acetylcholine at the neuromuscular junction (Jones, Bigland-Ritchie & Edwards, 1979). Although early work remains somewhat inconclusive, Potter (1970) utilized the phrenic nerve and diaphragm muscle to demonstrate no change in acetylcholine stores were present following 5 min of stimulation at 20 Hz. In contrast to these results a 25% decline in acetylcholine following 30 min of stimulation *in vivo* at 20 Hz in cat leg musculature was demonstrated (MacIntosh, 1963). Importantly, it has been suggested that depletion of transmitter may be a more significant contributor to fatigue during use of higher stimulation frequencies, as are normally applied during NMES protocols (MacIntosh & Collier, 1976). Thus, although not directly shown in humans, depletion of acetylcholine at the neuromuscular junction may prevent transmission of action potentials past the synaptic cleft. Moreover, distal to the neuromuscular junction, fatigue may develop due to impairments in transmission along the sarcolemma (Jones,

1979). Specifically, repeated activation of the Na^+-K^+ pump is thought to lead to an ionic imbalance, whereby K^+ ions accumulate and Na^+ ions are depleted within the extracellular space (Jones et al., 1979; Jones et al., 1996). In doing so, this ionic imbalance may hinder transmission of action potentials from the motor end plate to the T-tubule, thereby blocking impulses from propagating deep within the muscle belly.

Although a number of ionic factors, including diminished action potential propagation down the T-tubule and decreased troponin sensitivity have been investigated as potential mechanisms of fatigue deep within the muscle (Westerblad et al., 1993; Jones, 1996; Keeton & Binder-Macleod, 2006), mechanisms of fatigue located within the muscle appear to be primarily attributable to decreased release of Ca^{2+} from the sarcoplasmic reticulum (Jones, 1996; Chin et al. 1996; Keeton & Binder-Macleod, 2006). Because the relationship between interstitial Ca^{2+} and muscle tension is thought to be sigmoidal, in the steep part of the curve (i.e. at lower frequencies) small decrements in Ca^{2+} release can result in large decreases in torque (Westerblad et al., 1993; Keeton & Binder-Macleod, 2006). While the exact mechanisms of the decreased Ca^{2+} release have yet to be fully elucidated, a number of factors have been theorized to play a role in this form of fatigue to date. One hypothesis suggests that with repeated contractions, Ca^{2+} may remain in the intracellular space of the sarcoplasmic reticulum longer, and this elevated intracellular Ca^{2+} is known to inhibit release of Ca^{2+} (Keeton & Binder-Macleod, 2006). A second hypothesis proposes that a precipitate forms within the SR due to binding of Ca^{2+} to accumulated inorganic phosphate that is transported into the sarcoplasmic reticulum, leaving the lumen of the sarcoplasmic reticulum with less free Ca^{2+} to release (Keeton & Binder-Macleod, 2006).

Concomitant to lack of Ca^{2+} release, it has been suggested that structural damage to the muscle fibre itself may occur, (Jones, 1996; Keeton & Binder-Macleod, 2006). Some authors have suggested a redistribution of sarcomere lengths may occur during these types of contractions where the sarcomeres in the center of the muscle fibre become lengthened, while the sarcomeres at the end become shortened (Jones, 1996). When this occurs, the center portions produce minimal force, while the end sarcomeres determine the force produced by the muscle. As the sarcomeres are not in their ideal length according to the length-tension relationship, redistribution of sarcomere lengths can then lead to lower forces obtained for a given stimulation frequency, or in other words, a rightward shift of the length-tension relationship.

1.6 INTERLEAVED NMES AND MU OVERLAP ESTIMATIONS

As a strategy to reduce fatigability during NMES, by addressing the specific issue of unnaturally high MU discharge rates during conventional NMES, our lab developed interleaved NMES (iNMES; Lou et al., 2016a). iNMES involves a combination of nNMES and mNMES, wherein stimulation pulses are delivered to the two stimulation sites in an alternated fashion. The rationale for iNMES stems from a body of work demonstrating recruitment of different populations of MUs when stimulation is placed over a nerve versus over a muscle belly using fine wire EMG (Okuma et al., 2013; described in greater detail in Section 1.2.2.3.2). Briefly, when stimulation is placed over a muscle belly, those MUs closest to the surface of the skin (i.e. superficial MUs) are activated at lower stimulation amplitudes, and as stimulation intensity is increased, MUs located progressively deeper within the muscle are recruited. Conversely, when stimulation is placed over a nerve trunk, MUs distributed throughout the muscle are activated, independent of stimulation amplitude.

One indirect method to estimate the relative proportion of MUs recruited at multiple stimulation locations involves comparing the amount of torque produced at each stimulation site when stimulation is delivered separately and together, and is often referred to as MU overlap. Initially, methodology for estimating percent MU overlap was developed to determine the selectively of the MU subpopulations recruited within a given muscle when using implanted multi-electrode arrays and were conducted in the common peroneal nerve of the rat (Rutten, van Wier, & Put, 1991), the tibial (Yoshida & Horch, 1993) and sciatic (Branner, Stein, & Normann, 2001; Mcdonnall, Clark, & Normann, 2004) nerves of the cat, and have also been completed using implanted nerve cuff electrodes over the femoral nerve in humans with SCI (Fisher, Tyler, & Triolo, 2013). These percent MU overlap methods involve a comparison of the sum of the force produced when stimulation is sent through individual electrodes independently, to the evoked force when stimulation is sent through multiple electrodes simultaneously, at various stimulation amplitudes. In this way, 0% MU overlap would be indicative of recruitment of completely independent subpopulations of MUs by each electrode. Conversely, 100% MU overlap would indicate the same subpopulation of MUs was recruited by each electrode (Mcdonnall et al., 2004). However, these methods are invasive and require extensive expertise for insertion and operation of electrode arrays. In addition, estimating overlap with these methods is highly time consuming and is not feasible for most research in human participants.

Recently, a method to estimate percent MU overlap non-invasively was developed utilizing NMES placed transcutaneoulsy (Wiest et al., 2017a). Briefly, pulses of stimulation (pulse duration = 100 μs) were delivered transcutaneously over the tibialis anterior muscle belly and common peroneal nerve separately and simultaneously (the pulse of nNMES was delivered 2.8 ± 0.8 ms prior to the pulse of mNMES to ensure the signals arrived at the muscle at the same

time) to estimate the amount of MU overlap at a range of stimulation amplitudes (10, 20, 30, 40, 50, 60, 70, 80, 90, 100% peak twitch torque; PTT). Findings from this study indicated that the least amount of overlap (~5%) was generated at 10% PTT. Thereafter, MU overlap progressively increased with increasing intensities, however, no significant difference in MU overlap (~ 72%) was found between intensities ranging from 50-100% PTT (Figure 1-1). This study therefore, supports the idea that higher stimulation intensities (to a point) lead to greater MU overlap in the tibialis anterior. Importantly, however, this study used a second-order polynomial interpolation technique for its measures, and therefore, did not directly measure the magnitude of MU overlap at all contraction amplitudes utilized.

Although it is assumed that this greater percent overlap results in more MUs firing at higher rates than those MUs recruited at only one site (nerve or muscle) the examination of the functional outcomes of this greater percent MU overlap has not been investigated fully. Mcdonnall et al. (2004) demonstrated that when stimulation was placed directly over the cat sciatic nerve, electrode pairs with greater overlap were demonstrated to exhibit greater torque than electrode pairs with lesser overlap. However, as it has been established that MUs may be recruited differently when stimulation is placed directly over a nerve compared to when stimulation is delivered over the surface of the skin, the results of the aforementioned study may not be applicable during delivery of transcutaneous NMES as is more commonly conducted in rehabilitation. Therefore, this thesis aims to determine whether the amount of MU overlap is related to the amount of fatigue that occurs during contractions generated via NMES.

Previously, a study conducted in the ankle dorsiflexors of individuals without neurological impairment demonstrated that iNMES reduced fatigue during a 12-minute fatigue protocol (240 contractions) at 10-15% MVC compared to nNMES and mNMES delivered alone

(Figure 1-2, Panel A). Specifically, it was found that although torque decreased from its initial value at baseline by ~ 58% during nNMES (squares) and ~ 67% during mNMES (circles), torque only decreased by ~ 39% during iNMES (triangles). Concurrently, the first significant decrease in torque (from the torque produced at baseline) occurred after only 1 minute during nNMES and mNMES (as denoted by the dagger), but occurred considerably later at 3 minutes into the fatigue protocol, during iNMES (denoted by the double dagger). A second study involving individuals with SCI evaluated the amount of fatigue during iNMES with previously collected nNMES and mNMES data. Data for this study is reported in Panel B of Figure 1-2. This study demonstrated again that iNMES (grey bar) mitigated fatigue compared to mNMES alone (black bar). However, iNMES did not affect torque output differently than nNMES (white bars). The authors speculated that the attenuated fatigue during nNMES was due to greater central contributions (i.e. H-reflexes) to the evoked contractions, while the attenuated fatigue during iNMES was likely due to decreases in MU firing rates. However, while these studies display promise for utilizing iNMES in reducing fatigue, neither study explored the mechanisms behind the diminished fatigue during iNMES and could only speculate iNMES reduced MU firing rates.

Although these studies demonstrate the ability for iNMES to reduce fatigue compared to more conventional methods of NMES, in particular mNMES, at low stimulation amplitudes, neither study examined the effect of iNMES on fatigue at different stimulation amplitudes. Moreover, these studies did not directly examine the mechanism(s) responsible for this reduced fatigue during iNMES and could only speculate it was attributable to reduced firing rates, as no measure of MU overlap was quantified. These gaps limit our current understanding of how torque is produced with consecutive contractions elicited by iNMES. Thus, before recommendations for clinical implementation of iNMES can be made, an understanding of how

iNMES delivered at a range of contraction amplitudes affects the magnitude of MU overlap and fatigue during repeated contractions is essential.

1.7 THESIS OUTLINE

The main objective of this thesis was to compare contraction fatigue of the ankle dorsiflexors when iNMES was delivered to produce contractions over a range of amplitudes. We also examined several other measures of fatigue to gain a more complete understanding of how torque declines when iNMES is used to produce contractions of different amplitudes. We hypothesized that there would be more contraction fatigue, defined as the relative decline in torque from the beginning to end of the fatigue protocol, for large than for small contractions. We anticipated that large contractions would fatigue more than small contractions because progressively more MUs would be recruited by both the common peroneal and tibialis anterior muscle belly stimulation sites (i.e. greater MU overlap) as contraction amplitude increased. Therefore, we also hypothesized that there would be a significant, negative correlation between contraction fatigue and our measure of MU overlap, whereby more MU overlap would be associated with a greater decline in torque. This experiment was conducted in accordance with the goal of reducing the rapid fatigue associated with electrically-evoked contractions for individuals with neurological impairment.

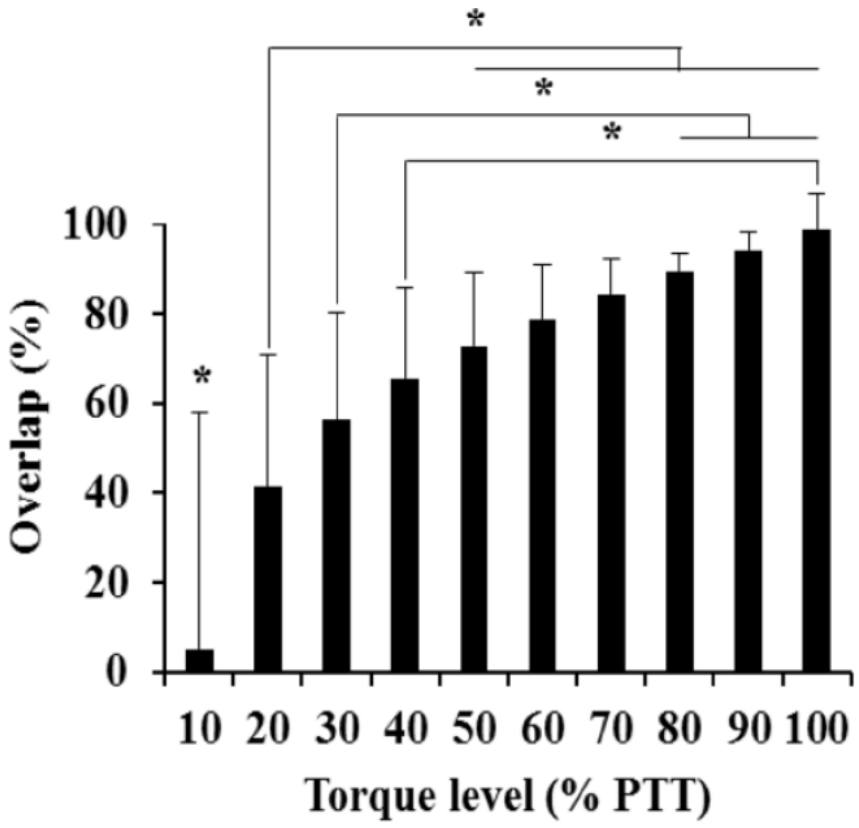

Figure 1-1. Motor unit (MU) recruitment overlap across a full range of stimulation amplitudes across participants. Each bar represents the estimated percent overlap (%). The cross over the 10% PTT bar indicates significant difference from all other torque levels. *($p<0.05$). *Adapted from Wiest et al. (2017a).*

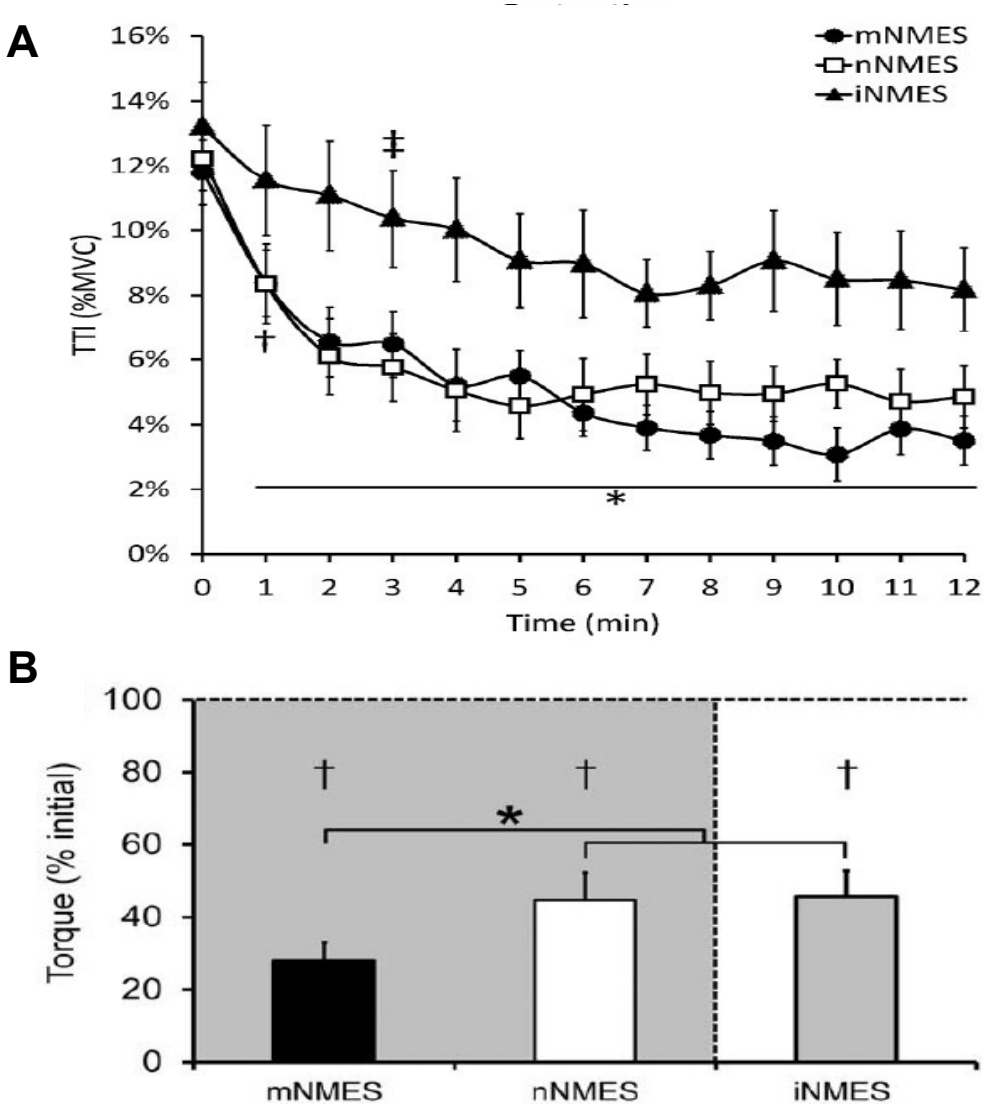

Figure 1-2. Fatigue during iNMES compared to nNMES and mNMES delivered alone. **Panel A.** Average torque-time-integrals (TTIs) as a % MVC for 13 data bins (240 contractions) across 10 neurologically-intact participants during mNMES (filled circles), nNMES (open squares) and iNMES (filled triangles) of the ankle dorsiflexors. The first significant decrease in TTI from the initial 5 trains (Time 0) is represented by the dagger (†) for mNMES and nNMES and by the double dagger (‡) for iNMES. The asterisk (*) indicates significant differences between iNMES and both mNMES and nNMES. *Adapted from Lou et al. (2016).* **Panel B**. Average percent decline in torque from the beginning to the end of each 75-contraction fatigue protocol during mNMES (triceps surae muscle belly; black bar; previously collected data as denoted by the shaded box), nNMES (tibial nerve; white bar; previously collected data as denoted by the shaded box) and iNMES (grey bar; presently collected data) of the ankle plantar flexors in 8 participants with a spinal cord injury. The asterisk (*) denotes significant differences between NMES types while the dagger (†) represents significant differences from initial (i.e., 100%; horizontally dashed lines). *Adapted from Bergquist et al. (2017)*. Error bars in both panels represent one standard error.

CHAPTER 2: CONTRACTION FATIGUE AND MOTOR UNIT OVERLAP IN THE TIBIALIS ANTERIOR DURING DIFFERENT INTENSITIES OF INTERLEAVED ELECTRICAL STIMULATION

2.1 INTRODUCTION

Neuromuscular electrical simulation (NMES) is used in rehabilitation to evoke contractions of paralyzed muscles. In doing so, NMES can help restore motor function and reduce secondary complications following neuromuscular injury or disease. Most commonly, NMES is delivered transcutaneously, either over a muscle belly (mNMES) or over a nerve trunk (nNMES). However, one major limitation of NMES when delivered in these ways is contraction fatigue, which manifests as a decline in torque over repeated contractions (Enoka & Duchateau, 2008; Gregory, Dixon, & Bickel, 2007; Kesar & Binder-Macleod, 2006). Much of this fatigue is attributable to the non-physiological way in which motor units (MUs) are recruited and discharge during NMES. For example, during NMES the same subset of MUs discharge synchronously at a latency time-locked to each stimulus pulse, which contrasts with the asynchronous MU discharge that occurs during voluntary contractions. Consequently, high NMES frequencies are required to achieve fused contractions of sufficient amplitude. These high NMES frequencies result in non-physiologically high MU discharge frequencies which contribute prominently to contraction fatigue during NMES.

High MU discharge frequencies during NMES are problematic as they increase the metabolic cost per contraction, augment inorganic phosphate accumulation, and affect both intramuscular pH and Ca^{2+} concentrations (Gorgey, Black, Elder, & Dudley, 2009; Gregory et al., 2007; Russ, Elliott, Vandenborne, Walter, & Binder-Macleod, 2002; Russ, Vandenborne, & Binder-Macleod, 2002). In addition, as stimulation frequency increases, the ability to depolarize

motor axons under the stimulating electrodes decreases, due to activity-dependent decreases in axonal excitability (Kiernan et al., 2004; Luu, Jones & Collins, *unpublished*). Decreased axonal excitability contributes to contraction fatigue when these axons "drop out" and the muscle fibres they innervate no longer produce force. Collectively, these mechanisms account for the relationship between NMES frequency and fatigue, whereby high NMES frequencies and their correspondingly high MU discharge rates, result in more contraction fatigue (Bigland-Ritchie, Jones, & Woods, 1979; Garland, Garner, & McComas, 1988; Gorgey et al., 2009; Gregory et al., 2007; Kesar & Binder-Macleod, 2006). Contraction fatigue reduces the intensity and duration of NMES-based programs, thereby limiting the physiological benefits of NMES (Binder-Macleod & Scott, 2001; Kesar, Chou, & Binder-Macleod, 2008; Maffiuletti, 2010)

With the goal of reducing contraction fatigue by minimizing MU firing rates, interleaved (iNMES) was developed to stimulate the muscles that dorsiflex the ankle (Lou et al., 2016). iNMES involves alternating, or "interleaving," stimulus pulses between the common peroneal nerve trunk and the tibialis anterior muscle belly. The rationale for iNMES is that stimulation over the muscle belly and nerve trunk can recruit distinct populations of MUs. At low stimulation amplitudes, NMES delivered over the tibialis anterior muscle belly recruits MUs located superficially (Maffiuletti, 2010; Mesin et al., 2010; Okuma et al., 2013). In contrast, NMES over the common peroneal nerve trunk recruits MUs distributed throughout the muscle (Okuma et al., 2013). iNMES exploits these differences in the spatial distribution of MUs recruited by the nNMES and mNMES sites, to recruit different subsets of MUs with every other pulse. In doing so, firing rates of MUs are reduced by half compared to stimulation over one site alone, despite the net frequency being the same during both types of NMES. Over the course of 240 contractions of the tibialis anterior, iNMES has been shown to reduce fatigue compared to

nNMES and mNMES (Lou et al., 2016). Specifically, when stimulation was set to produce an initial contraction amplitude of 10-15% of a maximal voluntary contraction (MVC), torque declined by 39% following iNMES, while torque declined by 67% during mNMES and 58% during nNMES (Lou et al., 2016).

Although iNMES reduces fatigue during relatively small contractions (i.e. 10-15% MVC; (Lou et al., 2016)), it is unclear whether iNMES will attenuate fatigue during larger contractions, compared to when nNMES or mNMES is delivered alone. Theoretically, in the Lou et al. (2016) study, the effectiveness of iNMES in reducing MU firing rates was contingent on the recruitment of different populations of MU with stimulation over the two stimulation sites (i.e. low MU overlap). However, as stimulation intensity increases, and more MUs are recruited, progressively more MUs will be recruited by both the nerve and muscle sites (i.e. high MU overlap; Wiest et al., 2017a), doubling their discharge rates relative to MUs recruited by one site only. Thus, there is likely to be a stimulation intensity and corresponding contraction amplitude at which overlap is so high that iNMES will no longer be effective in reducing MU firing rates and fatigue. As higher contraction amplitudes are often required in rehabilitative settings, determining the extent to which iNMES reduces contraction fatigue across a range of contraction amplitudes is important prior to its clinical implementation.

The main objective of the present investigation was to compare contraction fatigue of the ankle dorsiflexors when iNMES was delivered to produce contractions over a range of amplitudes. We anticipated, based on previous work, that overlap would increase as contraction amplitude increased (Wiest et al., 2017a) and, based on this, we predicted that larger contractions would fatigue more than smaller contractions. Our main outcome measure of contraction fatigue was the relative decline in torque from the beginning to end of a fatigue protocol, as this measure

provides a global measure of torque decline during NMES and is analogous to the fatigue index and similar measures used to assess fatigue in other studies. We hypothesized that there would be a greater relative decline in torque during larger contractions than smaller ones and that there would be a significant negative correlation between contraction amplitude and fatigue, whereby larger contractions are associated with a greater relative decline in torque. We also examined several other measures of fatigue to gain a more complete understanding of how torque declines when iNMES is used to produce contractions of different amplitudes. To explore the relationship between contraction fatigue and MU overlap, we estimated the proportion of MUs that were recruited by stimulation at both the common peroneal nerve and tibialis anterior muscle belly (i.e. MU overlap; Wiest et al., 2017a) across the range of contraction amplitudes tested. We hypothesized that there would be a significant negative correlation between MU overlap and fatigue, whereby more MU overlap would be associated with a greater relative decline in torque.

2.2 METHODS

2.2.1 Participant Characteristics

Eighteen healthy participants with no known neurological disorders or musculoskeletal injuries were recruited for participation using convenience sampling. However, four of these participants (all female) were excluded from participation. Two participants found the stimulation uncomfortable, even at very low current intensities. In another participant, dorsiflexion torque could not be achieved without excessive co-contraction of the ankle everters. The fourth participant was excluded as H-reflexes were consistently evoked in the tibialis anterior in this individual during nNMES. These H-reflexes indicate the recruitment of a different subset of MUs and at a different latency from those activated by depolarization of

motor axons (i.e. M-waves). The recruitment of two subsets of MUs at slightly different latencies with nNMES would confound our estimation of the amount of overlap of MUs recruited by the muscle and nerve stimulation sites (described below), thus, this participant was also excluded.

The 14 remaining participants (10 male, 4 female) completed all experimental sessions and were included in data analysis. The average age of participants was 26.2 ± 6.3 years and the average height of participants was 174.7 ± 8.8 cm. Ten participants had not received NMES prior to participating in the study. All participants verbally confirmed they had refrained from strenuous exercise 24 hours prior to each experimental session. Participants were given a thorough description of the procedures prior to providing written consent. All procedures were conducted in accordance with the University of Alberta Research Ethics Office and the Declaration of Helsinki.

2.2.2 General Methodology

2.2.2.1 Overview

This study employed a within-subjects, repeated measures design with all participants completing three experimental sessions. Sessions were pseudo-randomized in order and successive sessions were interspersed by at least 48 hours. Each experimental session employed a different stimulation intensity to initially generate one of three contraction amplitudes, LOW (~ 5% MVC), MID (~ 15% MVC) or MAX (the stimulation intensity that generated the greatest amount of torque tolerable). Figure 2-1 (Panel A) depicts a schematic of the experimental protocol which is described in detail in Section III (Experimental Procedure) below. Briefly, each testing session involved a series of pre-measurements, followed by a 180-contraction fatigue protocol delivered using iNMES, which was followed by post-measurements. The order

at which trains of stimulation were delivered over the nNMES and mNMES sites during the pre- and post- measurements were pseudo-randomized.

All participants were seated comfortably in a Biodex dynamometer (System 3, Biodex Medical Systems, Shirley, New York) to measure torque about the right ankle joint while NMES was delivered to activate the tibialis anterior muscle and dorsiflexors of the ankle (Figure 2-1, Panel B). The tibialis anterior muscle was selected for investigation as 1) it is commonly affected following injury to the central nervous system, resulting in a condition known as foot drop (Chae, Sheffler, & Knutson, 2008; Liberson, Holmquest, Scot & Dow, 1961); 2) it is easily accessible for stimulation via both the muscle belly and the common peroneal nerve and, thus, pulses can be alternated between the two sites and; 3) H-reflexes are typically small or not evoked in the tibialis anterior under resting conditions (Zehr, 2002) which is important for the present investigation as the presence of H-reflexes would confound the MU overlap estimation. Each participant was positioned with their knee flexed at ~ 120°, their right lateral malleolus in line with the motor axis and their ankle positioned at ~ 20° of plantar-flexion. This ankle angle was selected as it is optimal for producing dorsiflexion torque in individuals with and without SCI (Pelletier & Hicks, 2010) A force-sensitive resistor (FSR) was positioned under the head of the first metatarsal to assess the activity of the ankle everters during all experimental procedures.

2.2.2.2 EMG

As depicted in Figure 2-1 (Panel B) surface EMG was recorded from the right tibialis anterior muscle and peroneus longus muscles using pairs of disposable Ag-AgCl electrodes (2.25 cm^2; Vermed Medical, VT, USA) placed over the muscle belly and in parallel to the predicted path of the underlying muscle fibers. A ground electrode was placed over the shaft of the tibia.

Prior to placing the electrodes on the skin, shaving, abrasion and subsequent alcohol cleansing was conducted to reduce skin impedance to < 10 kΩ. Impedance was measured using a handheld multimeter (B&K Precision, California, USA). All EMG signals were amplified (500x) and band-pass filtered between 10 and 1000 Hz (Neurolog System; Digitimer, Welwyn Garden City, UK).

2.2.2.3 Electrical Stimulation

Two constant-current Digitimer stimulators (Digitimer, Welwyn Garden City, UK) were used to deliver rectangular pulses (pulse duration = 500 μs) to the nNMES (DS7A) and mNMES (DSA7AH) sites. For mNMES, the stimulating electrodes (5.1 x 5.1 cm, SuperStim Premium, Richmar®, Chattanooga, TN) were trimmed to fit over the middle third of the tibialis anterior muscle belly with the anode positioned ~1 cm proximal to the cathode, consistent with previous recommendations for stimulation of the main motor point for tibialis anterior (Botter et al., 2011; Figure 2-1, Panel B). For stimulation over the common peroneal nerve, the electrodes (3.2 cm round; SuperStim Premium, Richmar®, Chattanooga, TN) were positioned near the head of the fibula (Figure 2-1, Panel B) and were adjusted to find a location where dorsiflexion was generated with minimal ankle eversion. Typically, the cathode was placed just distal to the head of the fibula with the anode positioned ~1 cm distal/medial to the cathode. For iNMES, stimulation pulses were alternated between the nNMES sites and mNMES sites, with the first pulse of each train delivered to the nNMES site. Alternation of pulses was conducted using a square pulse generator (S88; Grass Products, Natus Neurology, Warwick), connected between the two stimulators. The stimulation was delivered such that a pulse from the DS7A stimulator was followed by a pulse from the DS7AH stimulator with a 25 ms delay. Thus, triggering the

DS7A at 20 Hz (50 ms inter-stimulus interval) resulted in the triggering of the DS7AH at 20 Hz (50 ms inter-stimulus interval + 180° phase lag) to result in a net frequency of 40 Hz.

2.2.3 Experimental Protocol

2.2.3.1 M-wave Recruitment Curves

At the beginning of each experimental session, data were collected to construct M-wave recruitment curves separately for stimulation over the nNMES and mNMES sites (Figure 2-1, Panel A). Thirty stimulus pulses were delivered ~5 s apart at random stimulation intensities ranging from below motor threshold to 1.2x the intensity which evoked the largest M-wave amplitude (M_{max}). M_{max} was used to normalize all subsequent M-wave amplitudes. In addition to measuring M_{max} at the start of each experimental session, M_{max} was also measured following the fatigue protocol in a subset of five participants. This was done by first delivering pulses of stimulation over the nNMES and mNMES sites at the simulation intensity that produced M_{max} at the start of the experimental session. Ten stimulus pulses at random stimulation intensities above and below this initial stimulation intensity were then delivered to ensure the M_{max} was achieved.

2.2.3.2 Maximum Voluntary Contractions

After data were collected for the M-wave recruitment curves, participants performed two maximum isometric voluntary contractions (MVC) by maximally dorsiflexing against the belt on the dynamometer footplate for 3-5 s. Subsequent MVCs were separated by at least 2 min. Participants were given verbal encouragement and visual feedback throughout each MVC trial to promote maximal effort. If the peak torques produced during the two MVC's were not within

10% of each other, a third MVC was performed. The MVC trial which elicited the largest peak torque was designated as the MVC used to normalize all subsequent torque measurements. Approximately 3 s after the final contraction of the fatigue protocol, participants performed another MVC. Three additional MVCs were performed throughout the experimental session (see Figure 2-1, Panel A) to ensure consistent levels of post-activation potentiation within the tibialis anterior during torque measurements.

2.2.3.3 Setting Stimulation Intensity

Target contraction amplitudes for the iNMES fatigue protocols (described below) were ~5% MVC (LOW), ~15% MVC (MID) and the highest tolerated stimulation intensity (MAX). To set these intensities, 6 pulses at 20 Hz were delivered every 5-10 s to the nerve and muscle sites separately to evoke approximately half of the target torque output. For example, to achieve an initial contraction of ~ 15% MVC, stimulation intensity was adjusted over the nerve and muscle sites separately so that the torque produced by each site equaled ~ 7.5% MVC. If these stimulation intensities did not result in the target net torque during iNMES (i.e. when pulses were delivered over each site at 20 Hz and alternated to produce a net frequency of 40 Hz), intensities were adjusted at each site until the target torque was achieved *and* a similar amount of torque was produced at the two stimulation sites when stimulation was delivered over each site separately. The stimulation intensity for MAX was set by increasing the simulation intensity over both the nerve and muscle sites until the participant could no longer tolerate increases in stimulation intensity, or when additional increases in torque could not be achieved. If these stimulation intensities produced different contraction amplitudes, stimulation was lowered over

the site producing the greater torque to match that produced at the site where the maximal tolerated intensity produced the least torque.

2.2.3.4 Motor Unit Overlap Estimation

To assess the extent to which the same MUs were recruited by both the nNMES and mNMES sites (i.e. MU "overlap"), trains of stimulation were delivered over the nerve and muscle stimulation sites separately (nNMES, mNMES) and together (m+nNMES). Representative torque traces produced from these trains of stimulation are presented in Figure 2-2. Separate MU overlap estimations were conducted prior to the fatigue protocols using each of the three contraction amplitudes. Over each stimulation site, trains consisted of 6 pulses at 20 Hz, with 5 s rest between subsequent trains. When trains of stimulation were delivered over both locations together (m+nNMES), a delay in the timing of pulses between the nerve and muscle sites was added to ensure MUs were activated simultaneously from the two stimulation sites (Wiest et al., 2017a). Given that the nNMES stimulation site was farther from the muscle, pulses of nNMES were delivered 1.6 ± 1.0 ms prior to pulses of mNMES. This delay was calculated for every participant by subtracting the latency of the M-wave produced with stimulation over the muscle site from the latency of the M-wave evoked with stimulation over the nerve site

2.2.3.5 Fatigue Protocol

A fatigue protocol consisting of 180 trains of iNMES (0.3s on; 0.7s off) was delivered at one of the three stimulation intensities (LOW, MID or MAX) in a given experimental session. This duty cycle was selected to mimic the bursts of tibialis anterior activity (200-300 ms) that

occurs during the stance to swing phases of gait (Byrne, O'Keeffe, Donnelly, & Lyons, 2007). Each iNMES train consisted of 12 pulses of iNMES delivered at a net frequency of 40 Hz. Participants were instructed to remain relaxed during the fatigue protocol and received frequent reminders to do so.

2.2.4 Data Acquisition and Analysis

All data were acquired at 5-8 kHz using custom-written Labview software (National Instruments, USA). Analogue signals were digitized using a 6040E A-D board (National Instruments, USA). All data were analyzed post-hoc using custom-written Matlab software (The Mathworks, USA).

2.2.4.1 Dorsiflexion Torque

Dorsiflexion torque produced by nNMES, mNMES or iNMES were quantified by averaging the torque over a 10 ms window centered on the peak. For each participant, these values were then averaged into bins, with 10 contractions per bin, giving a total of 18 bins. Torque recorded during MVCs were quantified by the average torque over a 0.3 s window centered on the peak.

2.2.4.2 Fatigue

Contraction fatigue was quantified as the relative decline in torque from the beginning (Bin 1) to the end (Bin 18) of the fatigue protocol, using Equation 2-1. However, to provide additional information regarding the time-course and functional consequences of torque decline, three other measures of torque decline were quantified. First, the torque produced at the

beginning (Bin 1), middle (Bin 9) and end (Bin 18) of the fatigue protocols was compared to determine if each contraction amplitude incurred a significant amount of torque decline and to provide information regarding the time-course in torque decline. The absolute decline in torque from Bin 1 to Bin 18 was also calculated (as a % MVC) by subtracting the torque produced during Bin 18, from that produced during Bin 1. Finally, fatigue was quantified as the percent decline in torque produced during the MVC performed prior to the fatigue compared to the MVC performed immediately after the fatigue protocol.

$$\% \text{ Decline in Torque} = \frac{(\text{Torque}_{(\text{Bin 18})} - \text{Torque}_{(\text{Bin 1})})}{\text{Torque}_{(\text{Bin 1})}} \times 100$$

Equation 2-1. Percent decline in torque from Bin 1 to Bin 18 equation.

2.2.4.3 Motor unit overlap calculation

Percent MU overlap was estimated for each contraction amplitude prior to each fatigue protocol using Equation 2-2, which has been described in greater detail previously by Wiest et al. (2017a). To determine percent MU overlap, the average torque evoked during the three trains of mNMES (T_{mNMES}) was added to the average torque evoked during the three trains of nNMES (T_{nNMES}). The averaged evoked torque when stimulation was delivered together ($T_{m+nNMES}$) was then subtracted from this sum (see numerator in Equation 2-2). This numerator was then divided by the mean torque produced between the nerve and muscle sites ($T_{meanTmNMES+TnNMES}$) and multiplied by 100 to achieve percent MU overlap.

$$\text{MU Overlap (\%)} = \frac{((T_{mNMES} + T_{nNMES}) - T_{m+nNMES}))}{(T_{meanTmNMES + TnNMES})} \times 100$$

Equation 2-2. MU overlap equation.

If mNMES and nNMES produced the same torque amplitude, and $T_{m+nNMES}$ was the exact sum of these two torques (i.e. $T_{mNMES} + T_{nNMES}$), we considered this to be 0% overlap (Figure 2-2), thereby suggestive of the idea that completely different populations of MUs were recruited at each site. Conversely, if $T_{mNMES} + T_{nNMES}$ was equal to $T_{m+nNMES}$, MU overlap was considered to be 100%, indicating an identical population of MUs was recruited at the two stimulation sites.

2.2.5 Statistical Analyses

All statistical analyses were conducted on group data. A 3 (TIME) x 3 (AMP) repeated measures analysis of variance (RM ANOVA) was run to compare the evoked peak torque at Bins 1, 9 and 18 across the 3 contraction amplitudes. As a significant interaction was discerned during this analysis, separate analyses were subsequently run for each factor of the RM ANOVA (TIME and AMP). Specifically, three 1 x 3 (AMP) RM ANOVAs were conducted separately to assess the torque evoked at Bins 1, 9 and 18 at each contraction amplitude, and three separate 1 x 3 (TIME) RM ANOVAs were run to assess changes in evoked torque at the three time points. For the relative decline in torque, the absolute decline in torque, and the percent change in volitionally-evoked torque during MVCs performed prior and subsequent to the fatigue protocols across amplitudes (LOW, MID, MAX), separate 1 x 3 (AMP) RM ANOVAs were performed. A 1 x 3 (AMP) RM ANOVA was also utilized to compare the percent MU overlap at the three contraction amplitudes.

A total of seven Pearson product-moment correlations were run to determine relationships among variables. First, a correlation was run between the initial torque generated and the percent MU overlap. Three separate Pearson product-moment correlations were run to determine the relationship between MU overlap and the relative decline in torque, the absolute decline in torque and the percent decline in voluntary torque evoked during MVCs. An additional three Pearson product-moment correlations were conducted to determine the relationship between the initial contraction amplitude as a percent of MVC and the same three measures of torque decline.

To assess differences in the amount of current utilized over each stimulation site (nerve vs. muscle) to achieve the target contraction amplitudes, a 2 (SITE) x 3 (AMP) RM ANOVA was run. For M-wave data, two 3 (TIME) x 3 (AMP) RM ANOVAs were run to compare M-wave amplitudes at three time points (Bins 1, 9, 18) at the three different contraction amplitudes. As it is inappropriate to compare M-wave amplitudes over the nerve and muscle stimulation sites, one 3 x 3 RM ANOVA was used for M-waves evoked with stimulation over the nerve site, and a separate 3 x 3 RM ANOVA was used for M-waves evoked with stimulation over the muscle site. Differences in M_{max} amplitudes evoked prior and subsequent to the fatigue protocol across the three amplitudes were assessed in five participants using two 2 (TIME) x 3 (AMP) RM ANOVAs. Again, separate analyses were run for M_{max} data over the two stimulation sites.

When appropriate, all pair-wise comparisons were conducted using a Bonferroni correction for multiple comparisons. When sphericity violations were present, Greenhouse-Gessier corrections were utilized. A p-value of < 0.05 was considered statistically significant. If a significant interaction was found, main effects were not reported. All data are reported as mean ± one standard deviation (sd).

2.3 RESULTS

Single Subject Data:

Data from a single subject are presented in Figure 2-3. Dorsiflexion torque recorded during the 1st, 90th and 180th contractions of the fatigue protocol for the LOW (Panel A), MID (Panel B) and MAX (Panel C) contraction amplitudes are displayed in the left column of the figure. In this participant, the mean torques produced during the first ten contractions of the fatigue protocol (i.e. Bin 1) were 5% MVC, 15% MVC and 36% MVC during the LOW, MID and MAX contraction amplitudes, respectively. From the beginning to the end of the fatigue protocols, torque declined by 13% during the LOW session, 17% during the MID session and 18% during the MAX session. The right column of Figure 2-3 displays averaged M-waves elicited with stimulation over the common peroneal nerve trunk (nNMES) and over the tibialis anterior muscle belly (mNMES), respectively, during the 1st, 90th and 180th contractions in the same participant. M-waves evoked by stimulation over the nerve were ~4%, 26% and 100% M_{max} at the beginning of the LOW, MID and MAX sessions, respectively, in this participant. M-waves evoked by stimulation over the muscle site were ~70%, 111% and 100% M_{max} during the LOW, MID and MAX sessions, respectively. MU overlap for this participant increased from 38% during LOW to 87% during MID and 99% during MAX.

Group Data:

Decline in Torque:

Figure 2-4 (Panel A) displays the torque produced throughout the fatigue protocol at each of the three contraction amplitudes averaged across the group of 14 participants. The torque generated for each contraction was averaged into 18 bins. Bins 1, 9 and 18 (highlighted by

dashed boxes) were selected for statistical analysis as they represented the beginning, middle and end of the fatigue protocol, respectively. A significant interaction was found between TIME and AMP ($F_{(1.8,22.8)} = 12.7$, $p < 0.001$). Pairwise comparisons revealed that the torque evoked during the beginning, middle and end time points of the fatigue protocols were all different ($p < 0.001$) from each other. As shown in Figure 2-4B, during the LOW and MID contraction amplitudes, the torque evoked at the beginning of the fatigue protocol was significantly higher ($p < 0.05$) than the torque produced during the middle and end of the fatigue protocol, however, no difference ($p > 0.05$) in evoked torque was found between the middle and end of the fatigue protocol during either condition. In this figure, individual subject data is denoted by circles, while bars represent group data. During the MAX contraction amplitude trials, initial contraction amplitudes ranged from 24 to 47% MVC across participants, and torque decreased throughout the fatigue protocol, as torques produced at all three times points were significantly different from each other ($p \leq 0.003$).

The magnitude of fatigue was quantified as the percent decline in torque, which is presented in Panel A of Figure 2-5. In this figure, individual subject data is denoted by circles, while bars represent group data. The relative decline in torque from the beginning to the end of the fatigue protocol was not different between any of the three contraction amplitudes ($F_{(2,26)} = 0.7$, $p = 0.50$) as displayed in Figure 2-5A, and, on average, torque decreased by ~ 23% across contraction amplitudes. Although our primary measure of fatigue was the relative decline in torque from the beginning to end of the fatigue protocol, we also examined the absolute decline in torque from the start to end of the fatigue protocol as a percent of MVC (Figure 2-5, Panel B) and the percent decline in torque produced during MVCs (Figure 2-5, Panel C). A significant main effect of contraction amplitude ($F_{(1.4,18.1)} = 15.2$, $p < 0.001$) was found when assessing the

decline in absolute torque (Figure 2-5, Panel B). Pairwise comparisons revealed the absolute decline in torque was significantly greater during the MAX condition than during both the LOW ($p < 0.001$) and MID ($p = 0.035$) conditions. There was no difference ($p = 0.051$) in the absolute decline in torque between the LOW and MID sessions. Across participants, the mean percent change in torque produced during MVCs performed prior and subsequent to the fatigue protocols were -6 ± 6%, -10 ± 10% and -15 ± 6%, respectively. A main effect of contraction amplitude was found ($F_{(2,24)} = 4.3$, $p = 0.025$) and subsequent pair-wise comparisons indicated that there was a significantly greater percent decline in maximal torque during the MAX session than during the LOW session ($p = 0.003$). No difference in the percent change in torque was found between LOW and MID ($p = 0.67$) or the MID and MAX ($p = 0.63$) contraction amplitudes.

MU Overlap

MU overlap was quantified to estimate the proportion of MUs that were recruited by both the nerve and muscle stimulation sites. Data for individual participants and group mean MU overlap across contraction amplitudes is displayed in Figure 2-5, Panel D. There was a significant main effect of AMP on MU overlap ($F_{(2,26)} = 18.7$, $p < 0.001$). Pairwise comparisons indicate MU overlap was significantly greater during the MAX condition than during the LOW ($p < 0.001$) and MID ($p = 0.004$) conditions, however, no difference in MU overlap was found between the LOW and MID conditions ($p = 0.248$). During the LOW contraction amplitude, MU overlap ranged from 0% to approximately 51% across participants with 5 participants exhibiting 0% overlap. During the MID contraction amplitude, MU overlap ranged from ~1% to 92%, and during the MAX condition, MU overlap ranged from ~35% to 99%.

Correlations

Figure 2-6 displays the initial torque generated (x-axis) plotted against the percent MU overlap. A significant, positive correlation was found between these two measures ($r = 0.67$, $n = 42$, $p < 0.001$). The left panels of Figure 2-7 display the MU overlap data (x-axis) plotted against the relative decline in torque (Panel A), the absolute decline in torque as a percent of MVC (Panel B) and the percent decline in torque produced during MVCs (Panel C). There was a moderate, negative correlation between MU overlap and the absolute decline in torque as shown in Panel B, which was statistically significant ($r = -0.51$, $n = 42$, $p = 0.001$). No significant relationships were found between MU overlap and the relative decline in torque ($p = 0.71$) or the percent decline in torque produced during MVCs ($p = 0.20$). The right panel of Figure 2-7 displays the initial contraction amplitude (x-axis) plotted against the relative decline in torque (Panel D), the absolute decline in torque (Panel E) and the percent decline in torque produced during MVCs (Panel F). Significant, negative relationships were found between the initial torque generated and the absolute decline in torque ($r = -0.77$, $n = 42$, $p < 0.001$) and the decline in torque evoked during MVCs ($r = -0.50$, $n = 39$, $p = 0.001$). No significant correlation was found between the initial torque generated and the relative decline in torque ($p = 0.11$).

Current and Torque Produced at Nerve and Muscle Sites During iNMES

Prior to the fatigue protocol, stimulation was delivered to each site separately at the stimulation intensity used in the fatigue protocol. Figure 2-8, Panel A displays the current delivered to the nerve and muscle sites at each of the three contraction amplitudes. At the nerve stimulation site, the current utilized for the LOW, MID and MAX conditions was 10 ± 4 mA, 14 ± 6 mA and 18 ± 7 mA. Over the muscle stimulation site, current amplitudes of 9 ± 2 mA, 21 ± 8

mA and 64 ± 38 mA were utilized to achieve the LOW, MID and MAX conditions, respectively. A significant SITE x AMP interaction was found ($F_{(1.1, 14.0)} = 23.4$, $p < 0.001$). Pair-wise comparisons revealed that although the current required to achieve the desired amplitude of contraction over the nerve and muscle sites was not different ($p = 0.46$) during LOW, the current required to achieve the desired torque was significantly higher for stimulation over the muscle site during the MID ($p = 0.017$) and MAX ($p < 0.001$) conditions.

The torque evoked by stimulation over the common peroneal nerve during LOW, MID and MAX was 3 ± 1 % MVC, 9 ± 2 % MVC and 22 ± 7 % MVC, respectively, while the torque evoked by stimulation over the tibialis anterior muscle belly during the three conditions was 3 ± 1 % MVC, 9 ± 2 % MVC and 21 ± 7 % MVC, respectively. These data are displayed in Figure 2-8, Panel B. Although no significant interaction was found, a main effect of contraction amplitude ($F_{(1.1,14.1)} = 68.0$, $p < 0.001$) was determined. In addition, though the torques produced over the two stimulation sites were matched as closely as possible, a main effect of stimulation location was identified ($F_{(1,13)} = 10.0$, $p = 0.008$). This latter finding is indicative that more torque was consistently generated with stimulation over the nerve versus the muscle belly.

M-waves

The amplitudes of M-waves recorded during the fatigue protocol could not be quantified for four participants, as the beginning of the M-waves were consistently indiscernible from the stimulus artifact. This was particularly problematic when the stimulation was delivered over the muscle belly due to the close proximity of the stimulating electrodes to the EMG electrodes. Thus, unless otherwise indicated, the following section describes M-wave data from 10 out of the 14 participants.

Averaged, M-wave amplitudes elicited throughout the fatigue protocol (18 bins; 10 averaged M-waves per bin) are displayed in Panel A of Figure 2-9. Of these 18 bins, three (Bins 1, 9, 18) were selected to statistically assess any changes in M-wave amplitude throughout the fatigue protocol. These data are reported in Panel B of Figure 2-9, where M-waves evoked by stimulation over the nerve and muscle sites are displayed in the left and right panels, respectively. For M-waves evoked with stimulation over the nerve, no significant interaction was found, however, there was a main effect of contraction amplitude ($F_{(2,18)} = 7.2$; $p = 0.005$). Subsequent pairwise comparisons indicated that M-waves elicited during the LOW condition were smaller ($p = 0.033$) in amplitude than M-waves elicited during the MAX condition, but were not different ($p = 0.34$) from the amplitudes of M-waves elicited during the MID condition. These data indicate that across the three time points of the fatigue protocol, the amplitude of M-waves elicited with stimulation over the nerve did not change. For M-waves evoked via stimulation over the muscle, a significant AMP x TIME interaction was found ($F_{(4,36)} = 4.03$, $p = 0.008$). However, subsequent pairwise comparisons did not reveal a significant difference between any individual values.

Although M_{max} was measured over the nerve and muscle sites prior to the fatigue protocol in all 10 participants included in M-wave data, M_{max} was also recorded in 5 participants subsequent to the fatigue protocol. Data from these five participants is reported in Figure 2-9 (Panel C), where M_{max} amplitudes elicited with stimulation over the nerve (left panel) and muscle belly (right panel) are displayed at each of the three contraction amplitudes (LOW, MID, MAX). A main effect of time was found when stimulation was delivered over the nerve ($F_{(1,4)} = 6.98$; $p = 0.035$). Subsequent pairwise comparisons revealed that the amplitude of M_{max} evoked following the fatigue protocol was higher ($p = 0.035$) than the amplitude of M_{max} evoked prior to the

fatigue protocol. This main effect of contraction amplitude is displayed in the left inset of Figure 2-9 (Panel C). Conversely, when stimulation was delivered over the muscle belly, no main effects of time or contraction amplitude were found.

2.4 DISCUSSION

The present experiments were designed to compare contraction fatigue of the ankle dorsiflexors when iNMES was delivered to produce contractions over a range of amplitudes. We hypothesized that there would be more contraction fatigue, defined as the relative decline in torque from the beginning to end of the fatigue protocol, for large than for small contractions. We anticipated that large contractions would fatigue more than small contractions because progressively more MUs would be recruited by both the common peroneal and tibialis anterior muscle belly stimulation sites (i.e. greater MU overlap) as contraction amplitude increased. Therefore, we also hypothesized that there would be a correlation between contraction fatigue and our measure of MU overlap. However, although there were some subtle differences in how torque declined across contraction amplitudes, the relative amount that torque declined from the beginning to the end of the fatigue protocols was not different over the range of contraction amplitudes tested, and there was no significant correlation between the amount of fatigue and either the initial contraction amplitude or the amount of MU overlap.

In the present study, the relative decline in torque was ~ 23%, which is comparatively lower than previously-reported values of torque decline during iNMES of the ankle dorsiflexors. During a 240-contraction fatigue protocol when iNMES was delivered at a stimulation intensity to evoke initial amplitudes of 10-15% MVC, dorsiflexion torque declined by ~ 40% following iNMES (Lou et al., 2016). The lesser fatigue in the present study may be explained by the

different duty cycle and total stimulation "on" time used in our study. We selected a duty cycle of 30% (0.3s on, 0.7s off) to mimic bursting activity of the tibialis anterior during gait and to approximate duty-cycles used in common clinical practice for FES cycling (Byrne et al., 2007; Doucet et al., 2012; Kesar & Binder-Macleod, 2006) and our total "on" time for iNMES was 60 s. In contrast, Lou et al. (2016) utilized a duty cycle of 67% (2 s on, 1 s off) and iNMES had a total "on" time of 480 s, which was 8 times greater than our "on" time (Lou et al., 2016). It is likely that the greater fatigue in the Lou et al. (2016) study is at least partially attributable to these differences as longer stimulation "off" or rest durations relative to stimulation "on" times are known to elicit lesser fatigue (Packman-Braun, 1988). With this in mind, it is possible that the parameters selected for our fatigue protocol were not taxing enough on the neuromuscular system to incur measurable differences in fatigue across amplitudes.

While our findings of contraction fatigue were not anticipated, it has been consistently demonstrated that increasing the stimulation intensity has little impact on the amount of contraction fatigue during repeated contractions evoked by conventional NMES. Unfortunately, these studies have adjusted other stimulation parameters simultaneously, making interpretation of the sole effect of contraction amplitudes on fatigue difficult (Adams et al., 1993; Behringer et al., 2016; Gorgey et al., 2009). Regardless, this lack of a relationship between contraction amplitude and fatigue is thought to be due to random recruitment of MUs with respect to MU type, as well as a relatively fixed metabolic demand per activated MU (Gorgey et al., 2009). Despite these findings, we expected that during iNMES, when stimulus pulses are alternated between two stimulation sites, larger contractions would result in more fatigue due to greater overlap in the proportions of MUs recruited by both stimulation sites, and thus, higher MU firing rates compared to smaller contractions. While we did find that there was more MU overlap

during the MAX condition than during the LOW condition, and that a significant positive relationship was found between the initial contraction amplitude and percent MU overlap, MU overlap and fatigue were not significantly correlated. These findings contrast previous work by Mcdonnall et al. (2004) who showed, using implanted electrode arrays over the sciatic nerve of cats, that electrode pairs exhibiting more MU overlap displayed enhanced fatigue compared to electrode pairs with minimal overlap (Mcdonnall et al., 2004). For the MAX trials in the present study, participants were only able to tolerate stimulation intensities that produced contractions that were on average ~30% MVC, and ranged between 24-47% MVC. It is possible these contraction amplitudes were not sufficiently large to result in enough MU overlap to have a measurable effect on contraction fatigue. Accordingly, the moderate range of contraction amplitudes (~5-30% MVC) used in our study limited our ability to test the influence of contraction amplitude on fatigue across a wider range of contractions.

Although we did not find significant relationships between the relative decline in torque from the beginning to end of the fatigue protocol and the initial contraction amplitude, or between the relative decline in torque and MU overlap, we did find subtle differences in our supplementary measures of fatigue. Specifically, only during the MAX condition did torque continue to decline during the latter half of the fatigue protocol. In addition, both the absolute decline in torque (as a %MVC) and the ability to voluntarily generate torque during MVCs declined more after the MAX condition than after the LOW condition. These data suggest there are differences in how contractions are produced and how torque declines when iNMES is delivered to produce contractions of different amplitudes. Moreover, our somewhat conflicting results between our measures of fatigue may highlight the complexity and multifaceted nature of

fatigue during NMES, and suggest that mechanisms other than higher MU firing rates were attributable to the fatigue that developed in the present study.

During NMES, multiple factors contribute to contraction fatigue. One such mechanism is decreased axonal excitability especially during high impulse loads (Kiernan et al., 2004; Vagg et al., 1998). This decrease in membrane excitability is thought to arise from an inability of Na^+/K^+ pumps to maintain ionic balance, resulting in a lowering of the membrane potential and leading to MU "drop-out" if current amplitude is not adjusted correspondingly (Kiernan et al., 2004; Matkowski et al., 2015). However, a hallmark of decreased axonal excitability is a progressive decrease in M-wave amplitude and in the present study M-waves did not decrease, thus, it is unlikely that decreases in axonal excitability contributed to the fatigue observed. This finding suggests that iNMES may attenuate decreases in axonal excitability and propagation of M-waves along the muscle sarcolemma, although further experimentation is needed to verify this as iNMES has led to decreased M-waves previously (Lou et al., 2016). Within the muscle, fatigue is thought to primarily result from decreased release of Ca^{2+} from the sarcoplasmic reticulum. Although we did not assess this type of fatigue using measurements of peak twitch torque, based on process of elimination, it is likely that the fatigue present within the present study is attributable to this intramuscular mechanism.

Limitations

The MU overlap estimation employed in the present study was used to estimate the proportion of MUs recruited by stimulation over the tibialis anterior muscle belly and the common peroneal nerve trunk and was founded on previous work involving implanted electrode arrays in animals or cuff electrodes in humans (Fisher et al., 2013; Mcdonnall et al., 2004). This

measure is susceptible to underestimation if the stimulus pulses are not timed to arrive at the muscle at the same time and, to date, the reliability and validity of this measure has not been verified. However, our findings follow previous work examining MU overlap with increasing stimulation intensity (Wiest et al., 2017a) and we found a significant positive correlation between contraction amplitude and percent MU overlap, as would be expected.

Significance and Clinical Implications

A similar amount of contraction fatigue was produced with iNMES over the range of contraction amplitudes tested (~5-30% MVC). Thus, even when using the maximal tolerable stimulation amplitude (i.e. MAX), torque output remained on average ~ 9 Nm by the end of the 180-contraction fatigue protocol. This torque is over four times greater than the amount of torque required to dorsiflex the ankle joint (Bogey, Gitter, & Barnes, 2010; Davy & Audu, 1987; Wiest et al., 2017a), which suggests that despite the contraction fatigue accumulated in the present study, the ability of the tibialis anteior to produce sufficient force for dorsiflexion would not be compromised following iNMES. This study also provides information regarding the range of contraction amplitudes over which iNMES can be used and tolerated by individuals with intact sensation. Although we did not directly examine discomfort in this study, our MAX condition provided information regarding the greatest tolerated contraction amplitude for each participant. Overall, participants were able to tolerate a mean torque output of ~31% MVC, with over half of the participants (n = 8) able to achieve initial contraction amplitudes of >30% MVC. In other work, participants were able to tolerate an average of ~50% MVC using iNMES, while participants were only able to tolerate stimulation intensities to evoke 33% MVC during mNMES (Wiest et al., 2017b). These findings suggest that iNMES delivered at a tolerated range

of stimulation amplitudes may be used effectively to produce fatigue-resistant and functionally-meaningful contractions during FES-assisted walking or cycling in rehabilitation.

Previously, the decline in torque during iNMES was compared to the decline in torque when mNMES and nNMES were delivered alone at 10-15% MVC (Lou et al., 2016). Lou et al. (2016) determined that iNMES produced significantly less fatigue compared to nNMES and mNMES during a 240-contraction fatigue protocol. In the present study, iNMES was not compared to nNMES or mNMES which limits our ability to determine if iNMES retains its advantage in reducing fatigue compared to conventional delivery of NMES at higher contraction amplitudes. Future work should examine the amount of fatigue during nNMES, mNMES and iNMES for a more complete understanding of the effectiveness of iNMES. In addition, the range of stimulation amplitudes at which iNMES was tolerated by participants in the present study was possibly not broad enough to detect differences in fatigue between conditions. Conducting similar experiments in individuals without intact sensation, such as individuals with spinal cord injury, may allow for the testing of a wider range of contraction amplitudes and a greater understanding of the effect of contraction amplitude on fatigue during iNMES.

Summary

Over the range of contraction amplitudes tested (~5-30% MVC), iNMES produced a similar amount of relative contraction fatigue, regardless of the initial contraction amplitude, and despite more MU overlap at larger contractions. While the implications of these results are somewhat unclear, they may suggest that iNMES holds promise in minimizing contraction fatigue across a wider range of low to moderate contraction amplitudes than previously tested. Future work should compare the magnitude of contraction fatigue during iNMES to that

produced during nNMES or mNMES during larger contractions to determine if iNMES retains its advantage in reducing fatigue across a broader range of contraction amplitudes.

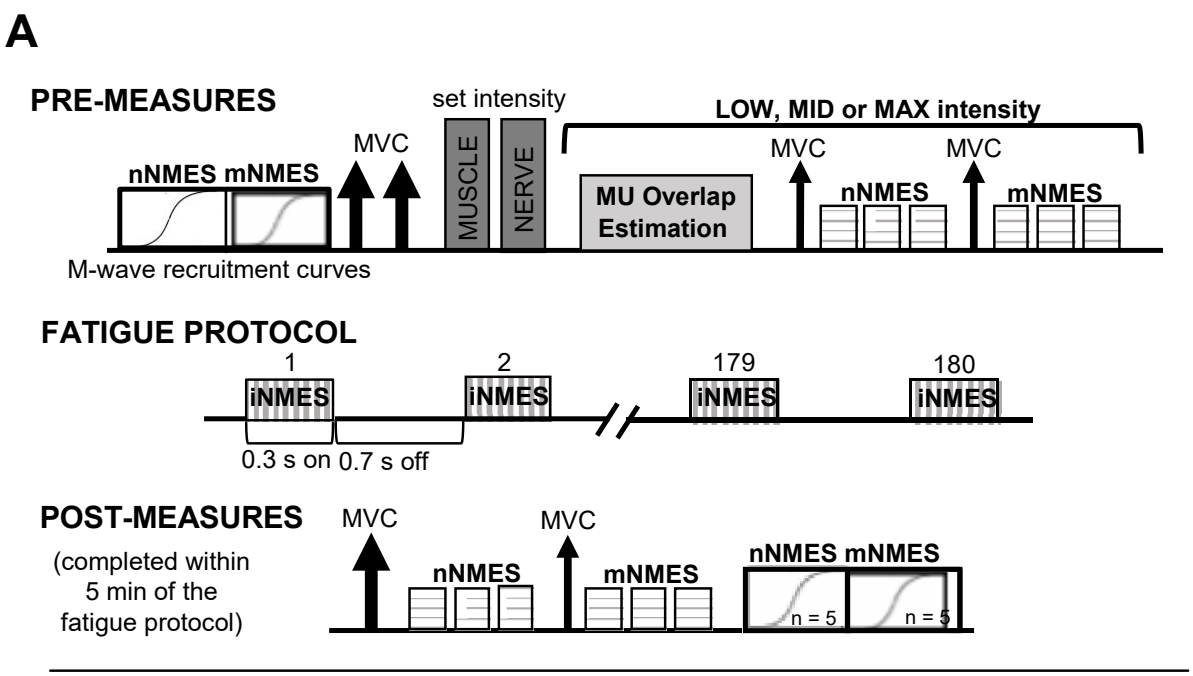

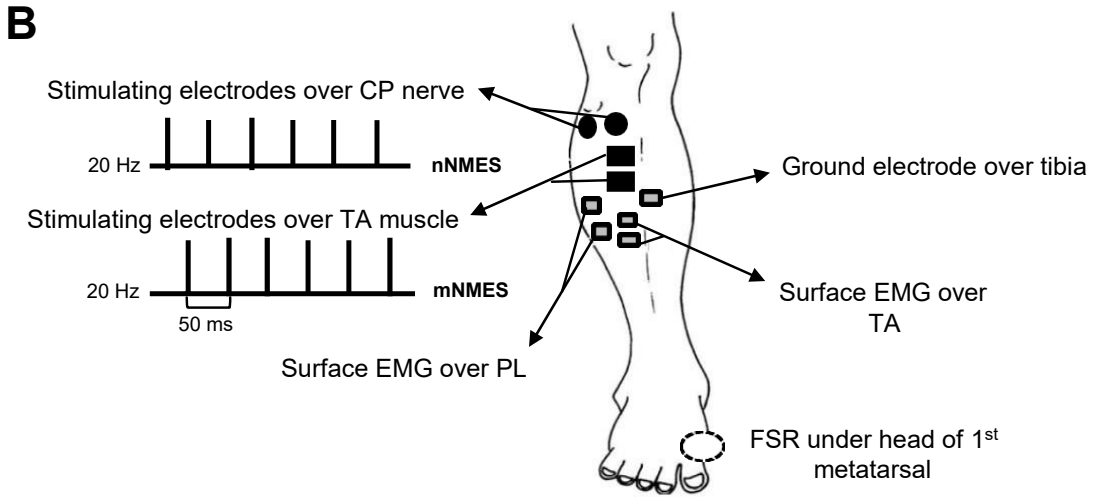

Figure 2-1. Overview of the experimental protocol. Panel A. Schematic procedures followed during a single session which included a fatigue protocol as well as pre- and post-fatigue protocol measures. **Panel B.** Placement of electrodes on the lower leg. The left side displays the location of the stimulating electrodes over the common peroneal (CP) nerve (black circles) and tibialis anterior (TA) muscle belly (black squares), as well as a representation of a single train of iNMES delivered at 40 Hz, when pulses (6 pulses per site) are alternated between the two sites at 20 Hz. EMG recording sites are displayed with grey squares over TA and peroneus longus (PL) with the reference electrode over the tibia. A force-sensitive resistor (FSR) was placed under the base of the first metatarsal to monitor eversion.

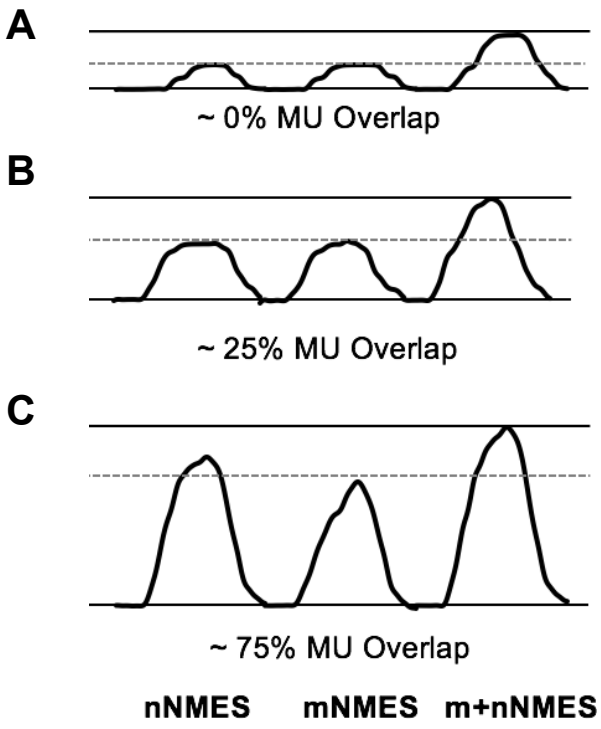

Figure 2-2. Torque recorded during contractions used to estimate percent motor unit (MU) overlap. Each panel first shows torque produced during nNMES, then mNMES and the third trace shows torque when both were delivered together (m+nNMES). **Panel A** shows data consistent with 0% overlap, indicating nNMES and mNMES recruit distinct subpopulations of MUs, with few if any MUs activated by both sites. **Panel B** shows data consistent with 25% overlap, indicating the activation of a small subset of MUs by both nNMES and mNMES. **Panel C** shows data consistent with 75% overlap, indicating that most MUs activated by mNMES are also activated by nNMES.

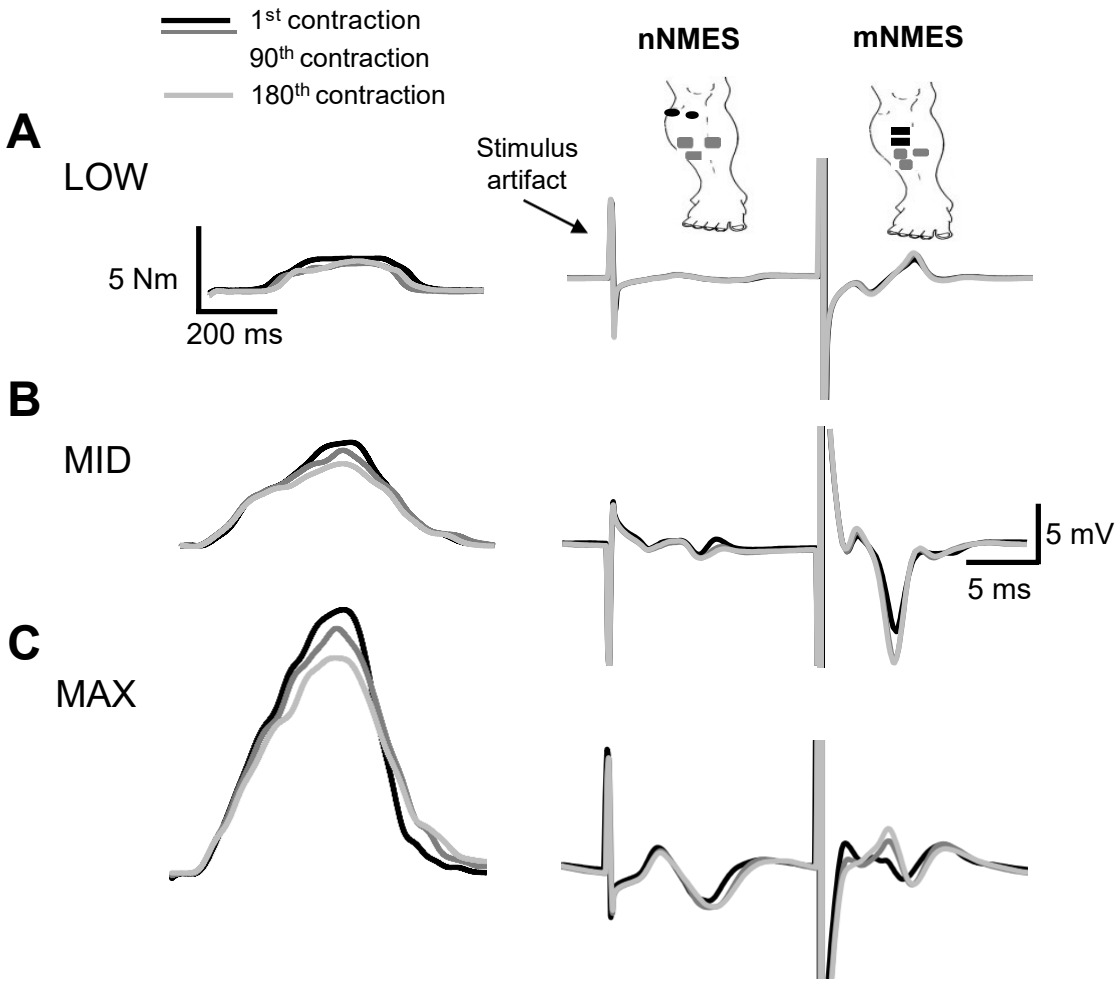

Figure 2-3. Torque and M-waves recorded from a single subject. Shown are data recorded during the LOW (**Panel A**), MID (**Panel B**) and MAX (**Panel C**) fatigue protocols. The left side of each panel displays dorsiflexion torque produced by iNMES at the beginning (1st contraction; black), middle (90th contraction; dark grey) and end (180th contraction; light grey) of each fatigue protocol. The right side of each panel shows overlaid, the average of the six M-waves produced by each stimulation site during those same contractions.

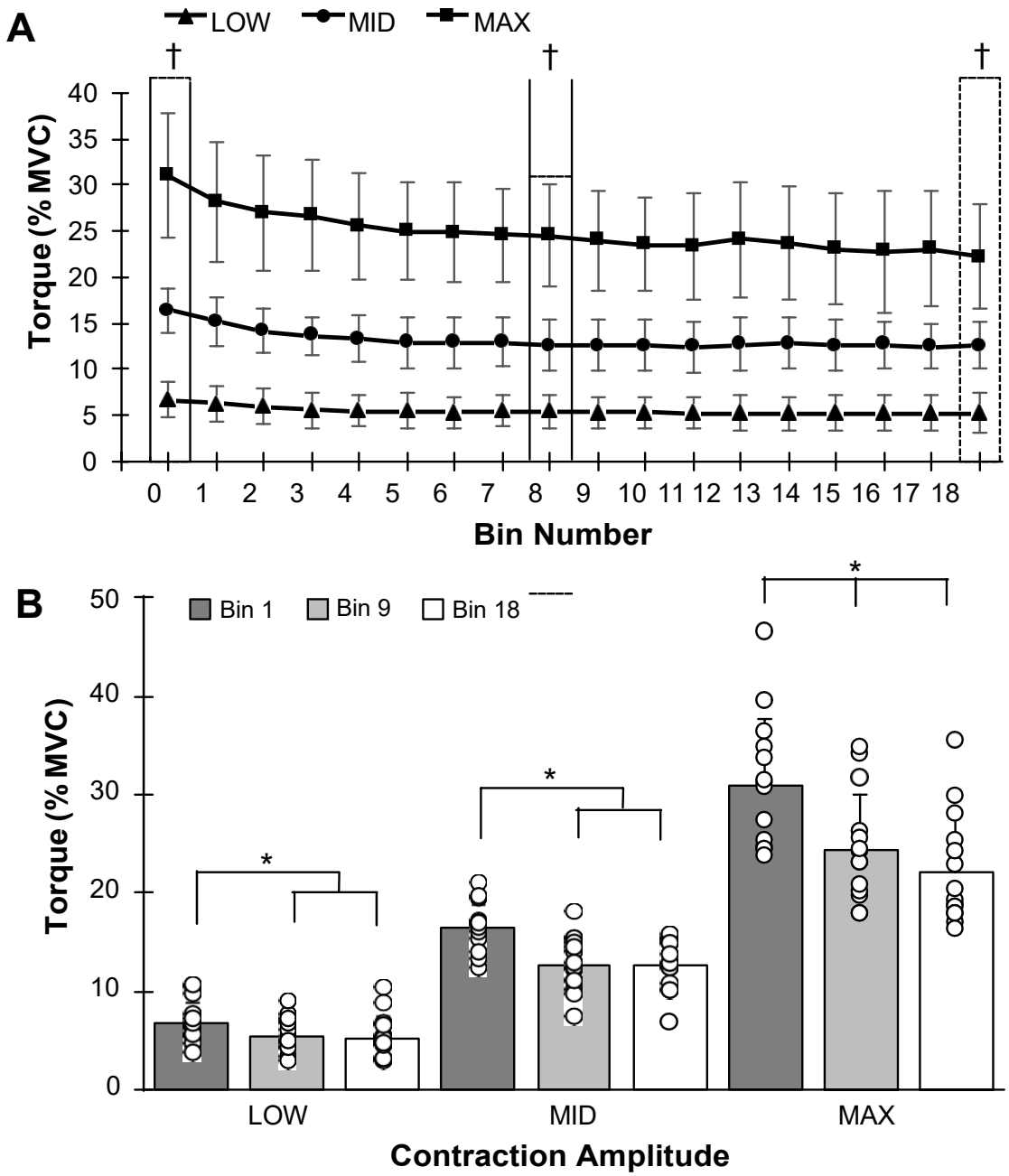

Figure 2-4. Torque generated during the fatigue protocols averaged across participants. Panel A. Torque recorded during the LOW (triangles), MID (circles) and MAX (squares) fatigue protocols. Torque generated during each contraction were averaged into 18 bins (10 contractions per bin). Dashed boxes indicate the three bins used for statistical comparison. **Panel B.** Torque recorded at the beginning (Bin 1; darks bars), middle (Bin 9; grey bars) and end (Bin 18; white bars) of the fatigue protocols averaged across participants. Error bars represent one standard deviation. † in Panel A denote significant differences between all three contraction amplitudes ($p < 0.05$). * in Panel B denote significant differences ($p < 0.05$).

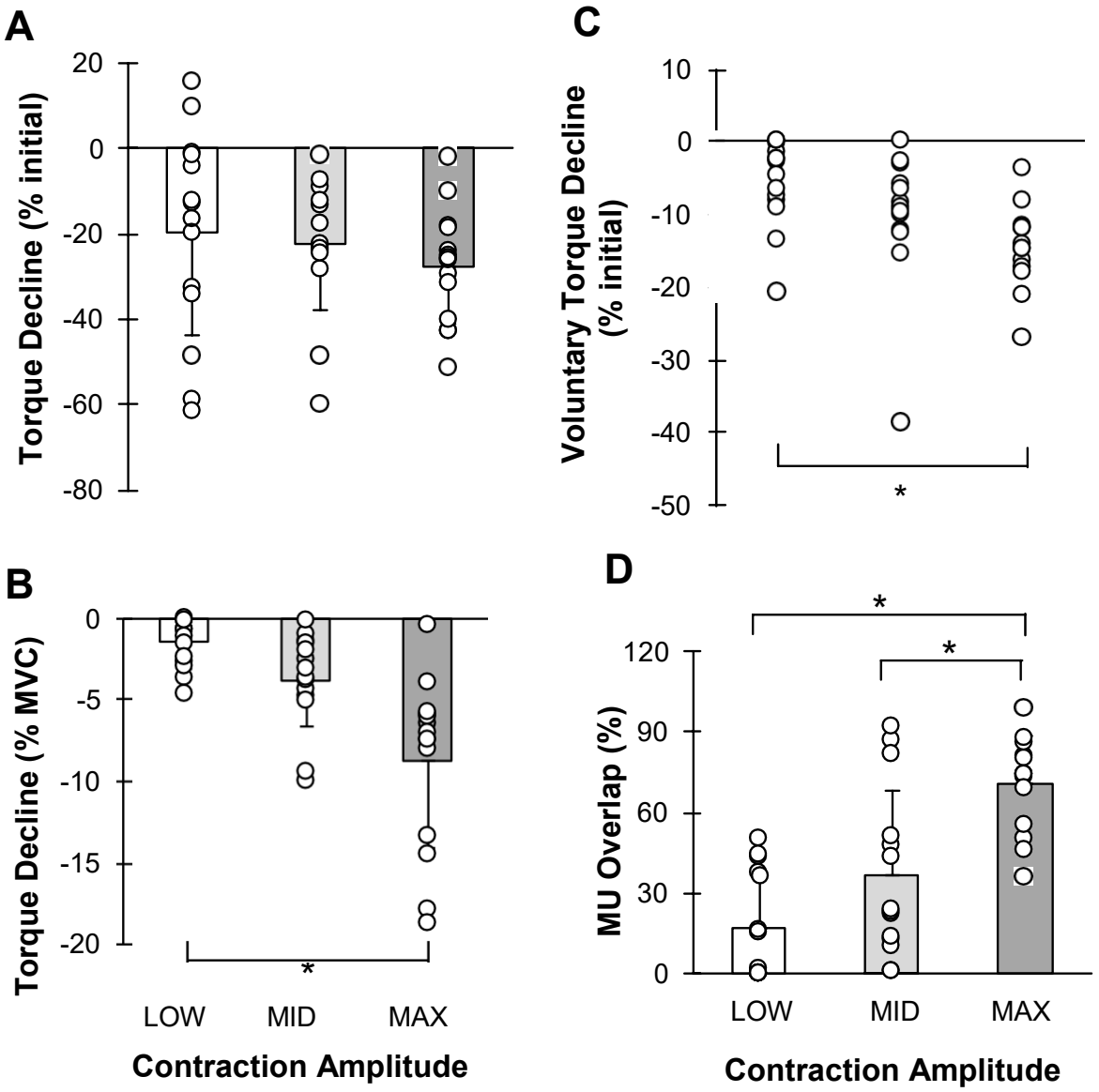

Figure 2-5. Average torque decline and motor unit (MU) overlap across participants during the LOW, MID and MAX sessions. Panel A. Relative decline in torque across participants for each contraction amplitude. To quantify this decline, the mean torque generated during the last ten contractions of each fatigue protocol (Bin 18) was expressed as a percent of that during the first ten contractions (Bin 1). **Panel B.** Absolute decline in torque (% MVC) across participants for each contraction amplitude. **Panel C.** Percent decline in the torque produced during maximal voluntary contractions performed before and immediately after each fatigue protocol**. Panel D.** Average estimated MU overlap across participants for the three contraction amplitudes. For all panels, open circles display individual subject data, while coloured bars represent group means. Error bars represent one standard deviation. * denotes statistical significance ($p < 0.05$).

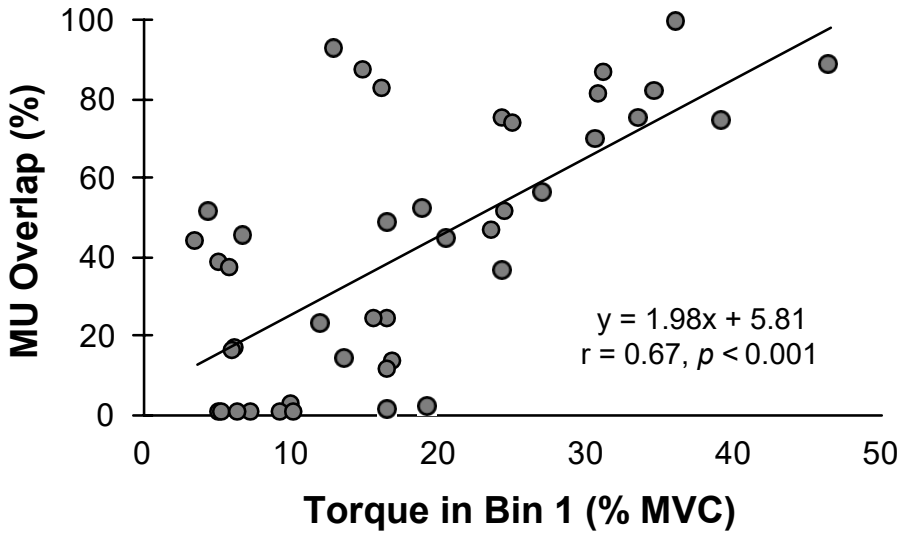

Figure 2-6. Relationship between initial contraction amplitude and MU overlap across participants. The torque generated at the beginning of the fatigue protocol (Bin 1) expressed as a percent of MVC is plotted on the x-axis against percent MU overlap on the y-axis. Regression lines, Pearson's r and p-values for the correlation are displayed.

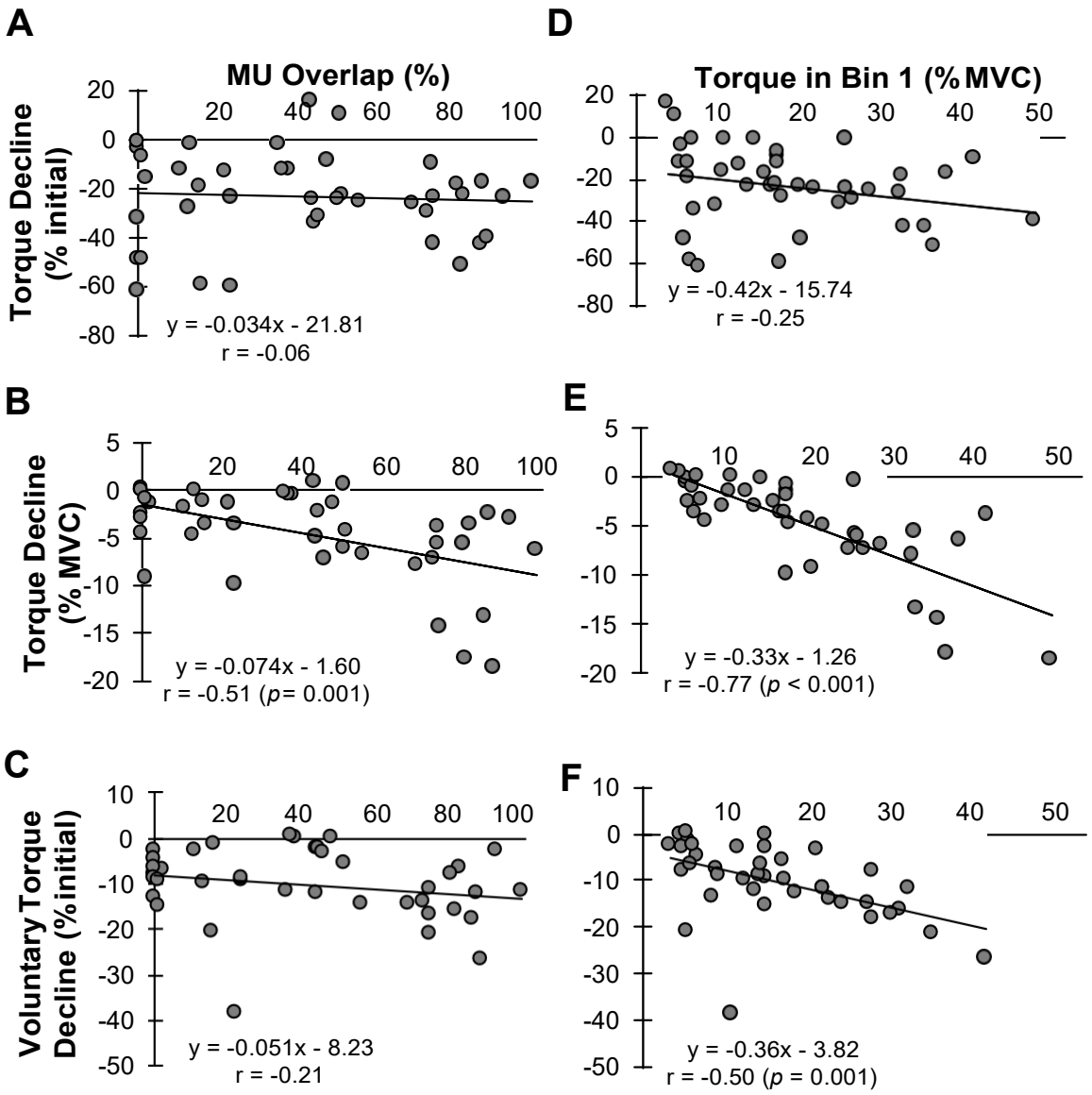

Figure 2-7. Correlations between three measures of fatigue and MU overlap and initial contraction amplitude using group data. The panels on the left side display the relationship between MU overlap and the relative decline in torque (**Panel A**), the absolute decline in torque (**Panel B**), and the relative decline in torque produced during maximum voluntary contractions performed before and after the fatigue protocol (**Panel C**). The panels on the right side display these same measures of fatigue **(Panels D, E, F)** plotted against torque generated at the beginning of the fatigue protocol (Bin 1) expressed as a percent of MVC. Regression lines, Pearson's r and p-values for the correlation are displayed.

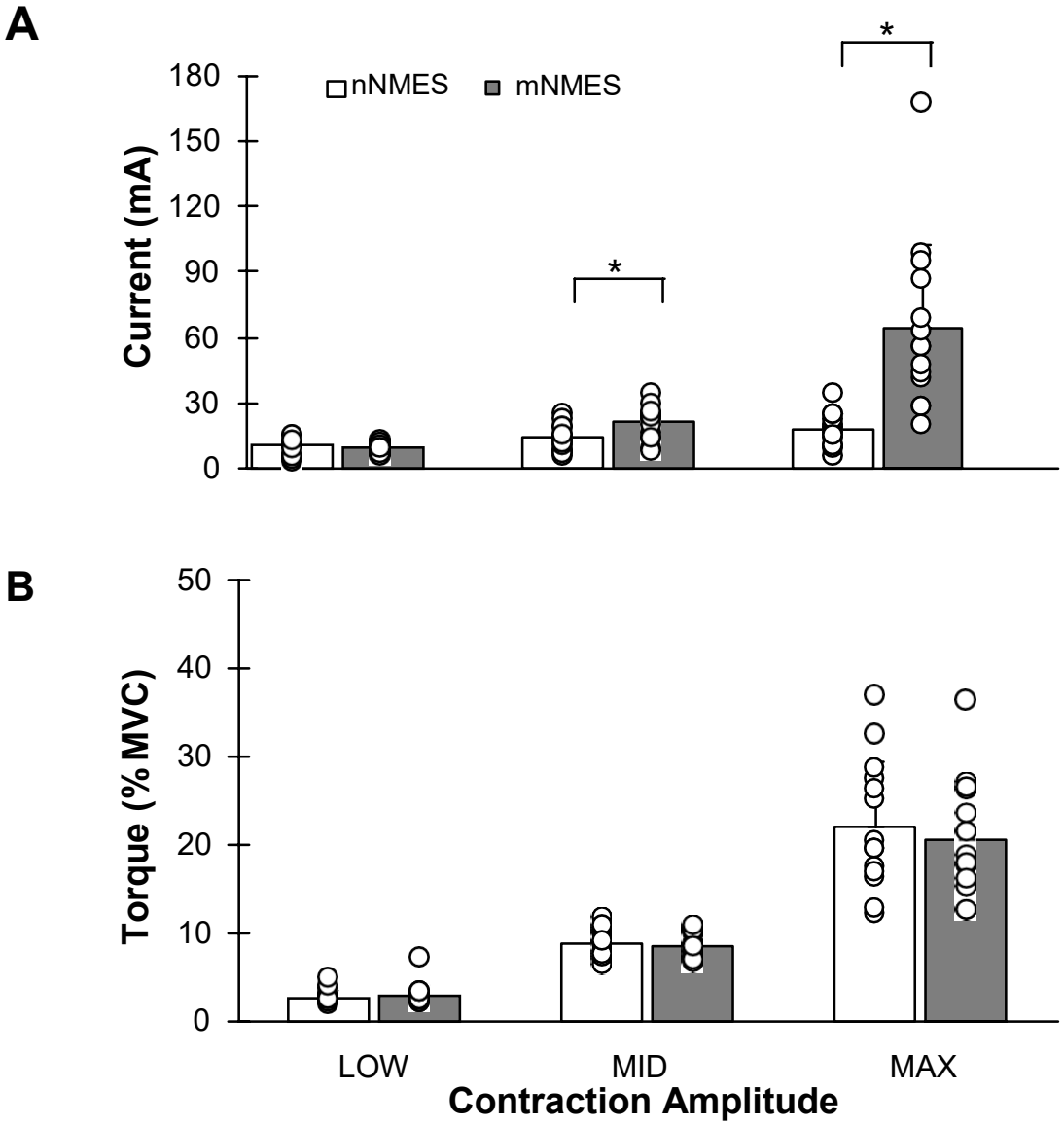

Figure 2-8. Group mean current delivered and torque evoked at each stimulation site for the LOW, MID and MAX fatigue protocols. Panel A. Average current delivered at the nerve (white bars) and muscle (grey bars) stimulation sites that summed to produce contraction amplitudes of ~5% MVC (LOW), ~15% MVC (MID) and ~31% MVC (MAX). * denotes statistical significance ($p < 0.05$). **Panel B.** Torque produced by 20 Hz trains of nNMES (white bars) and mNMES (grey bars).

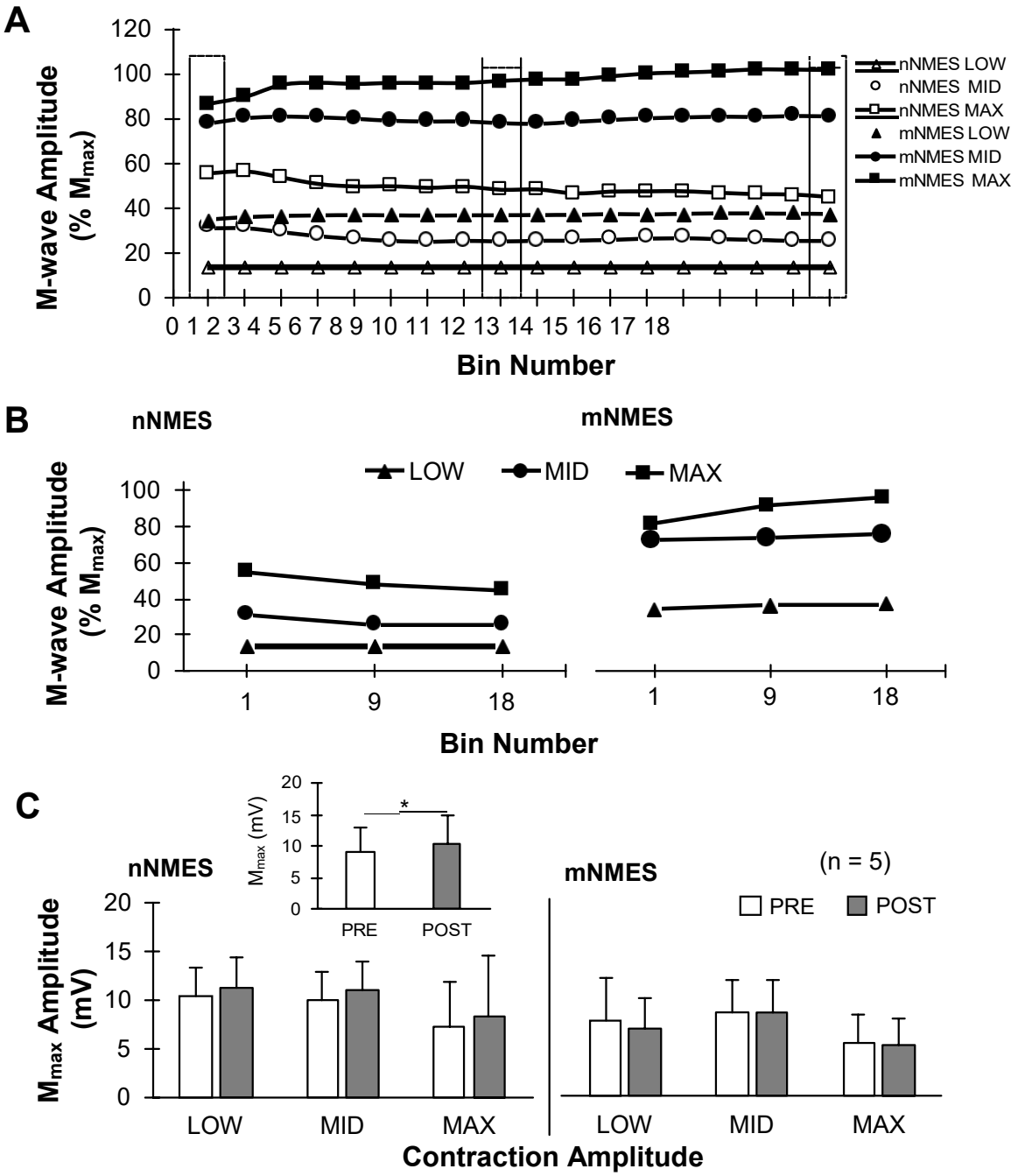

Figure 2-9. Mean M-wave amplitudes for the group recorded during the LOW, MID and MAX sessions. Panel A. Binned, averaged M-wave amplitudes (% M_{max}) across 10 participants during fatigue protocols at three contraction amplitudes. Bars around the contractions generate during Bins 1, 9 and 180 represent the three Bins utilized for statistical analysis in Panel C. **Panel B.** Group mean M-wave amplitudes (% Mmax) evoked during Bins 1, 9 and 18 over the nerve (a) and over the muscle belly (b). **Panel C**. Mmax amplitude (mV) over the common peroneal nerve (a) and muscle belly (b) before ("Pre"; white bars) and after ("Post"; grey bars) the fatigue protocol in a subset of participants (n = 5).

CHAPTER 3: GENERAL DISCUSSION

The work described in this thesis was designed to address gaps in knowledge about fatigue and MU recruitment during delivery of iNMES, a type of stimulation that involves interleaving stimulus pulses between a nerve trunk and muscle belly. iNMES has been shown to reduce fatigue compared to stimulation over a nerve trunk or muscle belly alone, however, this was the first study to examine contraction fatigue when iNMES was used to evoke larger contractions. The experimental procedures utilized and outlined in Chapter 2 were designed to compare the amount of fatigue of the ankle dorsiflexors during iNMES over a range of contraction amplitudes (~5-30% MVC). A secondary goal of the thesis project was to estimate the amount of overlap in the MUs recruited by each stimulation site at each contraction amplitude and to determine whether a relationship existed between contraction fatigue and MU overlap. Section 3.1 of this chapter provides an overview of the main results of the present investigation, while Section 3.2 presents some clinical implications associated with the experiments. Sections 3.3 and 3.4 describe the limitations and future directions of this thesis work, respectively, and Section 3.5 provides a brief summary of the present thesis.

3.1 OVERVIEW

The main finding of the present investigation was that contraction fatigue was not different between the contraction amplitudes tested and that torque decreased ~23% across our three conditions. In addition to no difference in contraction fatigue across amplitudes, fatigue was not significantly correlated with the initial torque generated. While this finding supports previous work that has examined fatigue across different contraction amplitudes (Behringer et al., 2016; Gorgey et al., 2009; Slade et al., 2003), we had expected higher stimulation intensities

to evoke large contractions that would lead to greater overlap in the MUs recruited by each stimulation site. In contrast to this hypothesis, we also did not find a relationship between the relative decline in torque and MU overlap. These data suggest that the percent MU overlap and, consequently, the proportion of MUs firing at twice the rate of those MUs only recruited by a single stimulation site, does not affect the amount of contraction fatigue. As higher NMES-frequencies are associated with enhanced fatigue due to greater metabolic demand of muscle fibres, intramuscular accumulation of inorganic phosphate ions and activity-dependent decreases in axonal excitability (Gregory et al., 2007; Luu et al., *unpublished*; Russ et al., 2002a; Russ et al., 2002b), we do not believe that our results suggest stimulation frequency has minimal bearing on fatigue. Rather, we speculate that the amount of MU overlap in our study was not sufficiently high to tease out the effects of greater MU overlap on contraction fatigue. In our study, we found MU overlap to range from ~20-70% across contraction amplitudes. However, because of the large amount of inter-individual variance in estimated MU overlap, this range in overlap may not have been wide enough to capture significant differences or correlations.

3.2 CLINICAL IMPLICATIONS:

The tibialis anterior is an important muscle for walking as it dorsiflexes the ankle during the swing phase of gait, thereby allowing for toe clearance and normal gait patterning (Kottink et al., 2004). Following a stroke, individuals commonly experience a condition known as foot drop, wherein the ability to dorsiflex the ankle becomes compromised, leading to compensation patterns and an increased risk of falls during walking (Everaert et al., 2010; Kottink et al., 2004). Accordingly, the common peroneal nerve and tibialis anterior muscle belly are frequently stimulated using foot-drop stimulators to allow for ambulation. In addition to the use of foot-

drop stimulators, the tibialis anterior muscle is commonly stimulated during FES-cycling and FES-walking in individuals with muscle paralysis, such as after a spinal cord injury.

Although only ~2 Nm of force is required to dorsiflex the ankle (Bogey et al., 2010; Davy & Audu, 1987; Wiest et al., 2017a), which was achieved during the LOW condition in some of our participants and during the MID condition in all participants, typically higher amplitudes of contraction are requisite to increase muscle strength (Maffiuletti, 2010). Indeed, use of contractions of at least 25-30% MVC are often recommended to increase strength, although much of the literature in this area has focused on the quadriceps muscle (Delitto et al., 1992). The data in the present study suggest that these greater amplitudes needed for strengthening can be utilized without large concern of enhanced relative fatigue. In doing so, iNMES may be used as a rehabilitative tool to increase muscle strength following a stroke or spinal cord injury. However, we found that some participants had difficulty tolerating stimulation intensities to evoke contraction amplitudes of >25% MVC and not a single participant was able to tolerate stimulation intensities to evoke contraction amplitudes of > 50% MVC during our MAX condition. Although we did not measure discomfort in the present study, most participants found stimulation over the muscle belly more uncomfortable than stimulation over the common peroneal nerve trunk. This finding is consistent with previous work that examined discomfort when stimulation was delivered over the common peroneal nerve and tibialis anterior muscle belly (Wiest et al., 2017b). The greater discomfort associated stimulation over the muscle belly can likely be explained by the significantly larger current required at the muscle stimulation site to achieve similar contraction amplitudes to those evoked with stimulation at the nerve site. For example, in our study, ~3.5 times the current was delivered over the muscle belly versus the nerve trunk in the MAX condition to achieved similar torque output between the two sites.

Therein, depending on individual participant tolerability, generating large contractions with iNMES may be unrealistic for some individuals, particularly those with partial or fully intact sensation.

To date, iNMES has been studied primarily in the ankle dorsiflexors, with emphasis on the tibialis anterior muscle. The tibialis anterior muscle is an ideal muscle for iNMES due to to the superficial location of both the common peroneal nerve as it runs adjacent to the fibular head and the tibialis anterior muscle belly which makes both easily accessible via transcuteanous stimulation. However, for muscles located in deeper regions of the leg segments, such as those located in the posterior thigh and innervated by the sciatic nerve, iNMES would not be possible. In addition to its ease in accessibility, the shape and smaller muscle size of the tibialis anterior makes the positioning of the stimulating electrode in relation to the common peroneal nerve trunk relatively stable, even during larger contractions. In contrast, larger muscles that "bulge" during contractions, such as the quadriceps, would be more likely to push the stimulating electrode away from the nerve trunk, thereby compromising the stability of the muscle contractions.

3.3 LIMITATIONS:

There are a number of limitations with the current study design. For one, the contractions generated via iNMES were isometric, with participants seated in a Biodex dynamometer. Whether comparable results would occur when iNMES is delivered in a weight bearing position (i.e. standing) or during functional contractions when joint angle and muscle fascicle lengths are changing, is presently unclear. In addition, all experimental procedures were conducted in individuals without a neurological impairment. As a multitude of metabolic, neuromuscular and

cardiovascular changes occur following neurological impairment and because MUs largely convert from Type S MU to Type FF MU, we would expect a significantly higher percent decline in these populations during iNMES than the average 23% decline found in our study.

Perhaps the largest limitation, however, was our measure of MU overlap, which estimates the proportion of MUs recruited at both the nerve and muscle stimulation sites. This MU estimation was founded on experiments that used direct stimulation of nerves using implanted electrode arrays or cuff electrodes (Fisher et al., 2013; Mcdonnall et al., 2004) and compares the amount of torque evoked when stimulation is delivered separately and together over the two stimulation sites. This MU overlap estimation can be underestimated if central pathways (i.e. activation of sensory pathways which synapse with motoneurons in the spinal cord) contribute to the evoked contractions, or if the stimulation is delivered over the stimulation sites is timed in such a way that the two signals do not arrive at the muscle at the same time, resulting in catch-like effects within the muscle. Despite the issues associated with examining MU overlap, our estimated MU overlap does impact the relationship between fatigue and contraction amplitude.

3.4 FUTURE DIRECTIONS:

Previous work has compared iNMES to nNMES and mNMES at lower contraction amplitudes and found that iNMES reduces fatigue compared to nNMES and mNMES delivered alone. To date, however, the magnitude of fatigue during iNMES compared to nNMES and mNMES at higher contraction amplitudes has not been investigated. Experiments to compare the amount of contraction fatigue during iNMES, mNMES and nNMES during larger contractions, such as the 30% MVC contraction amplitudes, produced in our MAX condition, are needed to determine whether iNMES retains its advantage in reducing contraction fatigue during larger

contractions. In addition to comparing iNMES to conventional methods of NMES during larger contractions, future work should attempt to test iNMES across a wider range of contraction amplitudes than was achieved in our study. We suspect that the range of stimulation amplitudes at which iNMES was tolerated by participants in the present study was not broad enough to detect differences in fatigue between conditions. Conducting similar experiments in individuals without intact sensation, such as individuals with spinal cord injury, may allow for the testing of a wider range of contraction amplitudes and a greater understanding of the effect of contraction amplitude on fatigue during iNMES. Finally, as iNMES has been studied most prominently in the tibialis anterior muscle, future work should focus on examining iNMES in other muscles such as the quadriceps or ankle plantarflexors. These muscles have greater central contributions (as evidenced by H-reflexes) when stimulation is delivered over the femoral or tibial nerves. As these central pathways would recruit a third subset of MUs, (in addition to the two subsets of MUs activated via depolarization of motor axons over the nerve trunk and muscle belly stimulation sites), iNMES may be even more effective in reducing fatigue in these muscles compared to the current data on the tibialis anterior.

3.5 SUMMARY

iNMES was shown to reduce fatigue of the ankle dorsiflexors during contractions of low amplitude compared to conventional types of NMES. This was the first study to examine the amount of contraction fatigue during larger contractions of the ankle dorsiflexors generated via iNMES. Our results demonstrate no difference in fatigue across a range of stimulation amplitudes to produce contraction amplitudes of ~5-30% MVC. Concomitantly, contraction fatigue was not significantly correlated with the initial amplitude of the contraction nor the

amount of overlap in MUs recruited by both the nerve and muscle stimulation sites, despite significantly larger MU overlap during larger contraction. Based on these findings, iNMES shows promise in minimizing fatigue of the ankle dorsiflexors during small to moderate contraction amplitudes.

REFERENCES

Ada, L., Dorsch, S., & Canning, C. G. (2006). Strengthening interventions increase strength and improve activity after stroke: a systematic review. *Australian Journal of Physiotherapy*, *52*(4), 241–248.

Adams, G. R., Harris, R. T., Woodard, D., Dudley, G. A., & Adams, R. (1993). Mapping of electrical muscle stimulation using MRI, *Journal of Applied Physiology*, *74*(2), 532–537.

Alon, G., Allin, J., & Inbar, G. F. (1983). Optimization of pulse duration and pulse charge during transcutaneous electrical nerve stimulation. *Australian Journal of Physiotherapy*, *29*(6), 195–201.

Amiridis, I., Arabatzi, F., Violaris, P., Stavropoulos, E., & Hatzitaki, V. (2005). Static balance improvement in elderly after dorsiflexors electrostimulation training. *European Journal of Applied Physiology*, *94*(4), 424–433.

Andersen, J. L., Mohr, T., Biering-Sørensen, F., Galbo, H., & Kjaer, M. (1996). Myosin heavy chain isoform transformation in single fibres from m. vastus lateralis in spinal cord injured individuals: effects of long-term functional electrical stimulation (FES). *Pflügers Archiv European Journal of Physiology*, *431*(4), 513–518.

Babault, N., Cometti, G., Bernardin, M., Pousson, M., & Chatard, J.-C. (2007). Effects of electromyostimulation training on muscle strength and power of elite rugby players. *Journal of Strength and Conditioning Research*, *21*(2), 431.

Bade, M. J., & Stevens-Lapsley, J. E. (2012). Restoration of physical function in patients following total knee arthroplasty: an update on rehabilitation practices. *Current Opinion in Rheumatology*, *24*(2), 208–214.

Bajd, T., Kralj, A., Turk, R., Benko, H., & Šega, J. (1989). Use of functional electrical stimulation in the rehabilitation of patients with incomplete spinal cord injuries. *Journal of Biomedical Engineering*, *11*(2), 96–102.

Baker, L. L., Rubayi, S., Villar, F., & Demuth, S. K. (1996). Effect of electrical stimulation waveform on healing of ulcers in human beings with spinal cord injury. *Wound Repair and Regeneration*, *4*(1), 21–28.

Baldi, J. C., Jackson, R. D., Moraille, R., & Mysiw, W. J. (1998). Muscle atrophy is prevented in patients with acute spinal cord injury using functional electrical stimulation. *Spinal Cord*, *36*(7), 463–9.

Behringer, M., Grützner, S., Montag, J., McCourt, M., Ring, M., & Mester, J. (2016). Effects of stimulation frequency, amplitude, and impulse width on muscle fatigue. *Muscle & Nerve*, *53*(4), 608–616.

Bergquist, A. J., Clair, J. M., & Collins, D. F. (2011). Motor unit recruitment when neuromuscular electrical stimulation is applied over a nerve trunk compared with a muscle belly: triceps surae. *European Journal of Applied Physiology*, *111*(10), 2399–2407.

Bergquist, A. J., Wiest, M. J., Okuma, Y., & Collins, D. F. (2017). Interleaved neuromuscular electrical stimulation after spinal cord injury. *Muscle & Nerve*.

Bickel, C. S., Gregory, C. M., & Dean, J. C. (2011). Motor unit recruitment during neuromuscular electrical stimulation: a critical appraisal. *European Journal of Applied Physiology*, *111*(10), 2399–2407.

Bigland-Ritchie, B., Jones, D., & Woods, J. (1979). Excitation frequency and muscle fatigue: electrical responses during human voluntary and stimulated contractions. *Experimental Neurology*, *64*(2), 414–427.

Bigland-Ritchie, B. R., Furbush, F. H., Gandevia, S. C., & Thomas, C. K. (1992). Voluntary discharge frequencies of human motoneurons at different muscle lengths. *Muscle & Nerve*, *15*(2), 130–137.

Binder, M. D., Hirokawa, N., & Windhorst, U. (Eds.). (2009). Cross-bridge Theory. In *Encyclopedia of Neuroscience* (p. 905). Berlin, Heidelberg: Springer Berlin Heidelberg.

Binder-Macleod, S., & Scott, W. (2001). Comparison of fatigue produced by various electrical stimulation trains. *Acta Physiologica*, *172*(3), 195–203.

Bø, K., Talseth, T., & Holme, I. (1999). Single blind, randomised controlled trial of pelvic floor exercises, electrical stimulation, vaginal cones, and no treatment in management of genuine stress incontinence in women. *Bmj*, *318*(7182), 487–493.

Bogey, R., Gitter, A. J., & Barnes, L. (2010). Determination of ankle muscle power in normal gait using an EMG-to-force processing approach. *Journal of Electromyography and Kinesiology*, *20*(1), 46–54.

Bostock, H., & Grafe, P. (1985). Activity-dependent excitability changes in normal and demyelinated rat spinal root axons. *The Journal of Physiology*, *365*(1), 239–257.

Branner, A., Stein, R. B., & Normann, R. A. (2001). Selective stimulation of cat sciatic nerve using an array of varying-length microelectrodes. *Journal of Neurophysiology*, *85*(4), 1585–1594.

Burke, D. (2016). Clinical Neurophysiology Practice Clinical uses of H reflexes of upper and lower limb muscles. *Clinical Neurophysiology Practice*, *1*, 9–17.

Burke, R. E. (1967). Motor unit types of cat triceps surae muscle. *The Journal of Physiology*, *193*(1), 141.

Burridge, J., Wood, D., Taylor, P., & McLellan, D. (2001). Indices to describe different muscle activation patterns, identified during treadmill walking, in people with spastic drop-foot. *Medical Engineering & Physics*, *23*(6), 427–434.

Byrne, C., O'Keeffe, D., Donnelly, A., & Lyons, G. (2007). Effect of walking speed changes on tibialis anterior EMG during healthy gait for FES envelope design in drop foot correction. *Journal of Electromyography and Kinesiology*, *17*(5), 605–616.

Castro, M. J., Apple, D. F., Staron, R. S., Campos, G. E., & Dudley, G. A. (1999). Influence of complete spinal cord injury on skeletal muscle within 6 mo of injury. *Journal of Applied Physiology*, *86*(1), 350–358.

Chae, J., & Hart, R. (1998). Comparison of discomfort associated with surface and percutaneous intramuscular electrical stimulation for persons with chronic hemiplegia1. *American Journal of Physical Medicine & Rehabilitation*, *77*(6), 516–522.

Chae, J., Sheffler, L., & Knutson, J. (2008). Neuromuscular electrical stimulation for motor restoration in hemiplegia. *Topics in Stroke Rehabilitation*, *15*(5), 412–426.

Christie, A., & Kamen, G. (2009). Motor unit firing behavior during prolonged 50 % MVC dorsiflexion contractions in young and older adults. *Journal of Electromyography and Kinesiology*, *19*(4), 543–552.

Connelly, D. M., Rice, C. L., Roos, M. R., & Vandervoort, A. A. (1999). Motor unit firing rates and contractile properties in tibialis anterior of young and old men. *J Appl Physiol (1985)*, *87*(2), 843–852.

Currier, D., & Mann, R. (1983). Muscular strength development by electrical stimulation in healthy individuals. *Physical Therapy*, *63*(6), 915–921.

Dalton, B. H., Harwood, B., Davidson, A. W., & Rice, C. L. (2009). Triceps surae contractile properties and firing rates in the soleus of young and old men. *J Appl Physiol (1985)*, *107*(6), 1781–1788.

Davy, D., & Audu, M. (1987). A dynamic optimization technique for predicting muscle forces in the swing phase of gait. *Journal of Biomechanics*, *20*(2), 187–201.

De Luca, C. J., & Hostage, E. C. (2010). Relationship between firing rate and recruitment threshold of motoneurons in voluntary isometric contractions. *Journal of Neurophysiology*, *104*(2), 1034–1046.

de Oliveira Melo, M., Aragão, F. A., & Vaz, M. A. (2013). Neuromuscular electrical stimulation for muscle strengthening in elderly with knee osteoarthritis–a systematic review. *Complementary Therapies in Clinical Practice*, *19*(1), 27–31.

Delitto, A., Strube, M. J., Shulman, A. D., & Minor, S. D. (1992). A study of discomfort with electrical stimulation. *Physical Therapy*, *72*(6), 410–421.

Doucet, B. M., Lam, A., & Griffin, L. (2012). Neuromuscular electrical stimulation for skeletal muscle function. *The Yale Journal of Biology and Medicine*, *85*, 201–215.

Duvoisin, M. R., Convertino, V. A., Buchanan, P., Gollnick, P., & Dudley, G. A. (1989). Characteristics and preliminary observations of the influence of electromyostimulation on the size and function of human skeletal muscle during 30 days of simulated microgravity. *Aviation, Space, and Environmental Medicine*, *60*(7), 671–678.

Edström, L., & Kugelberg, E. (1968). Histochemical composition, distribution of fibres and fatiguability of single motor units. Anterior tibial muscle of the rat. *Journal of Neurology, Neurosurgery, and Psychiatry*, *31*(5), 424–433.

Embrey, D. G., Holtz, S. L., Alon, G., Brandsma, B. A., & McCoy, S. W. (2010). Functional electrical stimulation to dorsiflexors and plantar flexors during gait to improve walking in adults with chronic hemiplegia. *Archives of Physical Medicine and Rehabilitation*, *91*(5), 687–696.

Enoka, R. M. (2002). Activation order of motor axons in electrically evoked contractions. *Muscle and Nerve*, *25*(6), 763–764.

Enoka, R. M., & Duchateau, J. (2008). Muscle fatigue: what, why and how it influences muscle function. *The Journal of Physiology*, *586*(1), 11–23.

Everaert, D. G., Thompson, A. K., Chong, S. L., & Stein, R. B. (2010). Does functional electrical stimulation for foot drop strengthen corticospinal connections? *Neurorehabilitation and Neural Repair*, *24*(2), 168–77.

Faghri, P. D., Glaser, R. M., & Figoni, S. F. (1992). Functional electrical stimulation leg cycle ergometer exercise: training effects on cardiorespiratory responses of spinal cord injured subjects at rest and during submaximal exercise. *Archives of Physical Medicine and Rehabilitation*, *73*(11), 1085–1093.

Feinstein, B., Lindegard, B., Nyman, E., & Wohlfart, G. (1955). Morphologic studies of motor units in normal human muscles. *Acta Anatomica*, *23*(2), 127–142.

Finkelstein, G. (2015). Mechanical neuroscience: Emil du Bois-Reymond's innovations in theory and practice, *Frontiers in Systems Neuroscience*, *9*, 1-4.

Finkelstein, G., & Finkelstein, G. (2014). Emil du Bois-Reymond on "The Seat of the Soul." *Journal of the History of Neurosciences*, *23*(1), 45-55.

Fisher, L. E., Tyler, D. J., & Triolo, R. J. (2013). Optimization of selective stimulation parameters for multi-contact electrodes, 1–8.

Fitzgerald, G. K., Piva, S. R., & Irrgang, J. J. (2003). A modified neuromuscular electrical stimulation protocol for quadriceps strength training following anterior cruciate ligament reconstruction. *Journal of Orthopaedic & Sports Physical Therapy*, *33*(9), 492–501.

Floeter, M. K. (2010). Structure and function of muscle fibers and motor units. *Disorders of Voluntary Muscle., 8th Ed. Cambridge University Press, Cambridge*, 1–10.

Fodstad, H., & Hariz, M. (2007). Electricity in the treatment of nervous system disease. *Acta Neurochirurgica. Supplement*, *97*(Pt 1), 11–19.

Garland, S. J., Garner, S., & McComas, A. (1988). Reduced voluntary electromyographic activity after fatiguing stimulation of human muscle. *The Journal of Physiology*, *401*(1), 547–556.

Garshick, E., Kelley, A., Cohen, S., Garrison, A., Tun, C., Gagnon, D., & Brown, R. (2005). A prospective assessment of mortality in chronic spinal cord injury. *Spinal Cord*, *43*(7), 408–416.

Gasser, H. S. (1935). Changes in nerve-potentials produced by rapidly repeated stimuli and their relation to the responsiveness of nerve to stimulation. *American Journal of Physiology--Legacy Content*, *111*(1), 35–50.

Gibbons, R., McCarthy, I., Gall, A., Stock, C., Shippen, J., & Andrews, B. (2014). Can FES-rowing mediate bone mineral density in SCI: a pilot study. *Spinal Cord*, *52*(s3), S4.

Gibbons, R., Stock, C., Andrews, B., Gall, A., & Shave, R. (2016). The effect of FES-rowing training on cardiac structure and function: pilot studies in people with spinal cord injury. *Spinal Cord*, *54*(10), 822–829.

Gibson, J., Smith, K., & Rennie, M. (1988). Prevention of disuse muscle atrophy by means of electrical stimulation: maintenance of protein synthesis. *The Lancet*, *332*(8614), 767–770.

Ginis, K. A. M., Hicks, A. L., Latimer, A. E., Warburton, D. E. R., Bourne, C., Ditor, D. S., & Goodwin, D. L. (2011). The development of evidence-informed physical activity guidelines for adults with spinal cord injury, *Spinal cord*, 49(11), 1088-1096.

Gondin, J., Cozzone, P. J., & Bendahan, D. (2011). Is high-frequency neuromuscular electrical stimulation a suitable tool for muscle performance improvement in both healthy humans and athletes? *European Journal of Applied Physiology*, *111*(10), 2473.

Gordon, T., & de Zepetnek, J. E. T. (2016). Motor unit and muscle fiber type grouping after peripheral nerve injury in the rat. *Experimental Neurology*, *285*, 24–40.

Gordon, T., & Mao, J. (1994). Muscle atrophy and procedures for training after spinal cord injury. *Physical Therapy*, *74*(1), 50–60.

Gorgey, A.S, Black, C., Elder, C., & Dudley, G. (2009). Effects of Electrical Stimulation Parameters on Fatigue in Skeletal Muscle. *The Journal of Orthopaedic and Sports Physical Therapy*, *39*(9), 684–692.

Gorgey, A. S., & Dudley, G. (2008). The role of pulse duration and stimulation duration in maximizing the normalized torque during neuromuscular electrical stimulation. *The Journal of Orthopaedic and Sports Physical Therapy*, *38*(8), 508–16.

Gorgey, A. S., Mahoney, E., Kendall, T., & Dudley, G. A. (2006). Effects of neuromuscular electrical stimulation parameters on specific tension. *European Journal of Applied Physiology*, *97*(6), 737–744.

Graham, M. T., Rice, C. L., & Dalton, B. H. (2016). Motor unit firing rates of the gastrocnemii during maximal brief steady-state contractions in humans. *Journal of Electromyography and Kinesiology*, *26*, 82–87.

Granat, M. H., Ferguson, A. C. B., Andrews, B. J., & Delargy, M. (1993). The role of functional electrical stimulation in the rehabilitation of patients with incomplete spinal cord injury - observed benefits during gait studies, *31*, 207–215.

Gregory, C., & Bickel, C. (2005). Recruitment patterns in human skeletal muscle during electrical stimulation. *Physical Therapy*, *85*(4), 358–364.

Gregory, C. M., Dixon, W., & Bickel, C. S. (2007). Impact of varying pulse frequency and duration on muscle torque production and fatigue. *Muscle & Nerve*, *35*(4), 504–509.

Gremeaux, V., Renault, J., Pardon, L., Deley, G., Lepers, R., & Casillas, J.-M. (2008). Low-frequency electric muscle stimulation combined with physical therapy after total hip arthroplasty for hip osteoarthritis in elderly patients: a randomized controlled trial. *Archives of Physical Medicine and Rehabilitation*, *89*(12), 2265–2273.

Griffin, L., Decker, M. J., Hwang, J. Y., Wang, B., Kitchen, K., Ding, Z., & Ivy, J. L. (2009). Functional electrical stimulation cycling improves body composition, metabolic and neural factors in persons. *Journal of Electromyography and Kinesiology*, *19*(4), 614–622.

Grobelnik, S., & Kralj, A. (1973). Functional electrical stimulation—a new hope for paraplegic patients. *Bull. Prosthet. Res*, *20*, 75–102.

Gruther, W., Kainberger, F., Fialka-Moser, V., Paternostro-Sluga, T., Quittan, M., Spiss, C., & Crevenna, R. (2010). Effects of neuromuscular electrical stimulation on muscle layer thickness of knee extensor muscles in intensive care unit patients: a pilot study. *Journal of Rehabilitation Medicine*, *42*(6), 593–597.

Hamid, S., & Hayek, R. (2008). Role of electrical stimulation for rehabilitation and regeneration after spinal cord injury: An overview. *European Spine Journal*, *17*(9), 1256–1269.

Harris, S., LeMaitre, J. P., Mackenzie, G., Fox, K. A., & Denvir, M. A. (2003). A randomised study of home-based electrical stimulation of the legs and conventional bicycle exercise training for patients with chronic heart failure. *European Heart Journal*, *24*(9), 871–878.

Häusser, M. (2000). The Hodgkin-Huxley theory of the action potential, *Nature Neuroscience*, *3*, 1165-1165.

Heckman, C. J., & Enoka, R. M. (2012). Motor Unit, *Comprehensive Physiology.*

Henriksson-Larsén, K. B., Lexell, J., & Sjöström, M. (1983). Distribution of different fibre types in human skeletal muscles. I. Method for the preparation and analysis of cross-sections of whole tibialis anterior. *The Histochemical Journal*, *15*(2), 167–178.

Ho, C. H., Triolo, R. J., Elias, A. L., Kilgore, K. L., Dimarco, A. F., Bogie, K., … Elias, A. L. (2014). HHS Public Access. *Phys Med Rehabil Clin N Am*, *25*(3), 1–30.

Hoff, H. E. (1936). Galvani and the pre-Galvanian electrophysiologists. *Annals of Science*, *1*(2), 157–172.

Hoffmann, P. (1910). Beitrag zur Kenntnis der menschlichen Reflexe mit beson- derer Berucksichtigung der elektrischen Erscheinungen. *Arch Anat Physiol 1*, *1*, 223–246.

Houghton, P. E., Kincaid, C. B., Lovell, M., Campbell, K. E., Keast, D. H., Woodbury, M. G., & Harris, K. A. (2003). Effect of electrical stimulation on chronic leg ulcer size and appearance. *Physical Therapy*, *83*(1), 17–28.

Hultman, E., Sjöholm, H., Jäderholm-Ek, I., & Krynicki, J. (1983). Evaluation of methods for electrical stimulation of human skeletal muscle in situ. *Pflügers Archiv European Journal of Physiology*, *398*(2), 139–141.

Johnson, M., Polgar, J., Weightman, D., & Appleton, D. (1973). Data on the distribution of fibre types in thirty-six human muscles: an autopsy study. *Journal of the Neurological Sciences*, *18*(1), 111–129.

Jones, D. A. (1979). Excitation Frequency and Muscle Fatigue: Mechanical Responses during Voluntary and Stimulated Contractions, *413*, 401–413.

Jubeau, M., Gondin, J., Martin, A., Sartorio, A., & Maffiuletti, N. A. (2007). Random motor unit activation by electrostimulation. *International Journal of Sports Medicine*, *28*(11), 901–904.

Kamen, G., & Knight, C. A. (2004). Training-Related Adaptations in Motor Unit Discharge Rate in Young and Older Adults, *The Journals of Gerontology Series A: Biological Sciences and Medical Sciences, 59*(12), 1334–1338.

Kandel, E. R., Schwartz, J. H., & Jessell, T. M. (1991). *Principles of Neural Science* (3rd ed.). New York: Elsevier Science Publishinging Co. Inc.

Kanning, K. C., Kaplan, A., & Henderson, C. E. (2010). Motor neuron diversity in development and disease. *Annual Review of Neuroscience*, *33*, 409–440.

Kernell, D. (1995). Neuromuscular frequency-coding and fatigue. In *Fatigue* (pp. 135–145). Springer.

Kesar, T., & Binder-Macleod, S. (2006). Effect of frequency and pulse duration on human muscle fatigue during repetitive electrical stimulation. *Experimental Physiology*, *91*(6), 967–76.

Kesar, T., Chou, L. W., & Binder-Macleod, S. A. (2008). Effects of stimulation frequency versus pulse duration modulation on muscle fatigue. *Journal of Electromyography and Kinesiology*, *18*(4), 662–671.

Kiernan, M. C., Lin, C. S., & Burke, D. (2004). Differences in activity-dependent hyperpolarization in human sensory and motor axons. *The Journal of Physiology*, *558*(1), 341–349.

Kiernan, M. C., Mogyoros, I., & Burke, D. (1996). Changes in excitability and impulse transmission following prolonged repetitive activity in normal subjects and patients with a focal nerve lesion. *Brain*, *119*(6), 2029–2037.

Kiernan, M., & Lin, C. (2012). Nerve excitability: a clinical translation. *Aminoff's Electrodiagnosis in Clinical Neurology. 6th Ed. Philadelphia: Saunders*, 345–365.

Kim, C. K., Bangsbo, J., Strange, S., Karpakka, J., & Saltin, B. (1995). Metabolic response and muscle glycogen depletion pattern during prolonged electrically induced dynamic exercise in man. *Scandinavian Journal of Rehabilitation Medicine*, *27*(1), 51–58.

Kim, K.-M., Croy, T., Hertel, J., & Saliba, S. (2010). Effects of neuromuscular electrical stimulation after anterior cruciate ligament reconstruction on quadriceps strength, function, and patient-oriented outcomes: a systematic review. *Journal of Orthopaedic & Sports Physical Therapy*, *40*(7), 383–391.

Kirk, E. A., & Rice, C. L. (2016). Contractile function and motor unit firing rates of the human hamstrings. *Journal of Neurophysiology*, (October), jn.00620.2016.

Kocina, P. (1997). Body composition of spinal cord injured adults. *Sports Medicine*, *23*(1), 48–60.

Kottink, A. I. R., Oostendorp, L. J. M., Buurke, J. H., Nene, A. V., Hermens, H. J., & IJzerman, M. J. (2004). The orthotic effect of functional electrical stimulation on the improvement of walking in stroke patients with a dropped foot: A systematic review. *Artificial Organs*, *28*(6).

Lake, D. A. (1992). Neuromuscular electrical stimulation. *Sports Medicine*, *13*(5), 320–336.

Laufer, Y., Ries, J. D., Leininger, P. M., & Alon, G. (2001). Quadriceps femoris muscle torques and fatigue generated by neuromuscular electrical stimulation with three different waveforms. *Physical Therapy*, *81*(7), 1307–1316.

Lee, S. C. K., Russ, D. W., & Binder-Macleod, S. A. (2009). Force-Frequency Relation of Skeletal Muscle. In M. D. Binder, N. Hirokawa, & U. Windhorst (Eds.), *Encyclopedia of Neuroscience* (pp. 1608–1611). Berlin, Heidelberg: Springer Berlin Heidelberg.

Liberson, W. T., Holmquest, H. J., Scot, D., & Dow, M. (1961). Functional electrotherapy: stimulation of the peroneal nerve synchronized with the swing phase of the gait of hemiplegic patients. *Archives of Physical Medicine and Rehabilitation*, *42*, 101–105.

Lou, J. W. H., Bergquist, A. J., Aldayel, A., Czitron, J., & Collins, D. F. (2016). Interleaved neuromuscular electrical stimulation reduces muscle fatigue. *Muscle & Nerve*.

Lundström, E., Smits, A., Terént, A., & Borg, J. (2010). Time-course and determinants of spasticity during the first six months following first-ever stroke. *Journal of Rehabilitation Medicine*, *42*(4), 296–301.

Luu, M. J., Jones, K. E. & Collins, D. F. (2017). Decreases in the excitability of motor axons contribute substantially to contraction fatigability during neuromuscular electrical stimulation. *unpublished manuscript*.

MacIntosh, F. (1963). Synthesis and storage of acetylcholine in nervous tissue. *Canadian Journal of Biochemistry and Physiology*, *41*(12), 2555–2571.

MacIntosh, F., & Collier, B. (1976). Neurochemistry of cholinergic terminals. In *Neuromuscular junction* (pp. 99–228). Springer.

Maffiuletti, N. A. (2006). The use of electrostimulation exercise in competitive sport. *International Journal of Sports Physiology and Performance*, *1*(4), 406–407.

Maffiuletti, N. A. (2010). Physiological and methodological considerations for the use of neuromuscular electrical stimulation. *European Journal of Applied Physiology*, *110*(2), 223–234.

Maffiuletti, N. A., Bramanti, J., Jubeau, M., Bizzini, M., Deley, G., & Cometti, G. (2009). Feasibility and efficacy of progressive electrostimulation strength training for competitive tennis players. *The Journal of Strength & Conditioning Research*, *23*(2), 677–682.

Mahoney, E. T., Bickel, C. S., Elder, C., Black, C., Slade, J. M., Apple, D., & Dudley, G. A. (2005). Changes in skeletal muscle size and glucose tolerance with electrically stimulated resistance training in subjects with chronic spinal cord injury. *Archives of Physical Medicine and Rehabilitation*, *86*(7), 1502–1504.

Martínez-López, E. J., Benito-Martínez, E., Hita-Contreras, F., Lara-Sánchez, A., & Martínez-Amat, A. (2012). Effects of electrostimulation and plyometric training program

combination on jump height in teenage athletes. *Journal of Sports Science & Medicine*, *11*(4), 727.

Matkowski, B., Lepers, R., & Martin, A. (2015). Torque decrease during submaximal evoked contractions of the quadriceps muscle is linked not only to muscle fatigue. *Journal of Applied Physiology*, *118*(9), 1136–1144.

Mayr, W., Bijak, M., Girsch, W., Hofer, C., Lanmüller, H., Rafolt, D., … Schnetz, G. (1999). MYOSTIM-FES to prevent muscle atrophy in microgravity and bed rest: preliminary report. *Artificial Organs*, *23*(5), 428–431.

Mcdonnall, D., Clark, G. A., & Normann, R. A. (2004). Selective motor unit recruitment via intrafascicular multielectrode stimulation. *Canadian Journal of Physiology and Pharmacology*, 82(8-9), 599–609.

Mesin, L., Merlo, E., Merletti, R., & Orizio, C. (2010). Investigation of motor unit recruitment during stimulated contractions of tibialis anterior muscle. *Journal of Electromyography and Kinesiology*, *20*(4), 580–589.

Milner-Brown, H. S., Stein, R. B., & Yemm, R. (1973). Changes in firing rate of human motor units during linearly changing voluntary contractions. *The Journal of Physiology*, *230*(2), 371–390.

Misiaszek, J. E. (2003). The H-reflex as a tool in neurophysiology: It's limitations and uses in understanding nervous system function. *Muscle & Nerve, 28*(2), 144–160.

Moe, J. H., & Post, H. W. (1962). Functional electrical stimulation for ambulation in hemiplegia. *The Journal-Lancet*, *82*, 285–288.

Mohr, T., Andersen, J. L., Biering-Sørensen, F., Galbo, H., Bangsbo, J., Wagner, A., & Kjaer, M. (1997). Long term adaptation to electrically induced cycle training in severe spinal cord injured individuals. *Spinal Cord*, *35*(1).

Molander, C., Xu, Q., & Grant, G. (1984). The Cytoarchitectonic Organization of the Spinal Cord in the Rat. I. The Lower Thoracic and Lurnbosacral Cord, *230*(1), 133–141.

Moore, K. N., Griffiths, D., & Hughton, A. (1999). Urinary incontinence after radical prostatectomy: a randomized controlled trial comparing pelvic muscle exercises with or without electrical stimulation. *BJU International*, *83*(1), 57–65.

Nash, M. S. (2005). Exercise as a health-promoting activity following spinal cord injury. *Journal of Neurologic Physical Therapy*, *29*(2), 87–103.

Neyroud, D., Dodd, D., Gondin, J., Maffiuletti, N. A., Kayser, B., & Place, N. (2014). Wide-pulse-high-frequency neuromuscular stimulation of triceps surae induces greater muscle fatigue compared with conventional stimulation. *Journal of Applied Physiology*, *116*(10), 1281–1289.

Okuma, Y., Bergquist, A. J., Hong, M., Chan, K. M., & Collins, D. F. (2013). Electrical stimulation site influences the spatial distribution of motor units recruited in tibialis anterior. *Clinical Neurophysiology*, *124*(11), 2257–2263.

Packman-Braun, R. (1988). Relationship between functional electrical stimulation duty cycle and fatigue in wrist extensor muscles of patients with hemiparesis. *Physical Therapy*, *68*(1), 51–56.

Pacy, P., Hesp, R., Halliday, D., Katz, D., Cameron, G., & Reeve, J. (1988). Muscle and bone in paraplegic patients, and the effect of functional electrical stimulation. *Clinical Science*, *75*(5), 481–487.

Palmieri, R. M., Ingersoll, C. D., & Hoffman, M. A. (2004). The Hoffmann Reflex: Methodologic Considerations and Applications for Use in Sports Medicine and Athletic Training Research, *Journal of Athletic Training, 39*(3), 268–277.

Pelletier, C.A., & Hicks, A.L. (2010). The length-tension relationship of human dorsiflexor and plantarflexor muscles after spinal cord injury. *Spinal Cord*, *48*(3), 202–6.

Pelletier, C., & Hicks, A.L. (2011). Muscle fatigue characteristics in paralyzed muscle after spinal cord injury. *Spinal Cord*, *49*(1), 125–130.

Person, R. (1974). Rhythmic activity of a group of human motoneurones during voluntary contraction of a muscle. *Electroencephalography and Clinical Neurophysiology*, *36*, 585–595.

Petterson, S. C., Mizner, R. L., Stevens, J. E., Raisis, L. E. O., Bodenstab, A., Newcomb, W., & Snyder-mackler, L. (2009). Improved function from progressive strengthening Interventions after total knee arthroplasty: A randomized clinical trial with an Imbedded prospective cohort. *Arthritis Care & Research, 61*(2), 174–183.

Piccolino, M., & Bresadola, M. (2013). *Shocking frogs: Galvani, Volta, and the electric origins of neuroscience*. Oxford University Press, USA.

Pollock, A., Farmer, S. E., Brady, M. C., Langhorne, P., Mead, G. E., Mehrholz, J., & van Wijck, F. (2013). Interventions for improving upper limb function after stroke. *The Cochrane Database of Systematic Reviews*, *11*.

Purves, D. E., Augustine, G. J., Fitzpatrick, D. E., & Katz, L. C. (1997). *Neuroscience.* Sunderland, MA, US: Sinauer Associates.

Querol, F., Gallach, J. E., Toca-Herrera, J., Gomis, M., & Gonzalez, L.-M. (2006). Surface electrical stimulation of the quadriceps femoris in patients affected by haemophilia A. *Haemophilia*, *12*(6), 629–632.

Quittan, M., Wiesinger, G. F., Sturm, B., Puig, S., Mayr, W., Sochor, A., … Fialka-Moser, V. (2001). Improvement of thigh muscles by neuromuscular electrical stimulation in patients with refractory heart failure: a single-blind, randomized, controlled trial. *American Journal of Physical Medicine & Rehabilitation*, *80*(3), 206–214.

Rafuse, V. F., & Gordon, T. (1996). Self-reinnervated cat medial gastrocnemius muscles. II. analysis of the mechanisms and significance of fiber type grouping in reinnervated muscles. *Journal of Neurophysiology*, *75*(1), 282.

Ragnarsson, K. T. (2008). Functional electrical stimulation after spinal cord injury: current use, therapeutic effects and future directions. *Spinal Cord*, *46*(4), 255–74.

Rexed, B. (1952). The cytoarchitectonic organization of the spinal cord in the cat. *Journal of Comparative Neurology*, *96*(3), 415–495.

Roig, M., & Reid, W. D. (2009). Electrical stimulation and peripheral muscle function in COPD: a systematic review. *Respiratory Medicine*, *103*(4), 485–495.

Roos, M. R., Rice, C. L., Connelly, D. M., & Vandervoort, A. A. (1999). Quadriceps muscle strength, contractile properties, and motor unit firing rates in young and old men. *Muscle & Nerve*, *22*(8), 1094–1103.

Rubinstein, S., & Kamen, G. (2005). Decreases in motor unit firing rate during sustained maximal-effort contractions in young and older adults, *Journal of Electromyography and Kinesiology*, *15*, 536–543.

Russ, D. W., Elliott, M. A., Vandenborne, K., Walter, G. A., & Binder-Macleod, S. A. (2002a). Metabolic costs of isometric force generation and maintenance of human skeletal muscle. *American Journal of Physiology - Endocrinology and Metabolism*, *282*(2), E448-E457.

Russ, D. W., Vandenborne, K., & Binder-Macleod, S. A. (2002b). Factors in fatigue during intermittent electrical stimulation of human skeletal muscle. *Journal of Applied Physiology*, *93*(2), 469–478.

Rutten, W. L., van Wier, H. J., & Put, J. H. (1991). Sensitivity and selectivity of intraneural stimulation using a silicon electrode array. *IEEE Transactions on Biomedical Engineering*, *38*(2), 192–198.

Ryu, J. S., Kang, J. Y., Park, J. Y., Nam, S. Y., Choi, S. H., Roh, J. L., … Choi, K. H. (2009). The effect of electrical stimulation therapy on dysphagia following treatment for head and neck cancer. *Oral Oncology*, *45*(8), 665–668.

Sabut, S. K., Sikdar, C., Kumar, R., & Mahadevappa, M. (2011). Functional electrical stimulation of dorsiflexor muscle: effects on dorsiflexor strength, plantarflexor spasticity, and motor recovery in stroke patients. *NeuroRehabilitation*, *29*(4), 393–400.

Sale, D. G. (1987). Influence of exercise and training on motor unit activation. *Exercise and Sport Sciences Reviews*, *15*(1), 95–152.

Sandow, A. (1965). Excitation contraction coupling in skeletal muscle. *Pharmacological Reviews*, *17*(3), 56.

Scremin, A. E., Kurta, L., Gentili, A., Wiseman, B., Perell, K., Kunkel, C., & Scremin, O. U. (1999). Increasing muscle mass in spinal cord injured persons with a functional electrical stimulation exercise program. *Archives of Physical Medicine and Rehabilitation*, *80*(12), 1531–1536.

Selkowitz, D. M. (1985). Improvement in isometric strength of the quadriceps femoris muscle after training with electrical stimulation. *Physical Therapy*, *65*(2), 186–196.

Silva, N. A., Sousa, N., Reis, R. L., & Salgado, A. J. (2014). From basics to clinical: a comprehensive review on spinal cord injury. *Progress in Neurobiology*, *114*, 25–57.

Smith, C. U. M., Frixione, E., Finger, S., & Clower, W. (2012). *The Animal Spirit Doctrine and the Origins of Neurophysiology*. Oxford University Press.

Stackhouse, S. K., Binder-Macleod, S. A., Stackhouse, C. A., McCarthy, J. J., Prosser, L. A., & Lee, S. C. K. (2007). Neuromuscular electrical stimulation versus volitional isometric strength training in children with spastic diplegic cerebral palsy: a preliminary study. *Neurorehabilitation and Neural Repair*, *21*(6), 475–85.

Stein, C., Fritsch, C. G., Robinson, C., Sbruzzi, G., & Plentz, R. D. M. (2015). Effects of electrical stimulation in spastic muscles after stroke: Systematic review and meta-analysis of randomized controlled trials. *Stroke*, *46*(8), 2197–2205.

Stein, R. B., Rolf, R., Everaert, D. G., Bobet, J., & Chong, S. (2008). Surface electrical stimulation for foot drop: control aspects and walking performance, *Journal of Automatic Control, 18*(2), 47–52.

Stevens-Lapsley, J. E., Balter, J. E., Wolfe, P., Eckhoff, D. G., & Kohrt, W. M. (2012). Early neuromuscular electrical stimulation to improve quadriceps muscle strength after total knee arthroplasty: a randomized controlled trial. *Physical Therapy*, *92*(2), 210–226.

Stock, M. S., & Thompson, B. J. (2014). Effects of Barbell Deadlift Training on Submaximal Motor Unit Firing Rates for the Vastus Lateralis and Rectus Femoris, *PloS one, 9*(12), e115567.

Vagg, R., Mogyoros, I., Kiernan, M. C., & Burke, D. (1998). Activity-dependent hyperpolarization of human motor axons produced by natural activity. *The Journal of Physiology*, *507*(3), 919–925.

van Swigchem, R., van Duijnhoven, H. J. R., den Boer, J., Geurts, A. C., & Weerdesteyn, V. (2012). Effect of peroneal electrical stimulation versus an ankle-foot orthosis on obstacle avoidance ability in people with stroke-related foot drop. *Physical Therapy*, *92*(3), 398–406.

Vanderthommen, M., & Duchateau, J. (2007). Electrical stimulation as a modality to improve performance of the neuromuscular system. *Exercise and Sport Sciences Reviews*, *35*(4), 180–185.

Vaynman, S., & Gomez-Pinilla, F. (2005). License to Run: Exercise Impacts Functional Plasticity in the Intact and Injured Central Nervous System by Using Neurotrophins. *Neurorehabilitation and Neural Repair*, *19*(4), 283–295.

Walls, R. J., McHugh, G., O'Gorman, D. J., Moyna, N. M., & O'Byrne, J. M. (2010). Effects of preoperative neuromuscular electrical stimulation on quadriceps strength and functional recovery in total knee arthroplasty. A pilot study. *BMC Musculoskeletal Disorders*, *11*, 119–119.

Warlow, C., Van Gijn, J., Dennis, M. S., Wardlaw, J. M., Sandercock, P. A., Rinkel, G., & Langhorne, P. (2008). Stroke: practical management.

Westerblad & Allen (2009) Human Muscle Fatigue textbook chapter (highlighted).pdf. (n.d.).

Wheeler, G. D., Andrews, B., Lederer, R., Davoodi, R., Natho, K., Weiss, C., … Steadward, R. D. (2002). Functional electric stimulation–assisted rowing: increasing cardiovascular

fitness through functional electric stimulation rowing training in persons with spinal cord injury. *Archives of Physical Medicine and Rehabilitation*, *83*(8), 1093–1099.

Wiest, M. J., Bergquist, A. J., Schimidt, H. L., Jones, K. E., & Collins, D. F. (2017a). Interleaved neuromuscular electrical stimulation: Motor unit recruitment overlap. *Muscle & Nerve*, *55*(4), 490–499.

Wiest, M. J., Bergquist, A. J., & Collins, D. F. (2017b). Torque, Current, and Discomfort During 3 Types of Neuromuscular Electrical Stimulation of Tibialis Anterior. *Physical Therapy*, *97*(8), 790–789.

Yamanishi, T., Yasuda, K., Sakakibara, R., Hattori, T., Ito, H., & Murakami, S. (1997). Pelvic floor electrical stimulation in the treatment of stress incontinence: an investigational study and a placebo controlled double-blind trial. *The Journal of Urology*, *158*(6), 2127–2131.

Yekutiel, M., Brooks, M., Ohry, A., Yarom, J., & Carel, R. (1989). The prevalence of hypertension, ischaemic heart disease and diabetes in traumatic spinal cord injured patients and amputees. *Spinal Cord*, *27*(1), 58–62.

Ying, Z., Roy, R. R., Edgerton, V. R., & Gómez-Pinilla, F. (2005). Exercise restores levels of neurotrophins and synaptic plasticity following spinal cord injury. *Experimental Neurology*, *193*(2), 411–419.

Yoshida, K., & Horch, K. (1993). Reduced fatigue in electrically stimulated muscle using dual channel intrafascicular electrodes with interleaved stimulation. *Annals of Biomedical Engineering*, *21*(6), 709–714.

Yoshimitsu, K., Shiba, N., Matsuse, H., Takano, Y., Matsugaki, T., Inada, T., … Nagata, K. (2010). Development of a training method for weightless environment using both

electrical stimulation and voluntary muscle contraction. *The Tohoku Journal of Experimental Medicine*, *220*(1), 83–93.

Zehr, E. P. (2002). Considerations for use of the Hoffmann reflex in exercise studies, European *Journal of Applied Physiology*, *86*(6), 455-468.